

Immobilization of Rhodamine Derivatives on Agarose Hydrogel for Heavy Metal
Detection

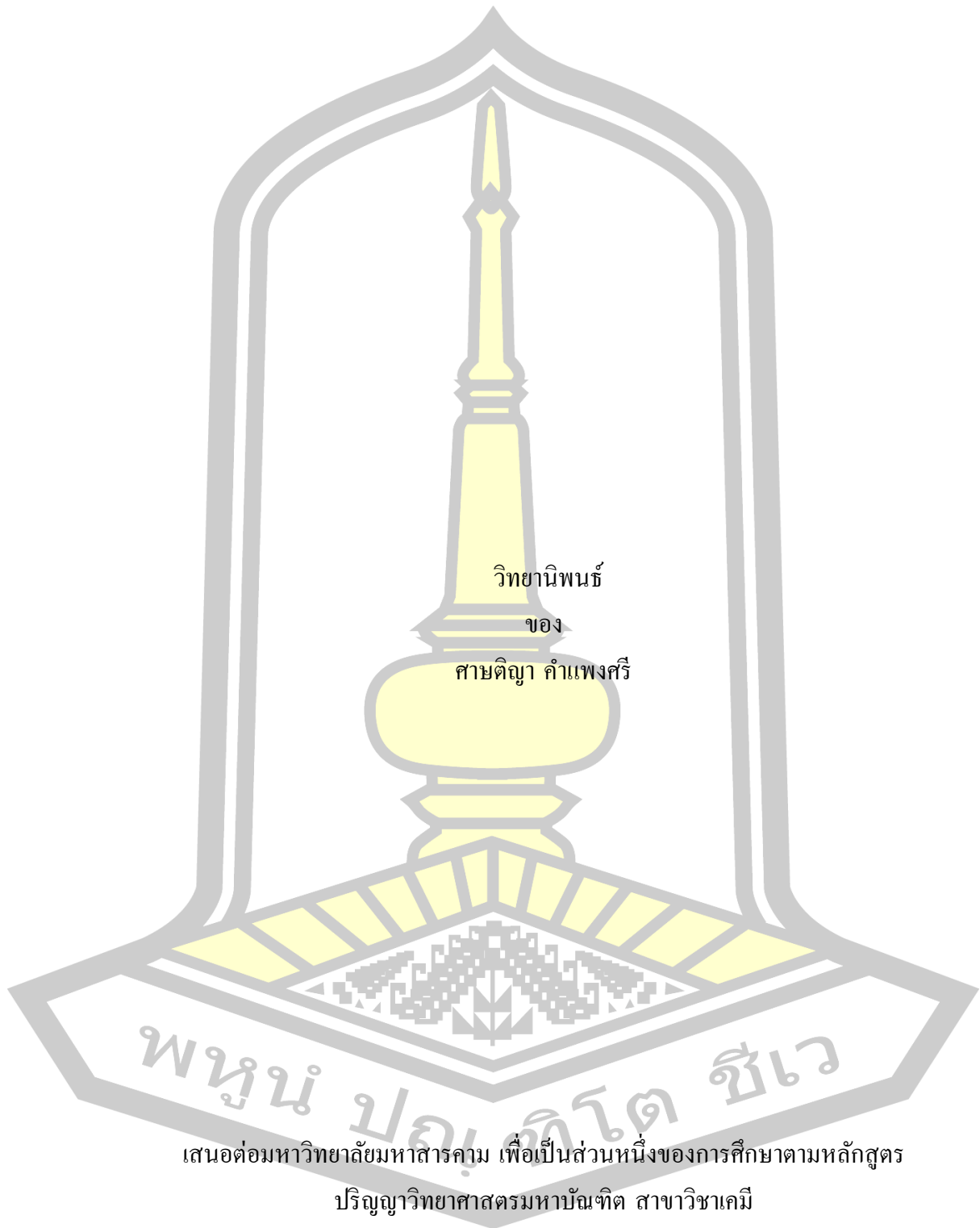
Sastiya Kampaengsri

A Thesis Submitted in Partial Fulfillment of Requirements for
degree of Master of Science in Chemistry

November 2018

Copyright of Maharakham University

การตรึงอนุพันธ์ของโรดามีน บนอะกาโรสไฮโดรเจล สำหรับการตรวจวัดโลหะหนัก



เสนอต่อมหาวิทยาลัยมหาสารคาม เพื่อเป็นส่วนหนึ่งของการศึกษาตามหลักสูตร

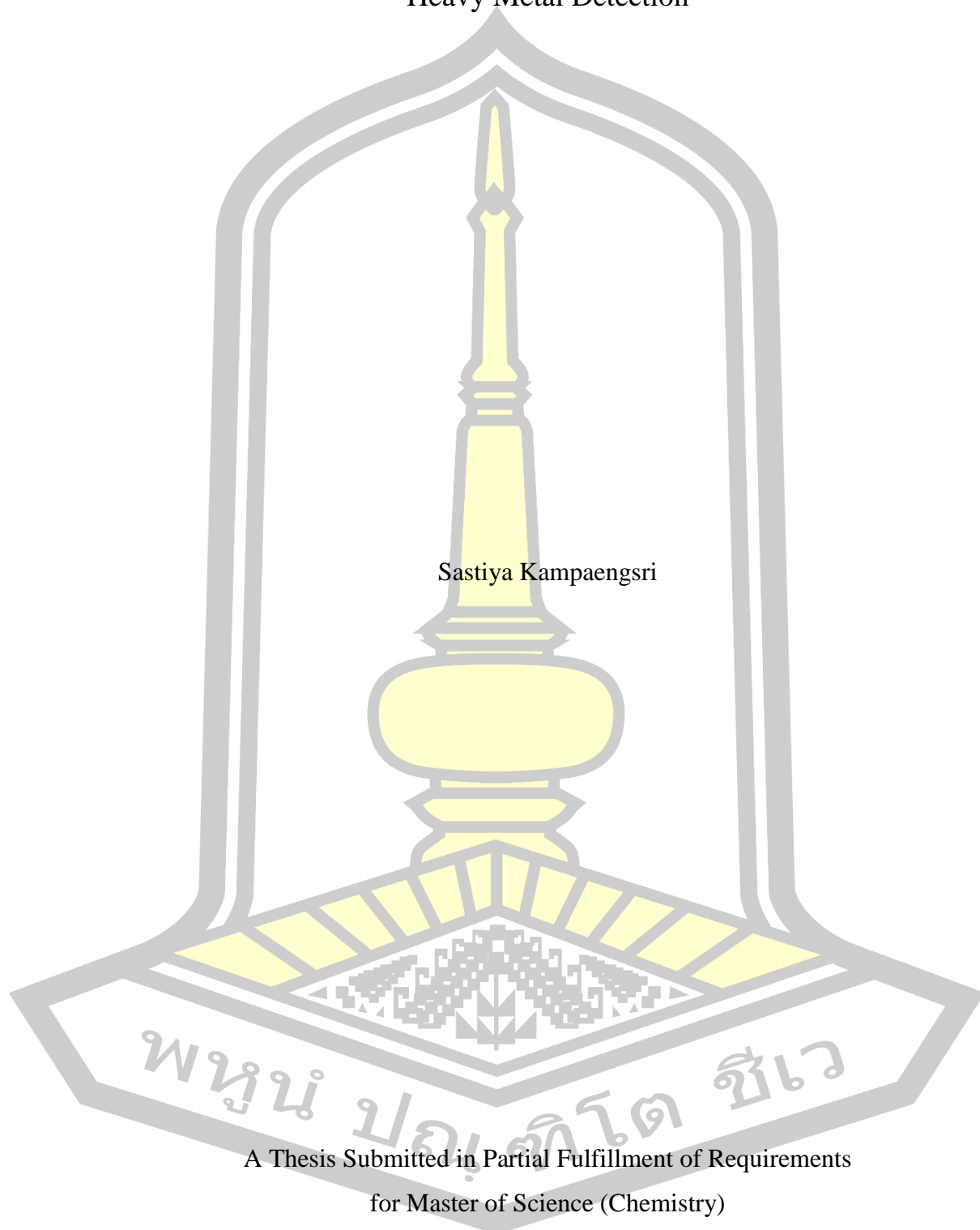
ปริญญาวิทยาศาสตรมหาบัณฑิต สาขาวิชาเคมี

พฤศจิกายน 2561

สงวนลิขสิทธิ์เป็นของมหาวิทยาลัยมหาสารคาม

Immobilization of Rhodamine Derivatives on Agarose Hydrogel for
Heavy Metal Detection

Sastiya Kampaengsri



A Thesis Submitted in Partial Fulfillment of Requirements
for Master of Science (Chemistry)

November 2018

Copyright of Mahasarakham University



The examining committee has unanimously approved this Thesis, submitted by Mr. Sastiya Kampaengsri , as a partial fulfillment of the requirements for the Master of Science Chemistry at Maharakham University

Examining Committee

(Asst. Prof. Burapol Singhana Ph.D.)	Chairman
(Assoc. Prof. Chatthai Kaewtong , Ph.D.)	Advisor
(Asst. Prof. Banchob Wanno , Ph.D.)	Co-advisor
(Asst. Prof. Prapairat Seephonkai , Ph.D.)	Committee
(Asst. Prof. Widchaya Radchatawedchakoon , Ph.D.)	Committee

Maharakham University has granted approval to accept this Thesis as a partial fulfillment of the requirements for the Master of Science Chemistry

(Prof. Pairot Pramual , Ph.D.)
Dean of The Faculty of Science

(Asst. Prof. Krit Chaimoon , Ph.D.)
Dean of Graduate School

Day.....Month.....Year.....

มหาวิทยาลัยราชภัฏรำไพพรรณี

TITLE	Immobilization of Rhodamine Derivatives on Agarose Hydrogel for Heavy Metal Detection		
AUTHOR	Sastiya Kampaengsri		
ADVISORS	Associate Professor Chatthai Kaewtong , Ph.D. Assistant Professor Banchob Wannoo , Ph.D.		
DEGREE	Master of Science	MAJOR	Chemistry
UNIVERSITY	Maharakham University	YEAR	2018

ABSTRACT

A highly sensitive and selective optical membrane for determination of Au^{3+} was synthesized by immobilization of a rhodamine derivative on agarose hydrogel. The sensing dye was synthesized by solvatochromism of rhodamine B via rhodamine lactone–zwitterion equilibrium. UV–vis spectroscopy, scanning electron microscopy (SEM), thermal gravimetric analysis (TGA) and attenuated total reflectance Fourier transform infrared spectroscopy (ATR-FTIR) were employed to confirm that the rhodamine-lactone (RhoL) was incorporated into the agarose hydrogel. The results showed that the sensor was highly selective for recognizing Au^{3+} over other metal ions in real systems. The DFT calculation results suggested that the membrane sensor formed stable complexes with Au^{3+} through a large number of cation-dipole and ion–ion interactions. In addition, rhodamine and a dansyl moiety (RhoL-DNS) were developed for highly selective detection of heavy metal based on fluorescence resonance energy transfer (FRET) due to the spectral overlap between the emission of the dansyl moiety and the absorption of the ring opened rhodamine moiety by dansyl energy donor to the rhodamine energy acceptor. UV–vis spectroscopy, fluorescent spectroscopy were employed to confirm that the rhodamine and a dansyl moiety were incorporated into the agarose hydrogel. This approach may provide an easily measurable and inherently sensitive method for Au^{3+} ion detection in environmental and biological applications.

Keyword : Heavy metal, Rhodamine lactone, Hydrogel, Solvatochromism, FRET

ACKNOWLEDGEMENTS

I would like to express my deepest and sincere gratitude to my advisor, Assoc. Prof. Dr. Chatthai Kaewtong for his kindness in providing an opportunity to be his advisee. I am also appreciated for her valuable supervision, suggestions, encouragement, supporting, guidance and criticism throughout the course of my study. I would like to express my greatest appreciation and sincere gratitude to my co-adviser, Asst. Prof. Dr. Banchob Wannoo, Department of Chemistry Faculty of Science, Maharakham University for his valuable advices, kindness, useful comment and suggestion. Sincere thank and appreciation are also due to my graduate committee, Assoc. Prof. Dr. Wittaya Ngeontae, Department of Chemistry, Faculty of Science, Khon Kaen University, Assoc. Prof. Dr. Chatthai Kaewtong, Asst. Prof. Dr. Banchob Wannoo, Asst. Prof. Dr. Prapairat Seephonkai and Asst. Prof. Dr. Somchai Keawwangchai, Department of Chemistry, Faculty of Science, Maharakham University for their helpful suggestion. I would like to express my gratitude to Department of Chemistry, Faculty of Science, Maharakham University for providing chemicals, instruments and all supporting facilities. I would like to express my sincere thanks to Department of Chemistry, Nanotechnology Research Unit and Supramolecular Chemistry Research Unit and Center of Excellence for Innovation in Chemistry (PERCH-CIC) for the financial support during my study. My appreciation is extended to all the staff members of the Department of Chemistry. I would like to thank my friends for their encouragement, making life enjoyable and friendship. Thanks are also expressed to many persons who have not been mentioned here for their help, directly and indirectly, during all stages of the work. More than anything else, I would like to special acknowledge my family especially my parents for their tender love, definite care, support, patience and many sacrifices throughout the extended period of my study.

Sastiya Kampaengsri

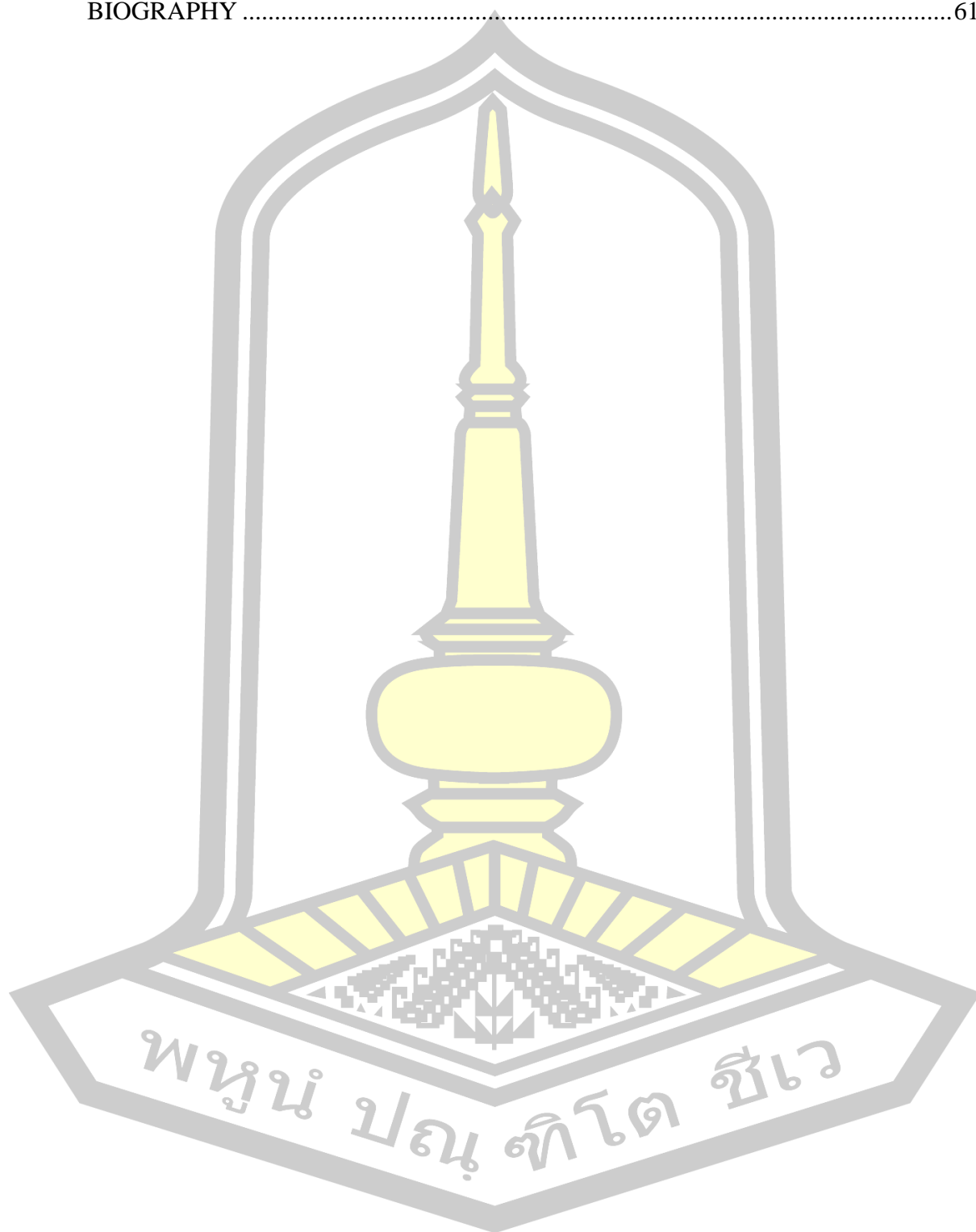
TABLE OF CONTENTS

	Page
ABSTRACT.....	D
ACKNOWLEDGEMENTS.....	E
TABLE OF CONTENTS.....	F
LIST OF FIGURES	I
CHAPTER I.....	1
INTRODUCTION	1
1.1 Definition of terms.....	4
1.1.1 Hydrogel.....	4
1.1.2 Fluorescence resonance energy transfer (FRET)	4
1.1.3 Rhodamine B.....	4
1.1.4 Chemical sensor	5
1.1.5 Fluorescence.....	5
1.1.6 Solvatochromic effect.....	5
1.2 Objectives	6
1.3 Scope of research.....	6
CHAPTER II.....	8
LITERATURE REVIEWS	8
2.1 Rhodamine derivative.....	8
2.2 Fluorescence resonance energy transfer of rhodamine-dansyl.....	18
2.3 Hydrogel.....	21
CHAPTER III.....	27
MATERIALS AND METHODS.....	27
3.1 Experimental.....	27
3.1.1 Reagents	27
3.1.2 Apparatus.....	27

3.2 Synthesize agarose hydrogel (Agr-RhoL)	28
3.2.1 Preparation of the rhodamine lactone (colorless L-form, RhoL)	28
3.2.2 Immobilization of rhodamine lactone (RhoL) to agarose hydrogel (Arg-RhoL).....	28
3.2.3 Sensor response studies of Arg-RhoL	29
3.3 Synthesize rhodamine derivative and dansyl chloride immobilized agarose hydrogel (AAgr-RhoL+DNS, Agr-RhoL-DNS)	29
3.3.1 Synthesize rhodamine ethylenediamine	29
3.3.2 Synthesize rhodamine-dansyl.....	31
3.3.3 Immobilization of rhodamine and dansyl chloride to agarose hydrogel ..32	
3.3.3.1 Activation of agarose hydrogel	32
3.3.3.2 Immobilization of rhodamine and dansyl chloride.....	33
3.3.4 Immobilization of rhodamine and dansyl chloride to agarose powder35	
3.3.4.1 Activation of agarose powder.....	35
3.3.4.2 Immobilization rhodamine and dansyl chloride.....	35
3.3.5 Immobilization of rhodamine-dansyl	37
CHAPTER IV	39
RESULTS AND DISCUSSION	39
4.1 Synthesize agarose hydrogel (Agr-RhoL)	39
4.1.1 The formation of the rhodamine lactone colorless L-form.....	39
4.1.2 Characterization of Arg-RhoL.....	39
4.1.3 Selectivity of Arg-RhoL.....	43
4.1.4 Computational methods.....	45
4.2 Immobilization of rhodamine derivative and dansyl chloride to agarose hydrogel.....	46
4.3 Immobilization of rhodamine derivative and dansyl chloride to agarose powder	49
4.4 Immobilization of rhodamine-dansyl.	50
CHAPTER V	54
CONCLUSIONS.....	54

REFERENCES55

BIOGRAPHY61

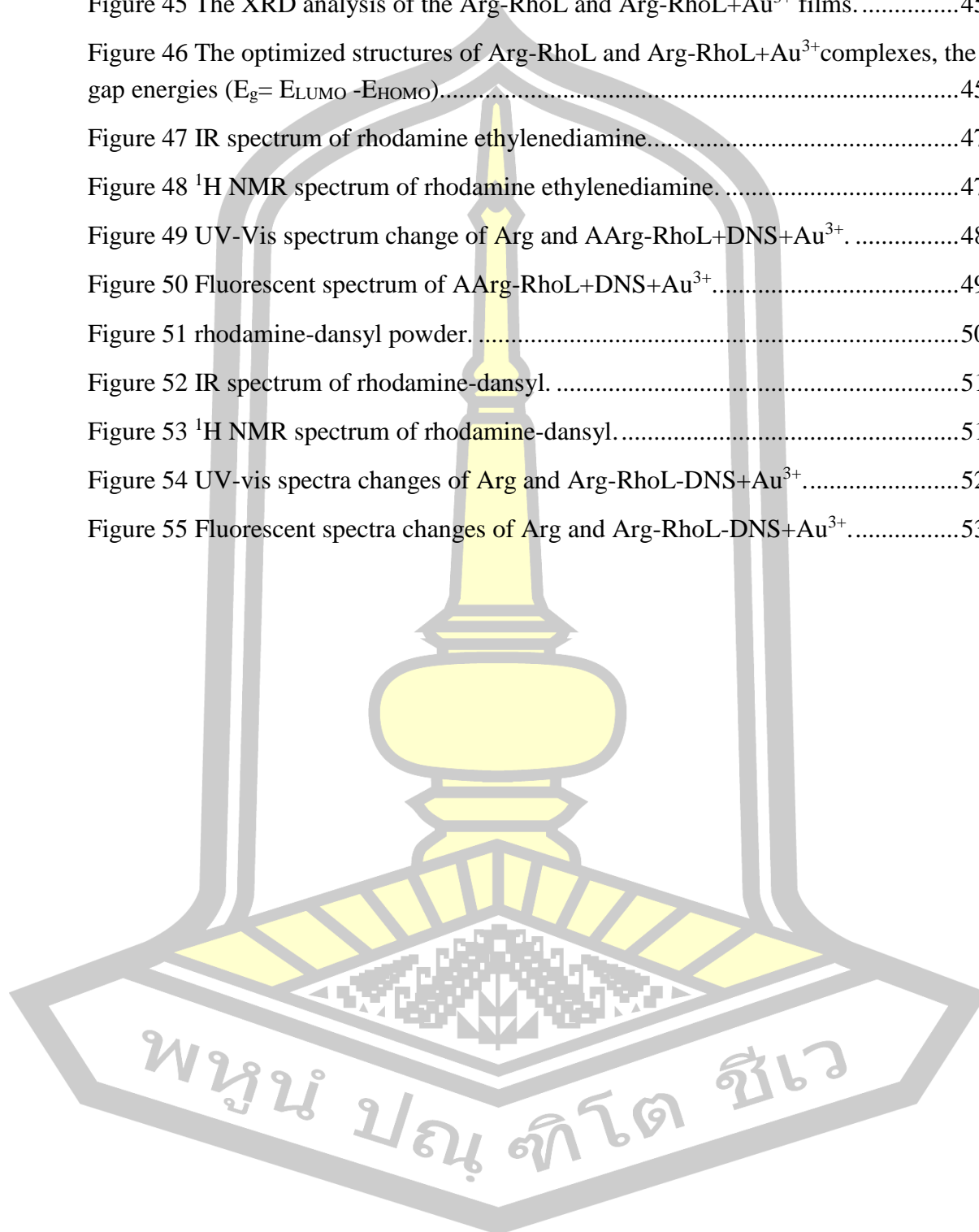


LIST OF FIGURES

	Page
Figure 1 Showing caught between host with guest to form host-guest complex.....	2
Figure 2 rhodamine B lactone–zwitterion equilibrium.....	3
Figure 3 fluorescence resonance energy transfer (FRET) of rhodamine-dansyl.	4
Figure 4 Synthesize rhodamine B (RhoL) and immobilized to agarose hydrogel (Agr-RhoL).....	7
Figure 5 Synthesize rhodamine-dansyl immobilized to agarose hydrogel (Agr-RhoL-DNS).....	7
Figure 6 Summary of crystal data for RB Lactone.....	8
Figure 7 lactone zwitterion of rhodamine B.....	9
Figure 8 Synthesis of rhodamine derivative and proposed Hg^{2+} binding mode.....	10
Figure 9 Proposed binding mechanism for PRC with Cu^{2+} and a photo of PRC (20 μM) as a selective naked-eye chemosensor for Cu^{2+}	11
Figure 10 The absorbance and fluorescence spectra of RhB in different solvents.....	11
Figure 11 Synthesis and metal detection of rhodamine derivative.....	12
Figure 12 Synthetic pathways to L1–L3.....	13
Figure 13 Synthetic route of rhodamine derivative.....	14
Figure 14 Synthesis procedures of RC and CS-RC.....	15
Figure 15 Synthesis and selective of RA.....	16
Figure 16 Synthesis and determination of Rho-Se with Hg^{2+}	17
Figure 17 Cu^{2+} -induced FRET off-on along with visual color changes upon irradiation at 420 nm.....	18
Figure 18 Structure, emission spectra and color change of chemo sensor up on addition of various metal ion in ethanol solution.....	19
Figure 19 Synthetic route to rhodamine-dansyl and proposed mechanism for FRET of rhodamine-dansyl with Hg^{2+}	20
Figure 20 Synthesis and selectivity of dansyl-appended rhodamine B sensor.....	21
Figure 21 (A) structure of Neutral red, (B) structure of Thionin.....	22

Figure 22 The structures of free calmagite and its 1:1 complex with Cu^{2+}	22
Figure 23 Optimized structures of free ligand and its 2:1 complex with Hg^{2+} ion.....	23
Figure 24 The structure of the dithizone complexes with metal and color change, absorbance spectra of the proposed optical sensor with metal ion.	24
Figure 25 Photographs of colorimetric sensing test of heavy metal ions, exclusively Cr^{6+} , Cu^{2+} , Fe^{3+} , Pb^{2+} , and Mn^{2+} , when loaded into the hydrogel films Agr/CD and Agr. And pictorial representation of fabrication of agarose/CD (Agr/CD) Hydrogel Film.	25
Figure 26 Structure of arsenazo III.	25
Figure 27 Chemical structure of orange (II) bonding to agarose membrane.....	26
Figure 28 Preparation of rhodamine B (RhoL-n).	28
Figure 29 Preparation of Agr-RhoL.....	29
Figure 30 Synthesis of rhodamine ethylenediamine.....	30
Figure 31 Synthesis of rhodamine-dansyl.	32
Figure 32 Activation of agarose gel membranes.	33
Figure 33 Immobilization of rhodamine derivative and dansyl chloride to agarose hydrogel.	34
Figure 34 Activation of agarose powder.....	35
Figure 35 Immobilization of rhodamine derivative and dansyl chloride to agarose powder.....	37
Figure 36 Preparation of agarose gel membranes.....	38
Figure 37 Immobilization of rhodamine-dansyl.	38
Figure 38 Visible absorption and emission spectra of rhodamine lactone in H_2O : THF solution.....	39
Figure 39 Attenuated total reflectance Fourier transform infrared spectroscopy (ATR-FTIR) spectrum of Arg-RhoL.....	40
Figure 40 Scanning electron microscope (SEM) image of Arg-RhoL (up) and Arg (below).	41
Figure 41 Thermogravimetric analysis of Arg and Arg-RhoL.	42
Figure 42 UV-visible spectra of Arg and Arg-RhoL.....	42
Figure 43 UV-vis spectra changes of Arg-RhoL after the addition of $10 \mu\text{M}$ of various cations.	43

Figure 44 Color changes of the Arg-RhoL with various cations.	44
Figure 45 The XRD analysis of the Arg-RhoL and Arg-RhoL+Au ³⁺ films.	45
Figure 46 The optimized structures of Arg-RhoL and Arg-RhoL+Au ³⁺ complexes, the gap energies ($E_g = E_{LUMO} - E_{HOMO}$).	45
Figure 47 IR spectrum of rhodamine ethylenediamine.	47
Figure 48 ¹ H NMR spectrum of rhodamine ethylenediamine.	47
Figure 49 UV-Vis spectrum change of Arg and AArg-RhoL+DNS+Au ³⁺	48
Figure 50 Fluorescent spectrum of AArg-RhoL+DNS+Au ³⁺	49
Figure 51 rhodamine-dansyl powder.	50
Figure 52 IR spectrum of rhodamine-dansyl.	51
Figure 53 ¹ H NMR spectrum of rhodamine-dansyl.	51
Figure 54 UV-vis spectra changes of Arg and Arg-RhoL-DNS+Au ³⁺	52
Figure 55 Fluorescent spectra changes of Arg and Arg-RhoL-DNS+Au ³⁺	53



CHAPTER I

INTRODUCTION

Although heavy metals have many beneficial uses such as in catalysts used in industry, they have also been involved in rampant pollution of the environment [1] resulting in contamination of food and drinking water [2]. The effects of heavy metal pollutants on aquatic ecosystems in urban, agricultural and industrial environments have been considered [3]. Therefore, it is essentially to find an effective method for the recovery of heavy metals from aqueous solution to support environmental monitoring and protection and also to support full utilization of gold resource. Conventional methods for the recovery of heavy metals from aqueous solutions included precipitation [4], ions exchange [5], and solvent extraction [6]. However, these methods are not effective (incomplete metal removal) or economical (high cost, high reagent and/or energy requirement).

Gold, one of the heavy metals, has been widely used in many fields (medicine [7], catalysis [8], and electronics [9]). Although the effect of gold ion on the cellular immune response is currently sparse. But Synchronously, Au^{3+} is known to be potentially toxic to humans [10–12], since soluble gold salts such as gold chloride are recognized to cause damage to the liver, kidneys [13], and the peripheral nervous system. And resulted in negative impacts on the environment.

Supramolecular is a science of chemistry. The study of molecular systems that are interlinked by molecular forces, which are called molecules and host molecules are molecules that are created through bonds by molecular building blocks (figure 1). The force between the molecules formed is called a molecular interaction [14]. Non-covalent interactions or interactions between molecules (Intermolecular Interactions) or molecular forces. Intermolecular forces are often found in large molecules that are caused by static electricity [15]. Interaction is important in large molecular studies (Macromolecules). Noncovalent interactions are ubiquitous in chemistry and are a main source of stability for many molecular complexes in nanoscience, materials chemistry, and biochemistry [16]. It is based on the principle of lock and key, which is specific to target substance or target ion, it has featured the science of molecular

sensor to detect metal ions. Molecular sensors measure the physical, chemical, and biological quantities at small scales, such as concentration of ions or proteins, existence of toxic molecules, and genetic information from cells, with a sensitivity and specificity at molecular scales [17]. Which requirement for molecular sensors in which molecules interact with an analyte to produce a detectable change, is becoming more demanding.

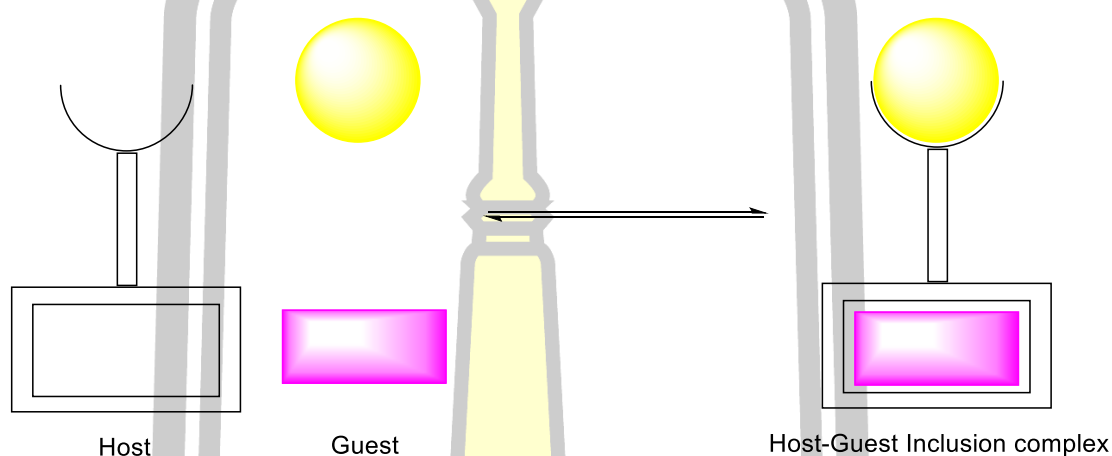


Figure 1 Showing caught between host with guest to form host-guest complex.

In the past few years, molecular sensors have become powerful tools for sensing of samples because of their simplicity and sensitivity. Nevertheless, these methods have also shown several problems such as low mechanical and thermal stability, weak chemical union with the metals, poor removal efficiency, high cost, etc. In contrast with molecular sensors, gel sensors exhibited prominent advantages, such as the ease of fabrication of devices, a wide choice of incorporating specific units into the gel, low cost, and so on [18]. Recently, a preparation of a Neutral Red (NR)-ACG optical sensor was reported as a long life pH optical sensor for pH measurements in a range of 2–8.5 and showed more stability than a standalone agarose membrane with easier handling and storage [4]. Dithizone has also been immobilized on agarose membrane for determination of Hg^{2+} and Pb^{2+} and had good selectivity for target ions compared with a large number of alkali, alkaline earth, transition, and heavy metal ions [2].

Rhodamine ethylenediamine is a derivatives of rhodamine dyes which are widely used as fluorescence probes owing to their high absorption coefficient and broad fluorescence in the visible region of the electromagnetic spectrum [19-20], high fluorescence quantum yields, and photostability after complexes with metal ions by activating a carbonyl group in a spirolactone or a spirolactam moiety [21-22]. The mechanism is based on the switch Off/On of the spirocyclic moiety mediated by guests. In general, spirolactone formation of rhodamine derivatives is non-fluorescent [23], whereas its ring-opened system by guests gives rise to a pink color and strong fluorescence emission (figure 2) [24-25]. In our earlier work, we developed a solvatochromic rhodamine-based sensor for Cr^{3+} using commercially available rhodamine simply dissolved in THF to produce rhodamine lactone (**RhoL**) via the rhodamine lactone–zwitterion equilibrium [26]. In this work, we exposed the preparation and response features of a new highly sensitive optical sensor on immobilization of rhodamine derivative on agarose hydrogel as a gold probe.

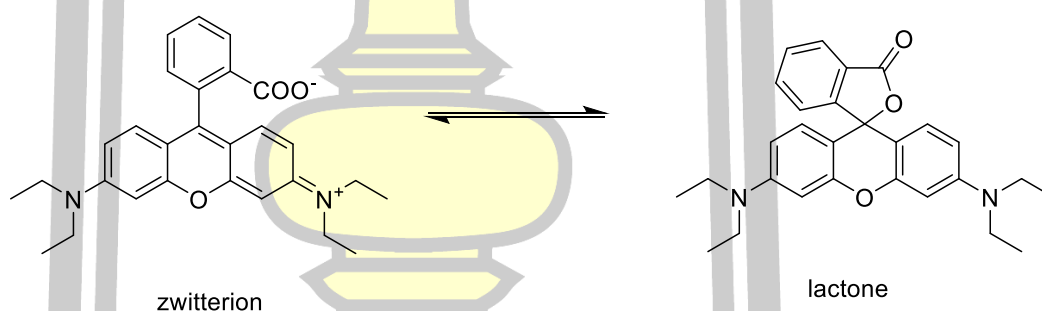


Figure 2 rhodamine B lactone–zwitterion equilibrium.

Moreover rhodamine and a dansyl moiety was developed for highly selective detection of heavy metal based on fluorescence resonance energy transfer (**FRET**) due to the spectral overlap between the emission of the dansyl moiety and the absorption of the ring opened rhodamine moiety by dansyl energy donor to the rhodamine energy acceptor [27-28]. In this work, we exposed the preparation and response features of a new highly sensitive optical sensor on immobilization of rhodamine derivative and dansyl chloride on agarose hydrogel as a gold probe by fluorescence resonance energy transfer (**FRET**) (figure 3).

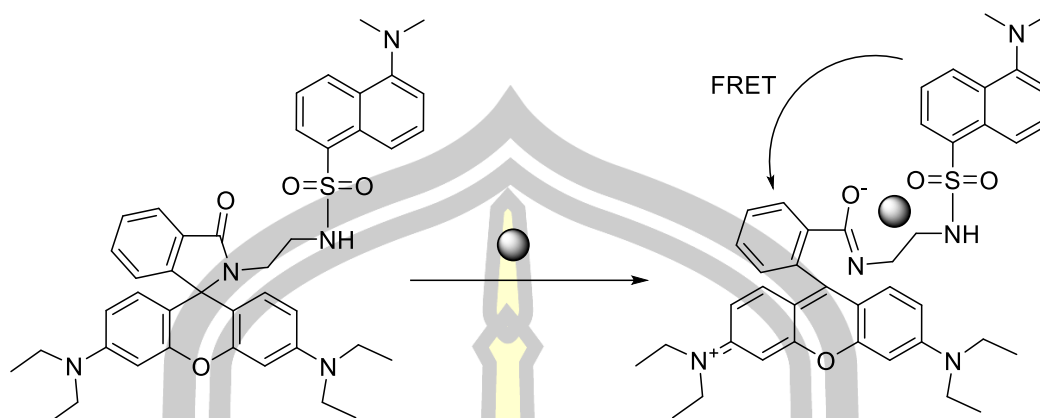


Figure 3 fluorescence resonance energy transfer (**FRET**) of rhodamine-dansyl.

1.1 Definition of terms

1.1.1 Hydrogel

Hydrogels are water-swollen polymeric materials that maintain a distinct three-dimensional structure. Hydrogels are synthesized from hydrophilic monomers by either chain or step growth, along with a functional cross linker to promote network formation.

1.1.2 Fluorescence resonance energy transfer (FRET)

A mechanism describing energy transfer between two light-sensitive molecules (chromophores). A donor chromophore, initially in its electronic excited state, may transfer energy to an acceptor chromophore through nonradiative dipole–dipole coupling. The efficiency of this energy transfer is inversely proportional of the distance between donor and acceptor, making **FRET** extremely sensitive to small changes in distance.

1.1.3 Rhodamine B

Rhodamine B is a chemical compound and a dye. It is often used as a tracer dye within water to determine the rate and direction of flow and transport. Rhodamine dyes fluoresce and can thus be detected easily and inexpensively with instruments called fluorometers.

1.1.4 Chemical sensor

A chemical sensor is a device that transforms chemical information (composition, presence of a particular element or ion, concentration, chemical activity, partial pressure) into an analytically useful signal. The chemical information, mentioned above, may originate from a chemical reaction of the analyte or from a physical property of the system investigated.

1.1.5 Fluorescence

Fluorescence is the emission of light by a substance that has absorbed light or other electromagnetic radiation. The emission of light by a substance that has absorbed light or other electromagnetic radiation. The most striking example of fluorescence occurs when the absorbed radiation is in the ultraviolet region of the spectrum, and thus invisible to the human eye, while the emitted light is in the visible region, which gives the fluorescent substance a distinct color that can be seen only when exposed to UV light. Fluorescent materials cease to glow nearly immediately when the radiation source stops, unlike phosphorescent materials, which continue to emit light for some time after.

1.1.6 Solvatochromic effect

The solvatochromic effect refers to a strong dependence of absorption and emission spectra with the solvent polarity. Since polarities of the ground and excited state of a chromophore are different, a change in the solvent polarity will lead to different stabilization of the ground and excited states, and thus, a change in the energy gap between these electronic states. Consequently, variations in the position, intensity, and shape of the absorption spectra can be direct measures of the specific interactions between the solute and solvent molecules.

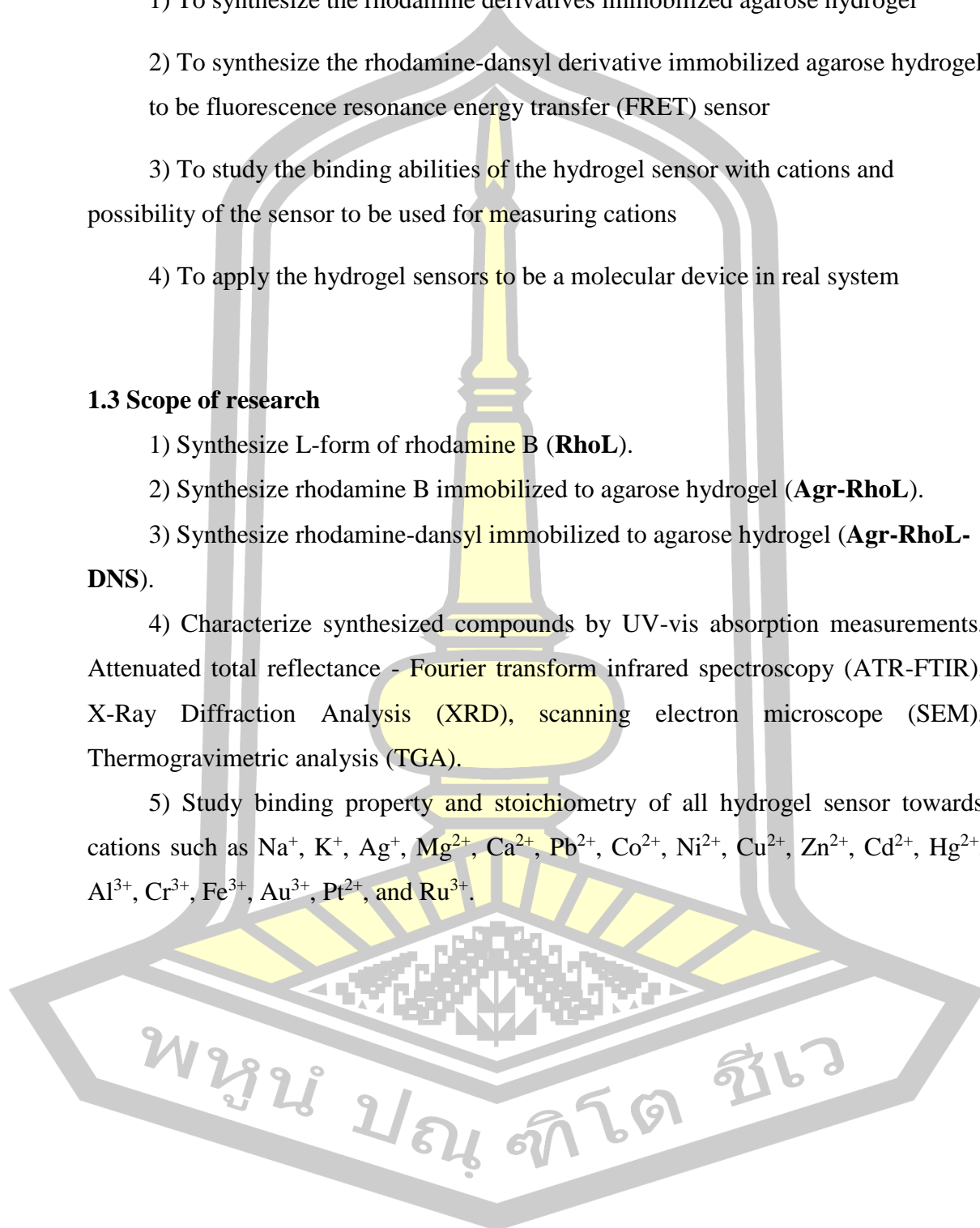
พหุ ประถมศึกษา

1.2 Objectives

- 1) To synthesize the rhodamine derivatives immobilized agarose hydrogel
- 2) To synthesize the rhodamine-dansyl derivative immobilized agarose hydrogel to be fluorescence resonance energy transfer (FRET) sensor
- 3) To study the binding abilities of the hydrogel sensor with cations and possibility of the sensor to be used for measuring cations
- 4) To apply the hydrogel sensors to be a molecular device in real system

1.3 Scope of research

- 1) Synthesize L-form of rhodamine B (**RhoL**).
- 2) Synthesize rhodamine B immobilized to agarose hydrogel (**Agr-RhoL**).
- 3) Synthesize rhodamine-dansyl immobilized to agarose hydrogel (**Agr-RhoL-DNS**).
- 4) Characterize synthesized compounds by UV-vis absorption measurements, Attenuated total reflectance - Fourier transform infrared spectroscopy (ATR-FTIR), X-Ray Diffraction Analysis (XRD), scanning electron microscope (SEM), Thermogravimetric analysis (TGA).
- 5) Study binding property and stoichiometry of all hydrogel sensor towards cations such as Na^+ , K^+ , Ag^+ , Mg^{2+} , Ca^{2+} , Pb^{2+} , Co^{2+} , Ni^{2+} , Cu^{2+} , Zn^{2+} , Cd^{2+} , Hg^{2+} , Al^{3+} , Cr^{3+} , Fe^{3+} , Au^{3+} , Pt^{2+} , and Ru^{3+} .



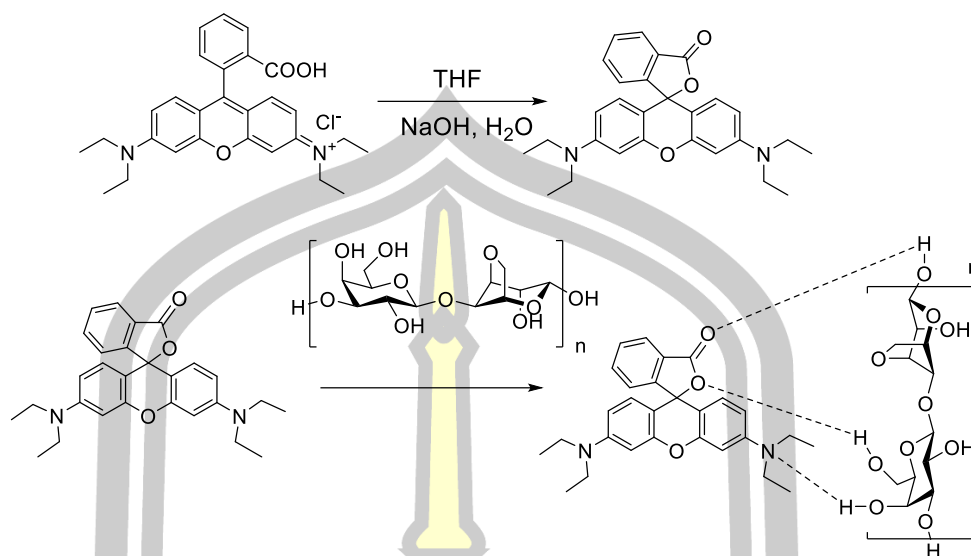


Figure 4 Synthesize rhodamine B (**RhoL**) and immobilized to agarose hydrogel (**Agr-RhoL**).

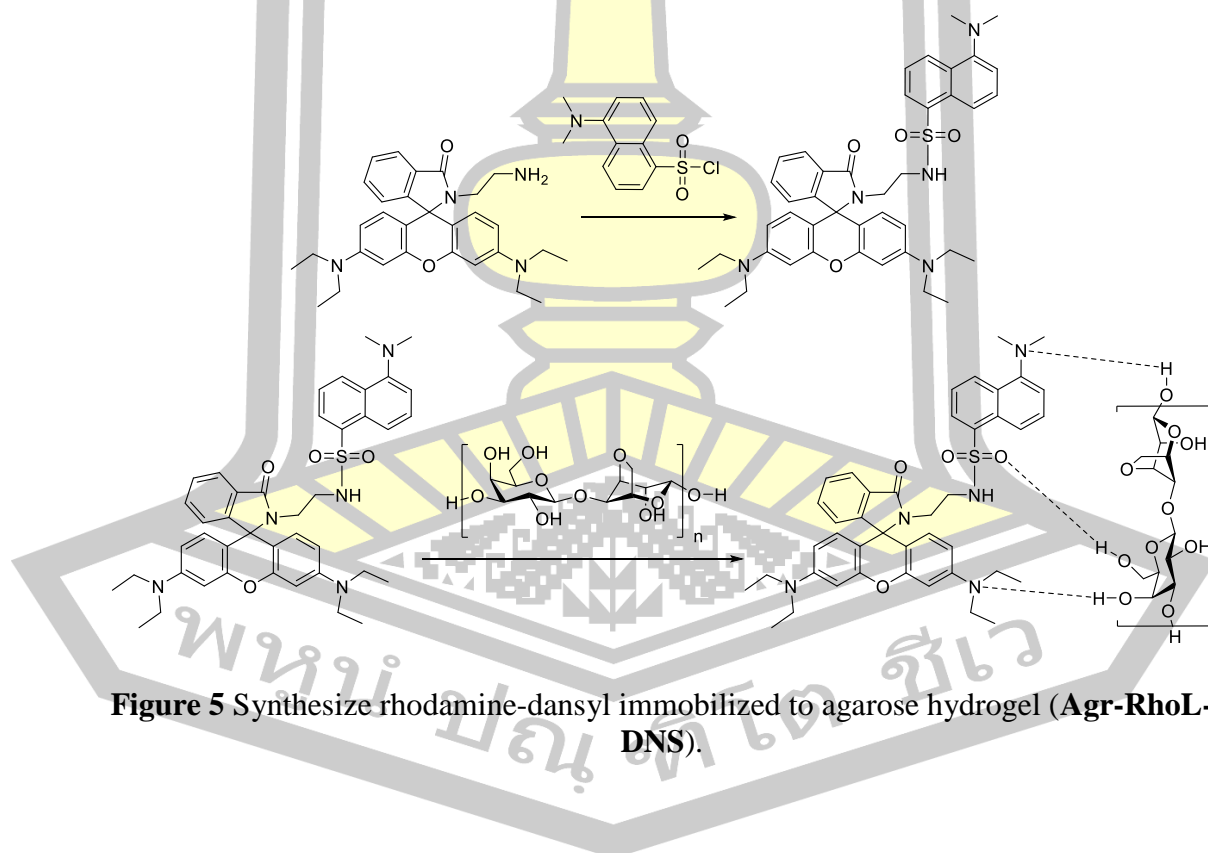


Figure 5 Synthesize rhodamine-dansyl immobilized to agarose hydrogel (**Agr-RhoL-DNS**).

CHAPTER II

LITERATURE REVIEWS

2.1 Rhodamine derivative

In 2001, Wang *et al.* synthesized the single crystals of a lactone form of rhodamine B (**RB** lactone) and its first detailed crystal structure analysis (figure 6). Perfect single crystals of **RB** lactone were hydrothermally prepared in a sol-gel system of rhodamine B-Na₂O-SiO₂-glycerol-H₂O [29].

Formula	C ₂₈ H ₃₀ N ₂ O ₃
M _r	442.55
Crystal color, habit	Slightly red, prismatic
Crystal system	Monoclinic
Space group	P2 ₁ /n
a (nm)	1.6559(3)
b (nm)	1.5657(3)
c (nm)	1.9381(2)
β (°)	100.10(1)
V (nm ³)	4.947(1)
Z	8
D _c (g cm ⁻¹)	1.188
μ (mm ⁻¹)	0.077
F (000)	1888.0
T (K)	293(1)
Max. 2θ	50.0
No. of unique reflection	9063
No. of observed reflection	3834 (I > 2.50σ(I))
Parameters refined	595
R	0.060
R _w	0.064
S (goodness of fit)	1.92
Largest diffraction peak and hole (e nm ⁻³)	360 to -230

Figure 6 Summary of crystal data for **RB** Lactone.

Moreover Hinckley and Seybold studied thermodynamics properties of rhodamine B. Rhodamine B (**RB**) exhibits several interesting equilibria (figure 7). In solution the spectrum of the dye is known to depend on temperature, solvent, and concentration. In protic solvents **RB** exists as an equilibrium mixture of a colorless lactone (**L**) and a colored zwitterion (**Z**) [30].

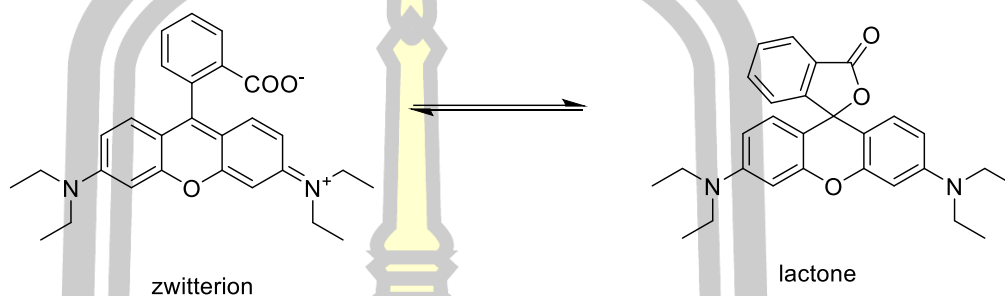


Figure 7 lactone zwitterion of rhodamine B.

In 2006, Zheng *et al.* synthesized chemosensors based on rhodamine spirolactams which have several advantages (figure 8). They display not only great absorbance and fluorescence intensity enhancement toward some specific metal ions, but also a strong color development against the colorless blank during the sensing event. A feature that would facilitate “naked-eye” detection, and very recently, an excellent example of opening the spiro ring of rhodamine spirolactam-based chemodosimeter was reported via the Hg²⁺-induced chemical reaction. Bearing this in mind, by incorporating proper binding sites, it would be possible to achieve a rhodamine spirolactam based chemosensor highly selective for Hg²⁺ via color/fluorescence changes. For the selective recognition of such a soft heavy metal ion, a sulfur-based functional group was considered and introduced, and the N, S binding sites might be a choice to be parts of a selective receptor [20].

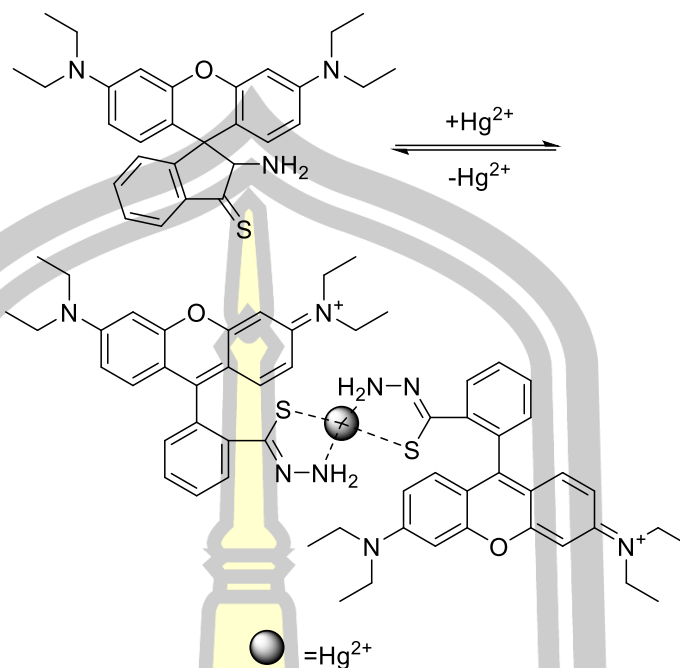


Figure 8 Synthesis of rhodamine derivative and proposed Hg^{2+} binding mode.

In 2009, Zhou *et al.* synthesized rhodamine fluorophore onto the pyrene moiety, which was utilized as a selective fluorescent and colorimetric sensor for Cu^{2+} in aqueous solution. Among the various metal ions, the chemosensor **PRC** (figure 9) displayed highly selective ratiometric changes upon the addition of Cu^{2+} . As expected, the pyrene moiety served successfully as a source of these ratiometric changes. As far as they were aware, **PRC** was the first ratiometric sensor based on rhodamine derivative. For comparison, pyrene-based compound was synthesized to test the fluorescence change with Cu^{2+} [24].

พหุพันธ์ ปณฺ ทิโต ชีเว

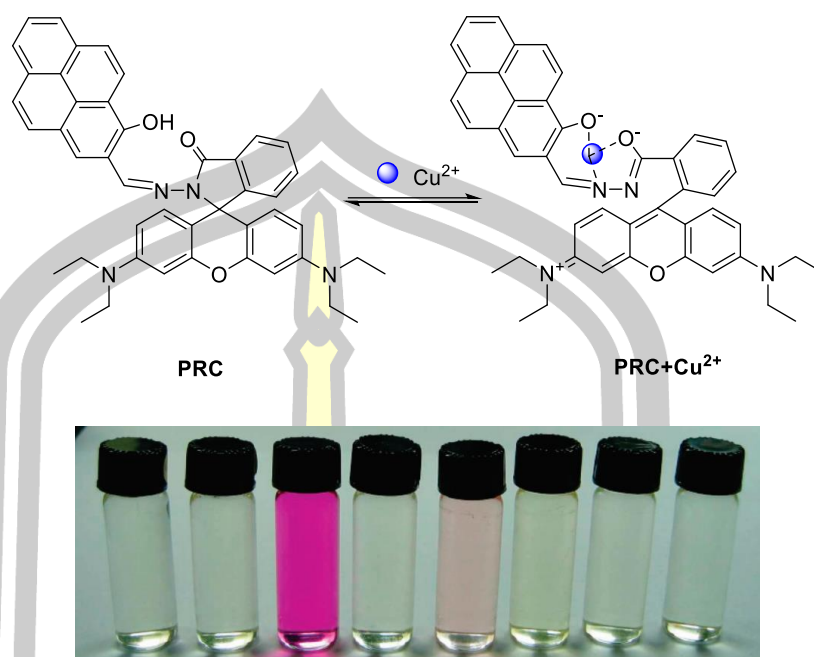


Figure 9 Proposed binding mechanism for **PRC** with Cu^{2+} and a photo of **PRC** (20 μM) as a selective naked-eye chemosensor for Cu^{2+} .

In 2013, Nathera *et al.* studied effect of solvents of various polarities on the electronic absorption and fluorescence spectra of **RhB**. The absorption and emission spectra of dyes with different solvents at various concentrations and the singlet-state excited dipole moments and ground state dipole moments (figure 10), as well as the values of the fluorescence quantum yield, were estimated. The interactions between the solvent and fluorophore molecules affect the energy difference between the ground and excited states. This energy difference is a property of the refractive index and dielectric constant of the solvent [31].

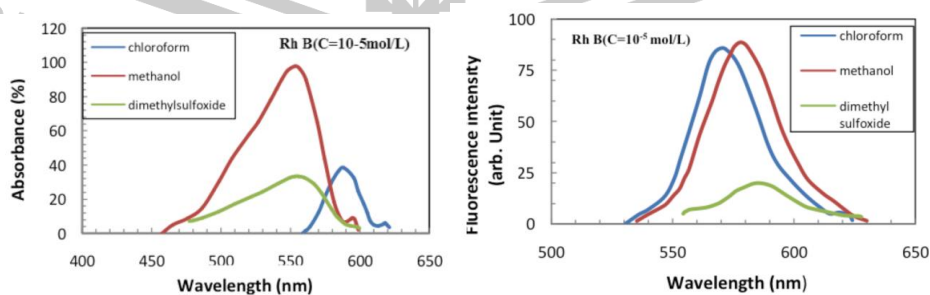


Figure 10 The absorbance and fluorescence spectra of **RhB** in different solvents.

In 2014, Li *et al.* synthesized rhodamine B salicylaldehyde hydrazone metal complex which was found to undergo intramolecular ring-open reactions upon UV irradiation (figure 11), which led to a distinct color and fluorescence change both in solution and in solid matrix. The complex showed good fatigue resistance for the reversible photochromism and long lifetime for the ring-open state. Interestingly, the thermal bleaching rate was tunable by using different metal ions, temperatures, solvents, and chemical substitutions. It was proposed that UV light promoted isomerization of the rhodamine B derivative from enol-form to keto-form, which induced ring opening of the rhodamine spirolactam in the complex to generate color. The photochromic system was successfully applied for photoprinting and UV strength measurement in the solid state. As compared to other reported photochromic molecules, the system in this study has its advantages of facile synthesis and tunable thermal bleaching rate, and also provides new insights into the development of photochromic materials based on metal complex and spirolactam-containing dyes [22].

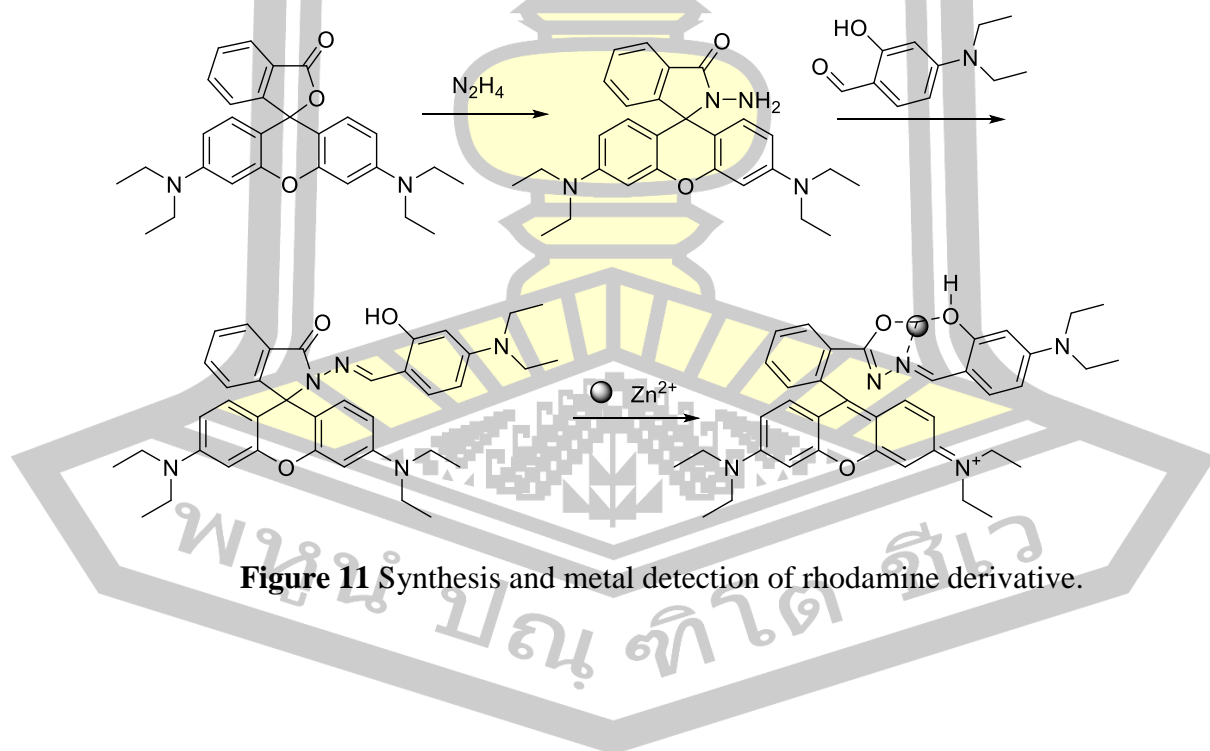


Figure 11 Synthesis and metal detection of rhodamine derivative.

In 2015, Mergu *et al.* synthesized a rhodamine derivatives **L1–L3** (figure 12). These compounds exhibited selective and sensitive “turn-on” fluorescent and colorimetric responses to Al^{3+} in methanol. Upon the addition of Al(III) , the spiro ring was opened and a metal-probe complex was formed in a 1:1 stoichiometry, as was further confirmed by ESI-MS spectroscopy. The chemo-dosimeters **L1–L3** exhibited good binding constants and low detection limits towards Al(III) . They also successfully demonstrated the reversibility of the metal to ligand complexation (opened ring to spirolactam ring) [32].

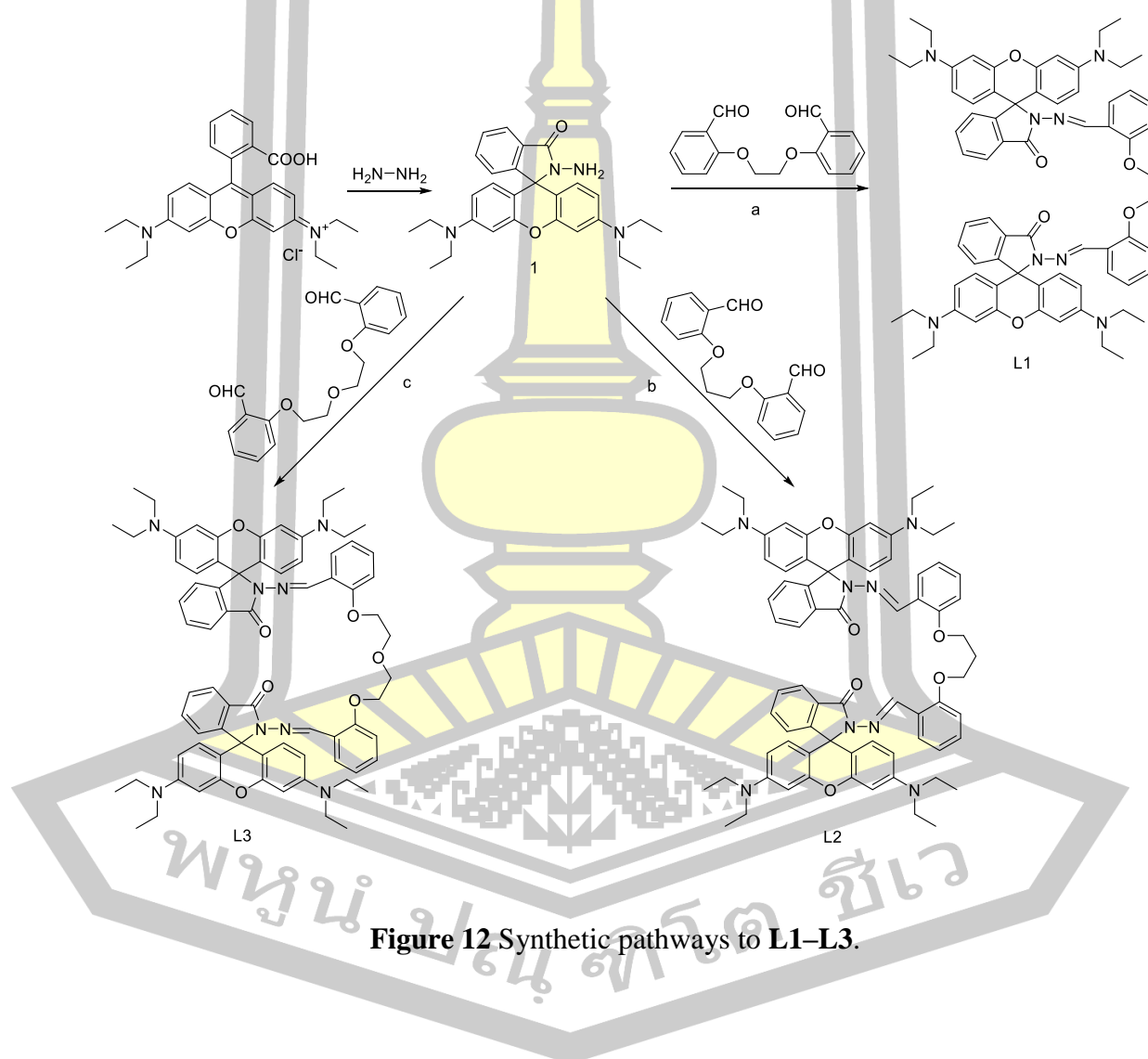


Figure 12 Synthetic pathways to **L1–L3**.

In 2015, Wang *et al.* designed and synthesized rhodamine derivative **L1** (figure 13) and its recognition mechanism for Hg^{2+} was studied using fluorescence spectroscopy in methanol–water solution. The results showed that **L1** was highly selective for recognizing Hg^{2+} , and that other metal ions did not interfere with this recognition. A good linear relationship was shown between the relative fluorescence intensity of **L1** and the concentration of Hg^{2+} within the range of 4–80 μM , with a detection limit of 0.19 μM . Job's plot method indicated 1:1 **L1**-to- Hg^{2+} stoichiometry in the complex. The mechanism of **L1** recognition for Hg^{2+} can be explained by the crystal structure of **L2**, which was the product of **L1** reacting with Hg^{2+} [33].

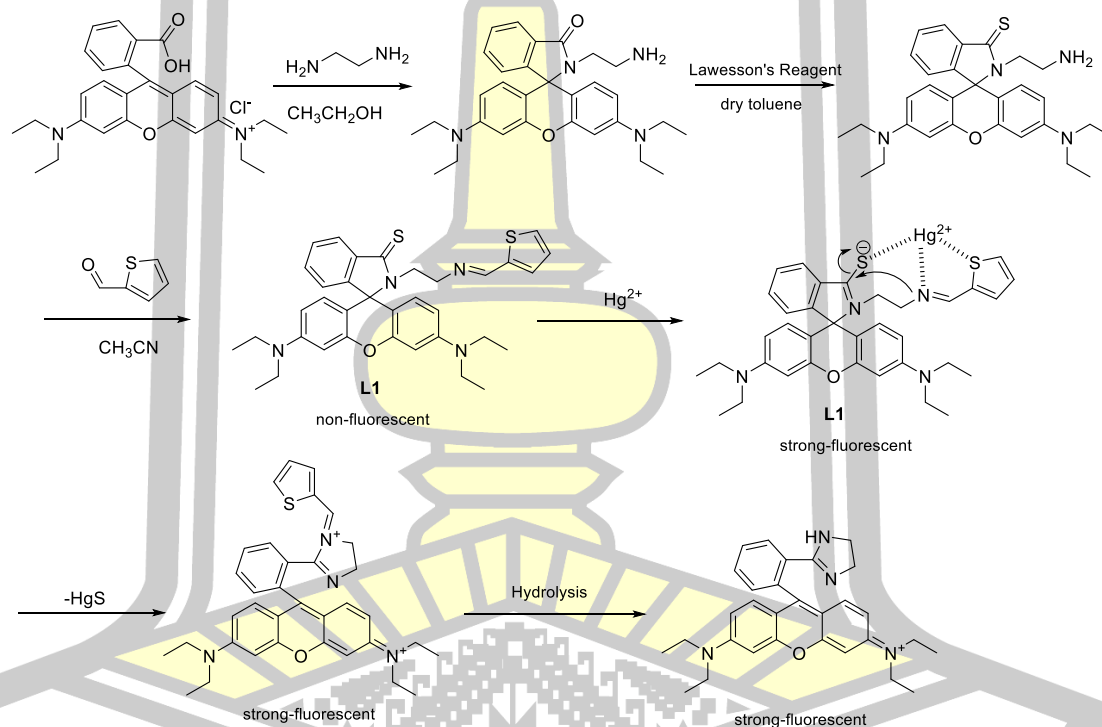


Figure 13 Synthetic route of rhodamine derivative.

In 2015, Shi *et al.* synthesized a rhodamine-based fluorescent probe **RC**, and then grafted it onto the surface of chitosan to demonstrate the first use of chitosan as the scaffolds for preparing novel functional adsorbent (figure 14). The resulting functional chitosan adsorbent not only showed both extraordinary adsorption capacity and super removal ability for Hg^{2+} , but also served as an excellent colorimetric and fluorescence turn-on “naked-eye” sensor for Hg^{2+} . The maximum adsorption rate was about 95%, which greatly exceed that of free chitosan under the same condition. Moreover, the adsorbent still exhibited very good adsorption performance after several regeneration cycles [34].

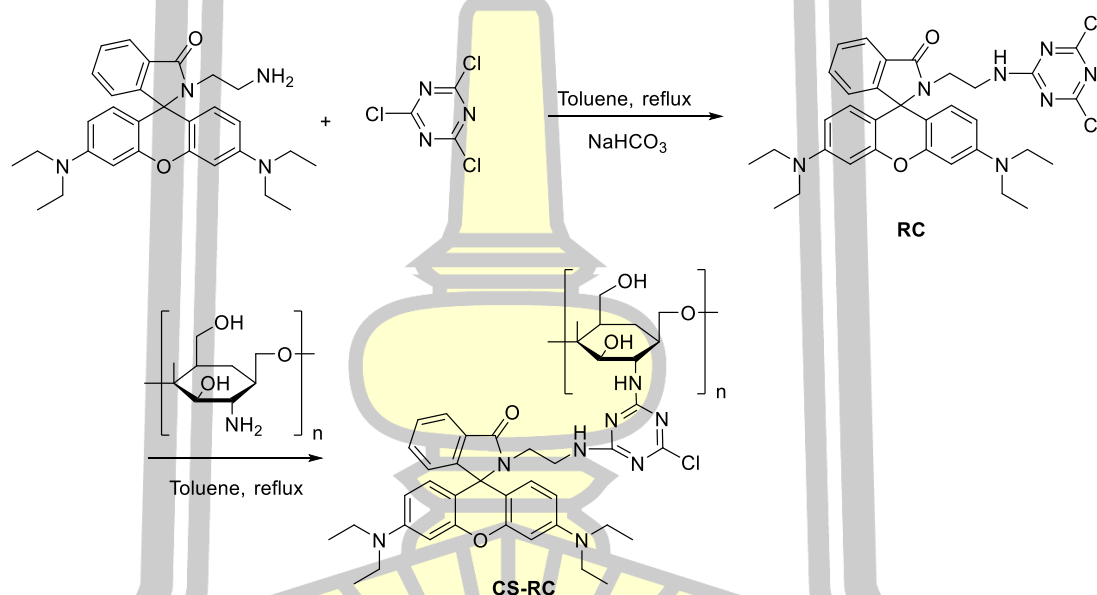


Figure 14 Synthesis procedures of **RC** and **CS-RC**.

In 2016, Jiao *et al.* presented the design, synthesis and photophysical property of a rhodamine B based fluorescence probe, which exhibited a sensitive and selective recognition towards mercury (II). The chemosensor **RA** (rhodamine-amide-derivative) contained a 5-aminoisophthalic acid diethyl ester and a rhodamine group, and the property of spiro lactone of this chemosensor **RA** was detected by X-ray crystal structure analyses. Chemosensor **RA** afforded turn-on fluorescence enhancement and displayed high brightness for Hg^{2+} , which led to the opening of

the spiro lactone ring and consequently caused the appearance of strong absorption at visible range, moreover, the obvious and characteristic color changed from colorless to pink was observed (figure 15). They envisioned that the chemosensor **RA** exhibited a considerable specificity with two mercury (II) ions which was attributed to the open of spiro lactone over other interference metal ions [35].

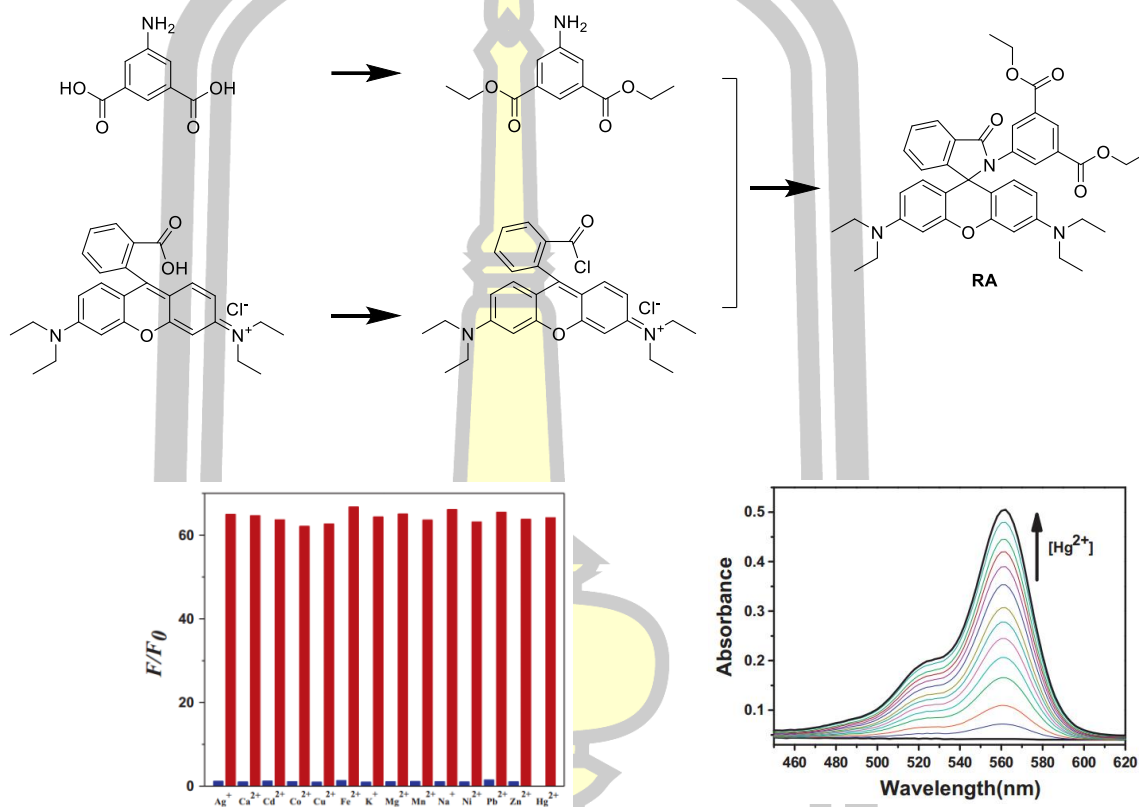


Figure 15 Synthesis and selective of **RA**.

In 2017, Parthiban *et al.* prepared a rhodamine B based chemosensor with diphenyl selenium (**RhoSe**) has been synthesized (figure 16), and its detection behavior towards various metal ions is studied via UV/Vis and fluorescence spectroscopy. The **RhoSe** showed a selective response to Hg^{2+} in CH_3OH/H_2O (v/v = 9:1) solutions over other metal ions. After addition of Hg^{2+} , the solution of **RhoSe** displayed an obvious color change from colorless to pink and a significant, 48-fold fluorescence enhancement. The color change and fluorescence enhancement were attributed to the ring-opening of the spiro lactam in the rhodamine fluorophore, which was induced by Hg^{2+} binding. The binding ratio of **RhoSe**- Hg^{2+} was determined by a

Job plot as a 1:1 ratio, and the effective pH range for Hg^{2+} detection was 4.0–10. Importantly, the reversibility of the **RhoSe**– Hg^{2+} complex was observed through the addition of Na_2S . For practical applications, the strip method was utilized to detect Hg^{2+} in water/methanol solution. In addition, confocal fluorescence microscopy experiments demonstrated that **RhoSe** is an effective fluorescent probe for Hg^{2+} detection in vitro and in vivo [36].

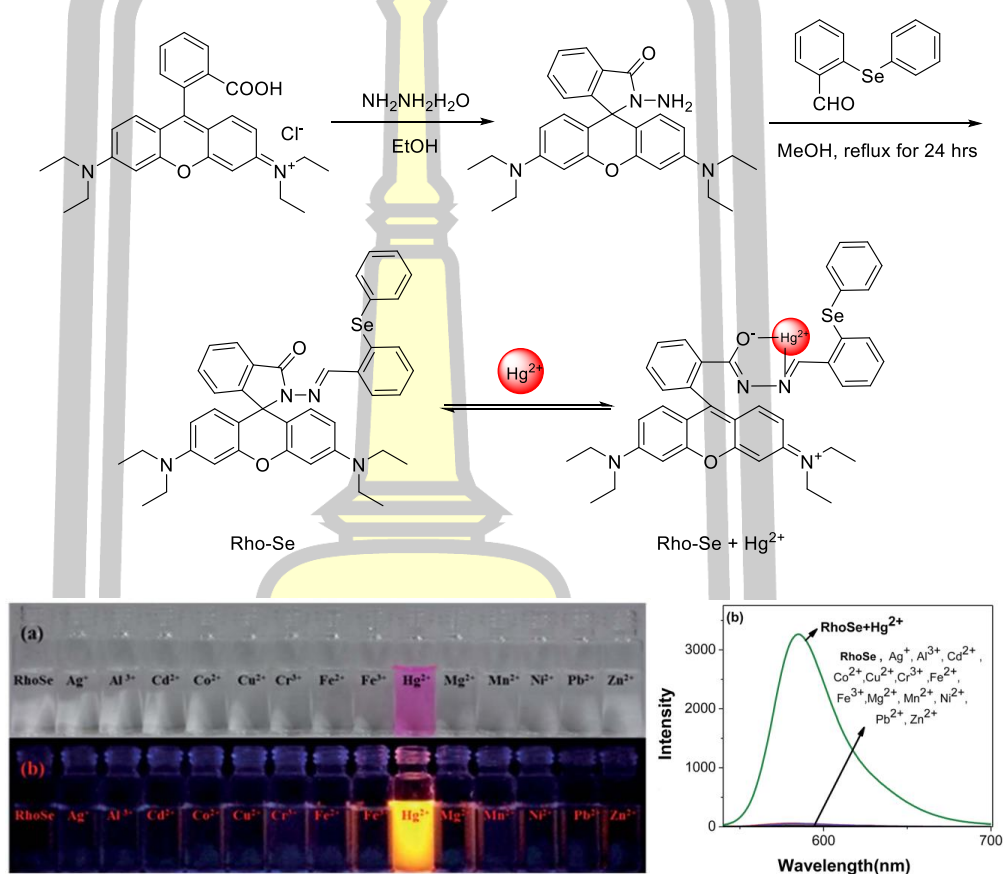


Figure 16 Synthesis and determination of **Rho-Se** with Hg^{2+} .

พหุ ประถมศึกษา

2.2 Fluorescence resonance energy transfer of rhodamine-dansyl

In 2008, Lee *et al.* synthesized a series of rhodamine B and dansyl fluorophores incorporated into a tren spacer and measured their optical properties upon the metal cations (figure 17). A series of new fluorescent probes bearing tren-spaced rhodamine B and dansyl groups have been synthesized. Compound of rhodamine B and dansyl exhibited selective changes in the absorption and the emission spectra toward Cu^{2+} ion over miscellaneous metal cations. Compound of rhodamine B and dansyl showed the best fluorescence resonance energy transfer (**FRET**) efficiency through dansyl emission to rhodamine absorption for the Cu^{2+} ion [37].

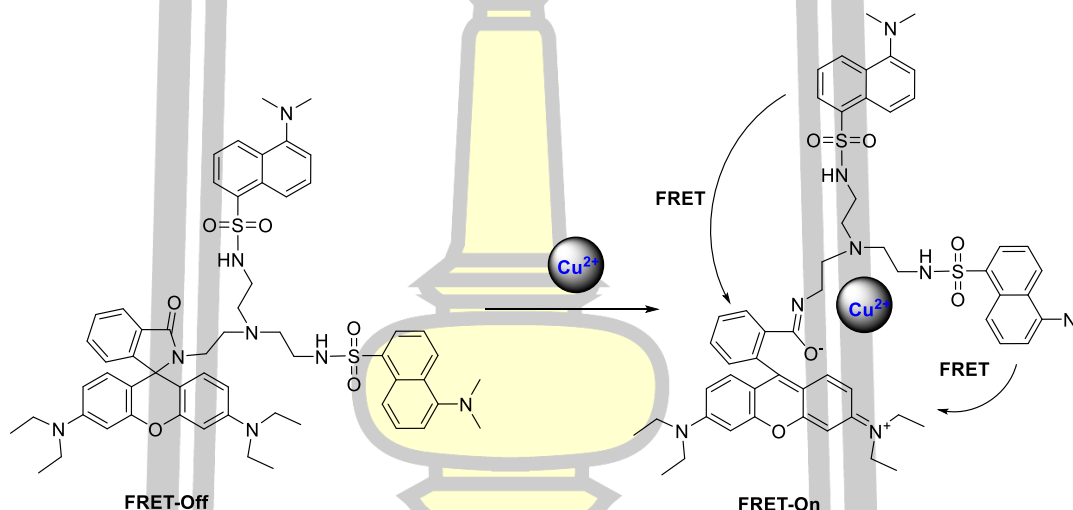


Figure 17 Cu^{2+} -induced FRET off-on along with visual color changes upon irradiation at 420 nm.

In 2014, Piao *et al.* synthesized rhodamine and dansyl moiety was developed for highly selective detection of Fe^{3+} based on **FRET** mechanism (figure 18). Binding of Fe^{3+} to the chemosensor induced spirolactam ring opening in the rhodamine moiety and subsequent off-on **FRET** from the dansyl energy donor to the rhodamine energy acceptor due to the spectral overlap between the emission of the dansyl moiety and the absorption of the ring opened rhodamine moiety. The success of off-on **FRET** from the dansyl energy donor to the rhodamine energy acceptor not only drastically reduced background signal by enlarging the pseudo-Stokes shift but also provided a good structural skeleton for designing Fe^{3+} chemosensor for more widely use. In

addition, the relatively high selectivity and sensitivity for Fe^{3+} over other metal ions showed the possibility for potential use in complex samples containing various competitive metal ions [28].

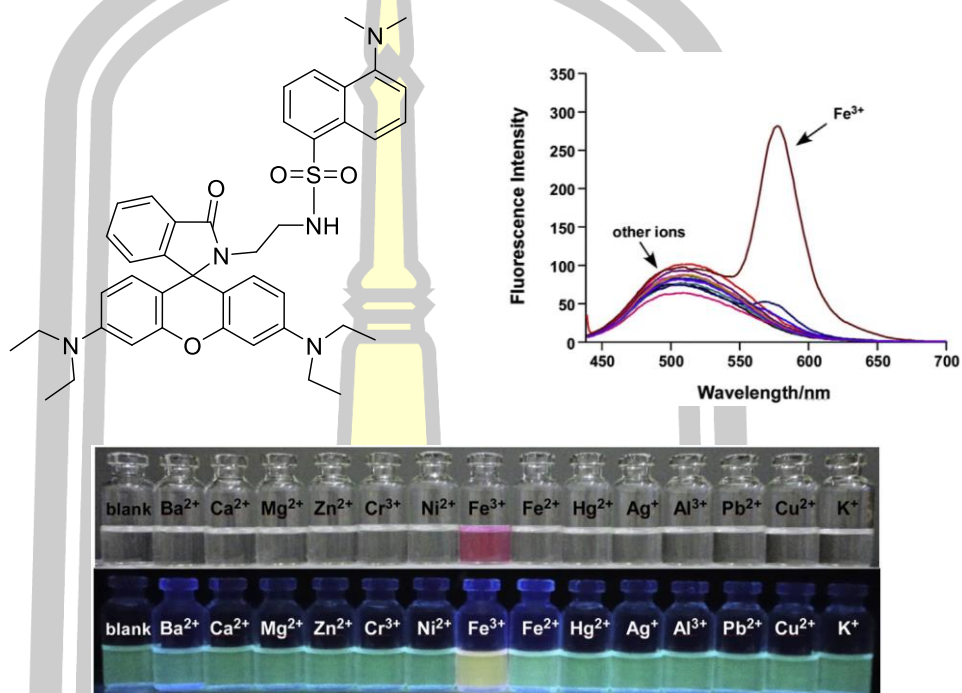


Figure 18 Structure, emission spectra and color change of chemo sensor up on addition of various metal ion in ethanol solution.

In 2015, Xie *et al.* synthesized dansyl-appended rhodamine 101 (rhodamine-dansyl) based FRET fluorescence probe which was developed as a ratiometric Hg^{2+} sensor (figure 19). A leuco-rhodamine derivative with unconjugated structures as fluorogenic and chromogenic sensors was chosen as a sensitive chemosensor for Hg^{2+} ions. This probe showed a fast, reversible and selective response toward Hg^{2+} in a wide pH range. The Hg^{2+} ion induced ring-opening reaction of the spirolactam rhodamine moiety of rhodamine-dansyl, leading to the formation of fluorescent derivatives that can serve as the FRET acceptors. Very large stokes shift (220 nm) was observed in this case. About 97-fold increase in fluorescence intensity ratio was observed upon its binding with Hg^{2+} [38].

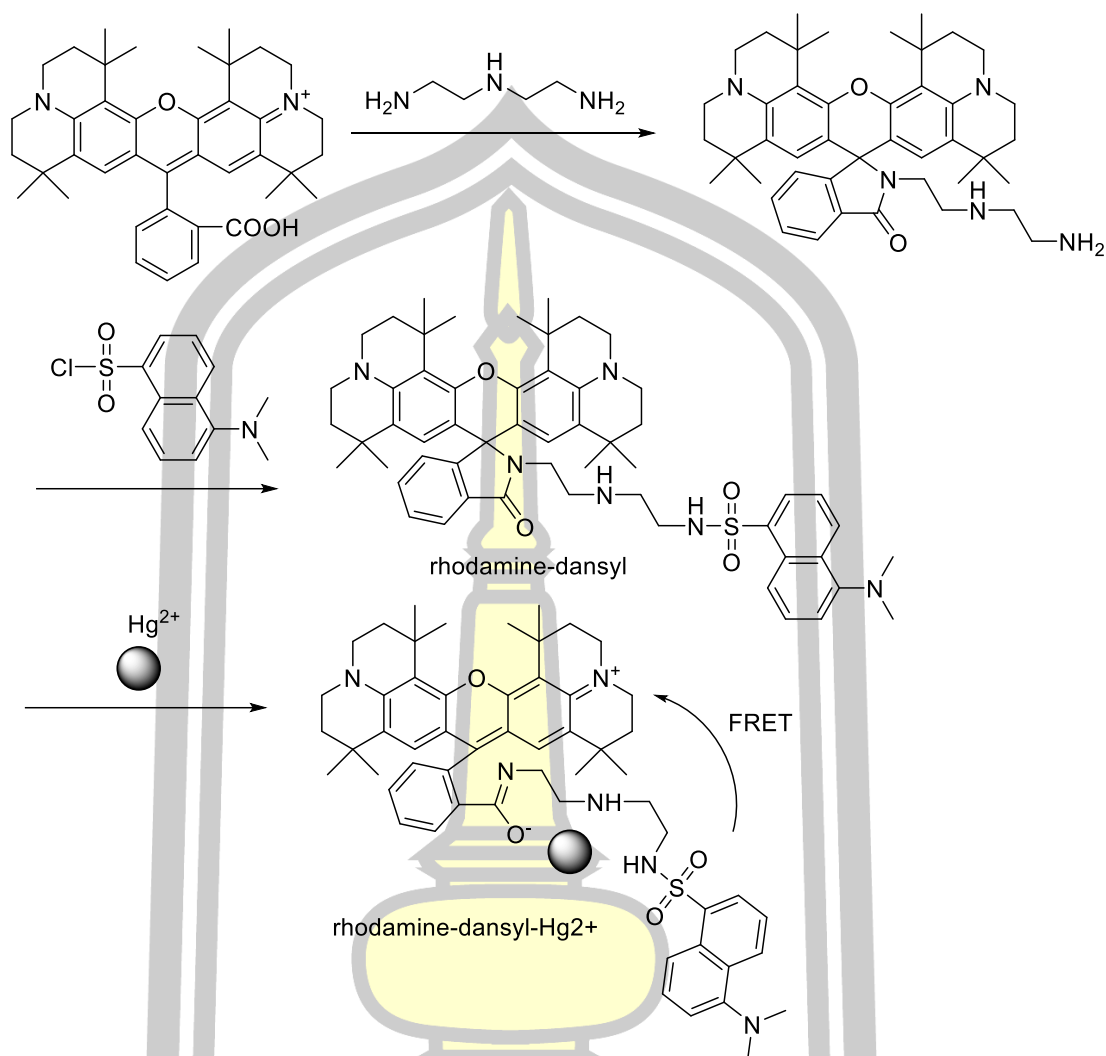


Figure 19 Synthetic route to rhodamine-dansyl and proposed mechanism for FRET of rhodamine-dansyl with Hg^{2+} .

In 2017, Yuan *et al.* synthesized dansyl-appended rhodamine B which was designed and synthesized for detection of Hg^{2+} and Cu^{2+} (figure 20). In MeCN/HEPES buffer solution, it gave a ratiometric fluorescent response to Hg^{2+} and a fluorescent quenched response to Cu^{2+} . Meanwhile, the probe gave colorimetric responses to Cu^{2+} and Hg^{2+} . The probe could selectively recognize and sense Hg^{2+} and Cu^{2+} from other common metal ions by showed unique fluorescence and absorption characteristics. In MeCN/HEPES buffer solution, the probe gave a ratiometric fluorescent response to Hg^{2+} , which was ascribed to the fluorescence resonance energy transfer from dansyl moiety to the ring-opened rhodamine B moiety, while the presence of Cu^{2+} causes fluorescence quenched. Beside the

fluorescence change, the presence of Cu^{2+} and Hg^{2+} could induce intensive absorption at about 555 nm, which resulted in a color change from colorless to pink [39].

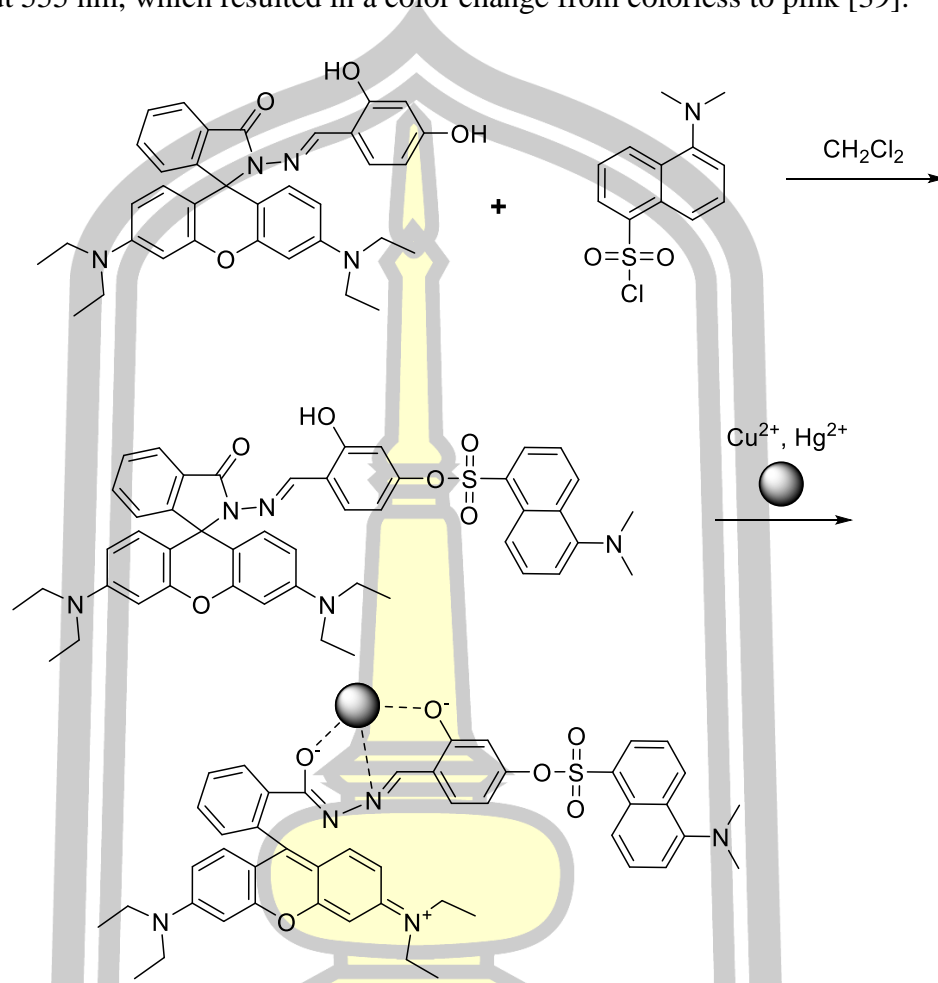


Figure 20 Synthesis and selectivity of dansyl-appended rhodamine B sensor.

2.3 Hydrogel

In 2007, Hashemi and Zarjani prepared by chemical immobilization of a mixture of two indicators of Neutral Red and Thionin (figure 21) on an agarose film coated glass slide (ACGS). For preparation of the sensor, the two dyes were immobilized on an epoxy activated agarose support and the effects of the coupling pH and the dyes ratio and concentrations were optimized. The sensor was mounted in a flow cell and successfully applied for on-line pH monitoring in a wide pH range of 0.5–12 with two linear calibration curve regions [40].

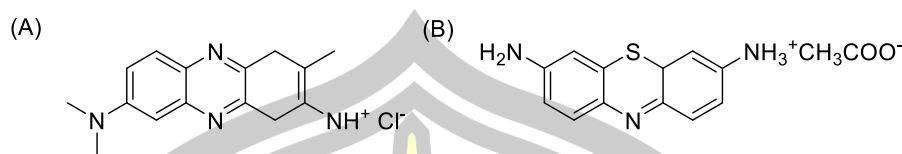


Figure 21 (A) structure of Neutral red, (B) structure of Thionin.

In 2008, Hashemi *et al.* prepared optical sensor for Cu²⁺ determination based on its complexation reaction with calmagite (figure 22). For this purpose, the stoichiometry and structure of the complex was carefully studied. A linear response curve was observed for the membrane sensor in Cu²⁺ concentration range of 0.4–200 $\mu\text{g L}^{-1}$ with an R^2 value of 0.997. The detection limit (3σ) of the method for Cu²⁺ was 0.07 $\mu\text{g L}^{-1}$. The influence of several potentially interfering ions on the determination of Cu²⁺ was studied and no significant interference was observed. The sensor showed a good durability and short response time with no evidence of reagent leaching. The dye was then immobilized on a transparent agarose membrane to be used as a selective membrane sensor for the spectrophotometric determination of Cu²⁺ in environmental water samples [41].

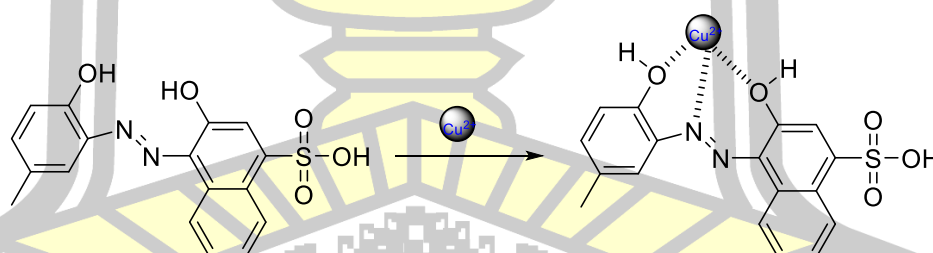


Figure 22 The structures of free calmagite and its 1:1 complex with Cu²⁺.

In 2011, Alizadeh *et al.* prepared optical sensor which was developed for the Hg²⁺ determination by chemical immobilization of 2-[(2 sulfanylphenyl) ethanimidoyl] phenol (**L**), on an agarose membrane (figure 23). Spectrophotometric studies of complex formation between the Schiff's base ligand **L** and Hg²⁺, Sr²⁺, Mn²⁺, Cu²⁺, Al³⁺, Cd²⁺, Zn²⁺, Co²⁺ and Ag⁺ in methanol solution indicated a substantially larger stability constant for the mercury ion complex. Consequently, the

Schiff's base **L** was used as an appropriate ionophore for the preparation of a selective Hg^{2+} optical sensor by its immobilization on a transparent agarose film. A distinct color change, from yellow to green-blue, was observed by contacting the sensing membrane with Hg^{2+} ions at pH 4.5. The effects of pH, ionophore concentration, ionic strength and reaction time on the immobilization of **L** were studied. A linear relationship was observed between the membrane absorbance at 650 nm and Hg^{2+} concentrations in the range from 1×10^{-2} to 1×10^{-5} mol L^{-1} with a detection limit of 1×10^{-6} mol L^{-1} . No significant interference from 100 times concentrations of a number of potentially interfering ions was detected for the mercury ion determination. The optical sensor was successfully applied to the determination of mercury in amalgam alloy and spiked water samples [42].

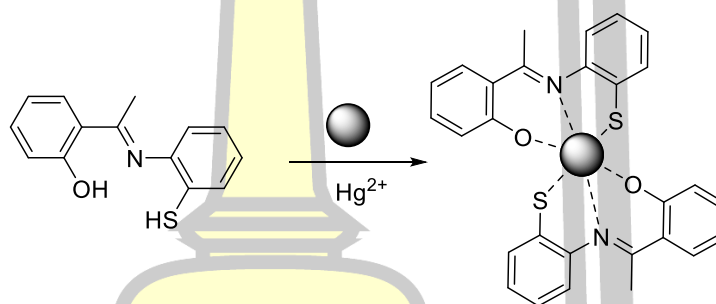


Figure 23 Optimized structures of free ligand and its 2:1 complex with Hg^{2+} ion.

In 2014, Zargoosh and Babadi prepared the covalent immobilization of dithizone on agarose membrane (figure 24). In addition to its high stability, reproducibility, and relatively long lifetime, the proposed optical sensor revealed good selectivity for target ions over a large number of alkali, alkaline earth, transition, and heavy metal ions. The proposed optical membrane displayed linear responses from 1.1×10^{-8} to 2.0×10^{-6} mol L^{-1} and 1.2×10^{-8} to 2.4×10^{-6} mol L^{-1} for Hg^{2+} and Pb^{2+} , respectively. The limits of detection (**LOD**) were 2×10^{-9} mol L^{-1} and 4×10^{-9} mol L^{-1} for Hg^{2+} and Pb^{2+} , respectively. The prepared optical membrane was successfully applied to the determination of Hg^{2+} and Pb^{2+} in industrial wastes, spiked tap water, and natural waters without any preconcentration step [2].

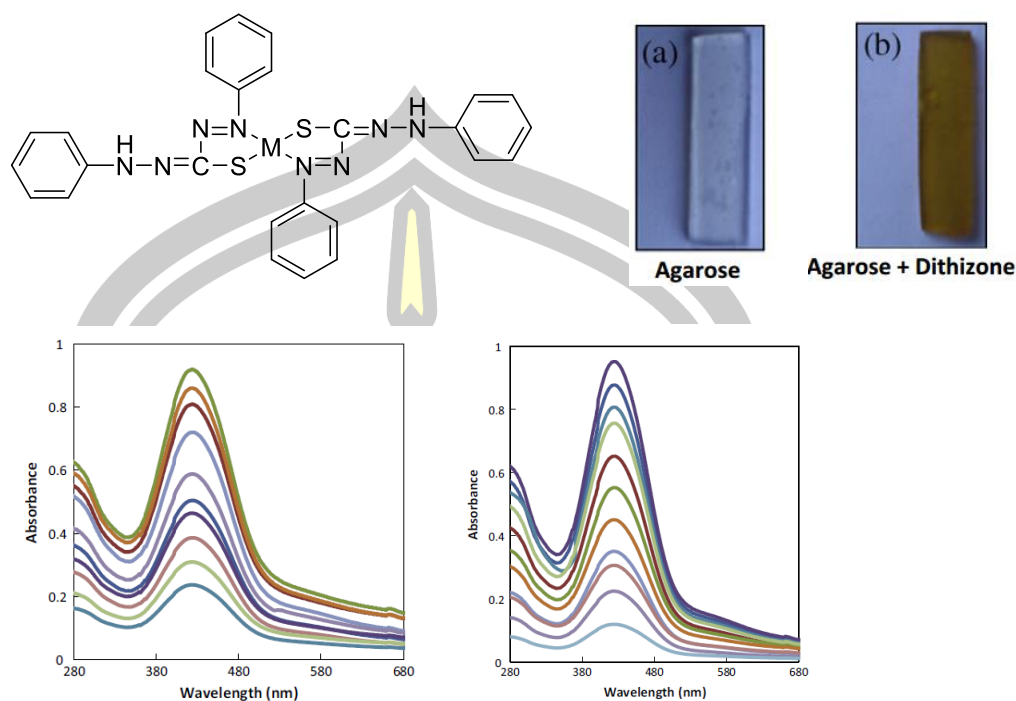


Figure 24 The structure of the dithizone complexes with metal and color change, absorbance spectra of the proposed optical sensor with metal ion.

In 2015, Gogoi *et al.* prepared chitosan based carbon dots rooted agarose hydrogel film (figure 25) as a hybrid solid sensing platform for detection of heavy metal ions. The fabrication of the solid sensing platform was centered on simple electrostatic interaction between the -NH_3^+ group presented in the carbon dots and the OH^- groups presented in agarose. Simply on dipping the hydrogel film strip into the heavy metal ion solution, in particular Cr^{6+} , Cu^{2+} , Fe^{3+} , Pb^{2+} , Mn^{2+} , the strip displayed a color change, viz., $\text{Cr}^{6+} \rightarrow$ yellow, $\text{Cu}^{2+} \rightarrow$ blue, $\text{Fe}^{3+} \rightarrow$ brown, $\text{Pb}^{2+} \rightarrow$ white, $\text{Mn}^{2+} \rightarrow$ tan brown. The optical detection limit of the respective metal ion was found to be 1 pM for Cr^{6+} , 0.5 μM for Cu^{2+} , and 0.5 nM for Fe^{3+} , Pb^{2+} , and Mn^{2+} by studying the changes in UV-visible reflectance spectrum of the hydrogel film. Moreover, the hydrogel film showed applicability as an efficient filtration membrane for separation of these quintet heavy metal ions. The strategic fundamental feature of this sensing platform was the successful capability of chitosan to form colored chelates with transition metals [1].

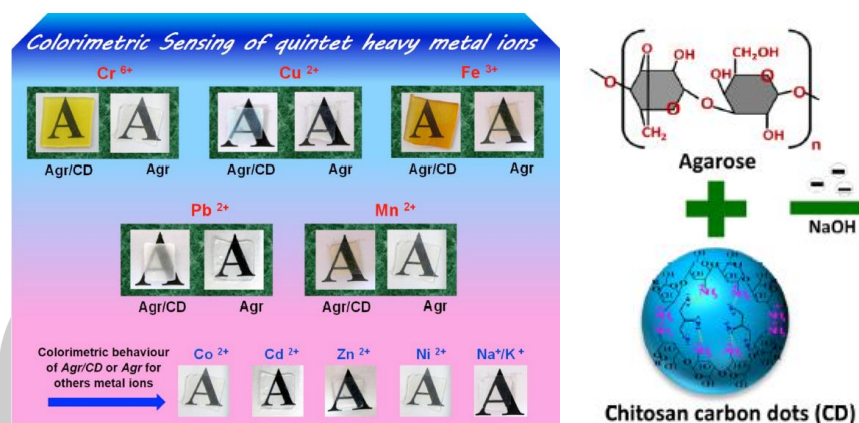


Figure 25 Photographs of colorimetric sensing test of heavy metal ions, exclusively Cr^{6+} , Cu^{2+} , Fe^{3+} , Pb^{2+} , and Mn^{2+} , when loaded into the hydrogel films Agr/CD and Agr. And pictorial representation of fabrication of agarose/CD (Agr/CD) Hydrogel Film.

In 2016, Serenjah *et al.* prepared immobilization of arsenazo III on an epoxy-activated agarose membrane support (figure 26). The optical properties of the agarose–arsenazo III membrane were carefully studied and a new selective and sensitive optical sensor for uranyl ion determination in water samples was introduced. The immobilization conditions were optimized and the prepared optical sensor showed a distinct color change from purple to dark violet upon increasing the analyte concentration in a buffered solution at pH 2. The optical sensor was successfully applied to the determination of UO_2^{2+} in spiked water samples [43].

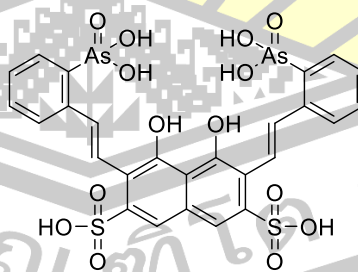


Figure 26 Structure of arsenazo III.

In 2016, Heydari *et al.* prepared of a new optical pH sensor with a suitable working range. The response change range of orange (II) indicator with pH was enhanced using covalent immobilization of this pH indicator on the agarose membrane (figure 27). For the first time, immobilized orange (II) on agarose membrane was applied as a pH optical sensor. The behavior of this optical sensor was monitored at different pHs. Factors affecting the performance of the sensor, such as pH of dye bonding to agarose membrane, dye concentration, ionic strength, reversibility, response time and storage time, have been investigated and optimized [44].

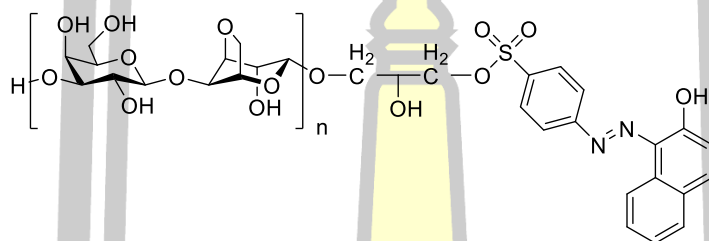
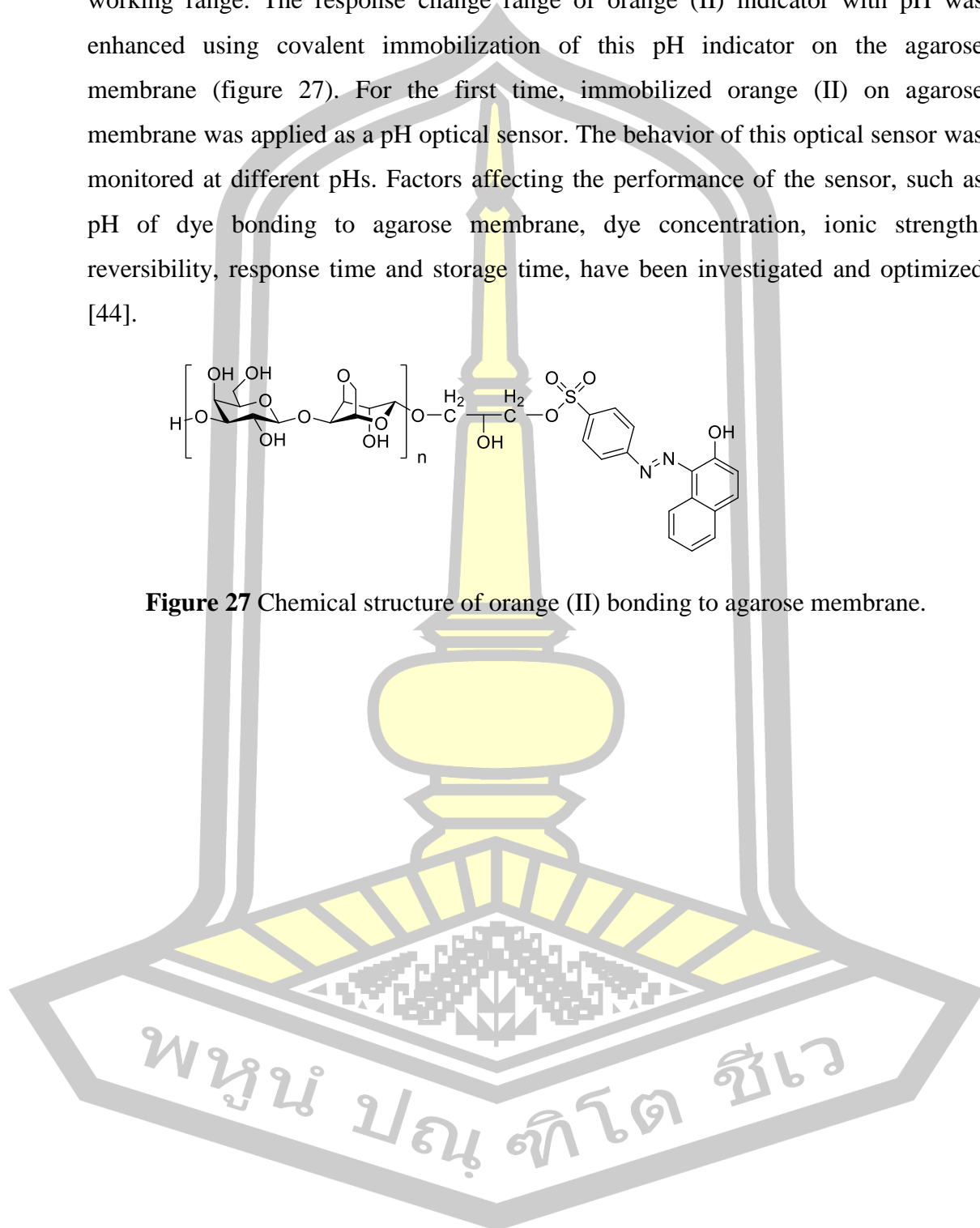


Figure 27 Chemical structure of orange (II) bonding to agarose membrane.



CHAPTER III

MATERIALS AND METHODS

3.1 Experimental

3.1.1 Reagents

All reagents were standard analytical grade. Rhodamine B, agarose (quality of analytical and preparative electrophoresis), tetrahydrofuran, sodium hydroxide were purchased from Sigma-Aldrich and CARLO ERBA. Dansyl chloride, Sodium nitrate (NaNO_3), potassium nitrate (KNO_3), silver nitrate ($\text{AgNO}_3 \cdot 9\text{H}_2\text{O}$), magnesium nitrate ($\text{Mg}(\text{NO}_3)_2 \cdot 6\text{H}_2\text{O}$), calcium nitrate ($\text{Ca}(\text{NO}_3)_2 \cdot 4\text{H}_2\text{O}$), Lead nitrate ($\text{Pb}(\text{NO}_3)_2$), cobalt nitrate ($\text{Co}(\text{NO}_3)_2 \cdot 6\text{H}_2\text{O}$), nickel nitrate ($\text{Ni}(\text{NO}_3)_2 \cdot 6\text{H}_2\text{O}$), copper nitrate ($\text{Cu}(\text{NO}_3)_2 \cdot 6\text{H}_2\text{O}$), zinc chloride (ZnCl_2), cadmium nitrate ($\text{Cd}(\text{NO}_3)_2 \cdot 4\text{H}_2\text{O}$), mercury nitrate ($\text{Hg}(\text{NO}_3)_2 \cdot \text{H}_2\text{O}$), aluminum nitrate ($\text{Al}(\text{NO}_3)_3 \cdot 6\text{H}_2\text{O}$), chromium chloride ($\text{CrCl}_3 \cdot 6\text{H}_2\text{O}$), iron chloride ($\text{FeCl}_3 \cdot 6\text{H}_2\text{O}$), gold chloride (AuCl_3), platinum chloride (K_2PtCl_4), ruthenium chloride ($\text{RuCl}_3 \cdot \text{H}_2\text{O}$) were purchased from Merck and Sigma-Aldrich.

3.1.2 Apparatus

Characterization of hydrogel+Rhodamine and hydrogel+rhodamine-dansyl were investigated by many technique. UV-vis absorption measurements were performed on a Perkin Elmer Lambda 25 UV/VIS spectrometer, Attenuated total reflectance Fourier transform infrared spectroscopy (ATR-FTIR) (Tensor 27, Bruker), scanning electron microscope (SEM) (LEO 01455VP, Cambridge, England) and Thermogravimetric analysis (TGA) was carried out using TA instruments, SDT Q600. Composition of hybrid materials were investigated by X-Ray Diffraction Analysis (XRD) advance d8 bruker.

3.2 Synthesize agarose hydrogel (Agr-RhoL)

3.2.1 Preparation of the rhodamine lactone (colorless L-form, RhoL)

Rhodamine lactone B (**RhoL**) was prepared by our modified method [26]. Briefly, 1.82 mL of 1.1×10^{-3} M rhodamine B, 1 mL of 3 N NaOH, 3.18 mL of distilled water and 4 mL of tetrahydrofuran were mixed and then agitated for 2 days. The resulting colorless of rhodamine lactone B (**RhoL**) solution (figure 28). Which represents close Spiro lactone ring of rhodamine B. UV-visible spectrum exhibited an absorbance peak at around 300 nm, namely $\pi - \pi^*$, $n - \pi^*$ which was a characteristic of rhodamine B. In the case of agarose hydrogel, no absorption peak was observed around 300 nm.

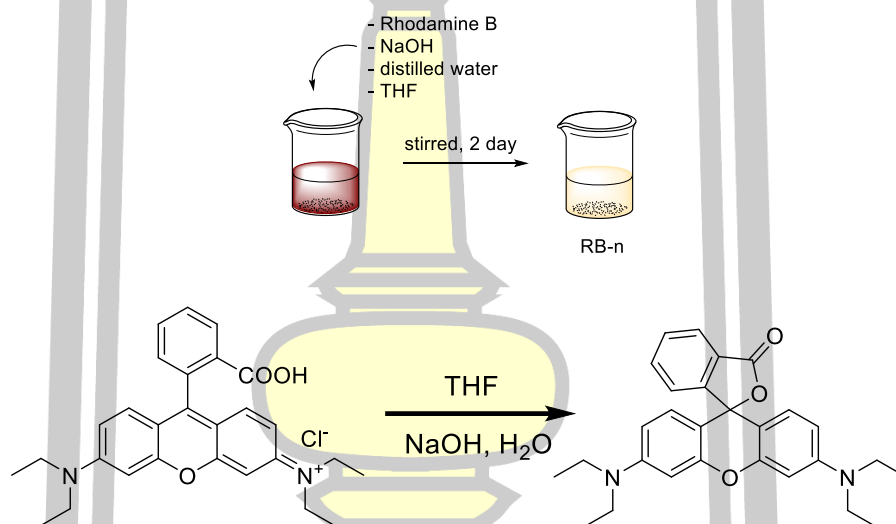


Figure 28 Preparation of rhodamine B (**RhoL-n**).

3.2.2 Immobilization of rhodamine lactone (RhoL) to agarose hydrogel (Arg-RhoL)

Rhodamine B hydrogel was prepared using modified optimal conditions from previous work [1]. Briefly, dissolving 0.4 g of agarose powder in 10 mL of rhodamine B (**RhoL**) solution followed by boiling in microwave for 30 s. Film casting was done by pouring the above solution into a petri dish and cooling to room temperature for about 1 day (figure 29). The pH of **Arg-RhoL** was adjusted by washing with water until pH 7 was reached and then dried at room temperature for 1 day. UV-visible spectrum exhibited an absorbance peak at around 300 nm, namely $\pi - \pi^*$, $n - \pi^*$ which

was a characteristic of Rhodamine B. In the case of agarose hydrogel, no absorption peak was observed around 300 nm.

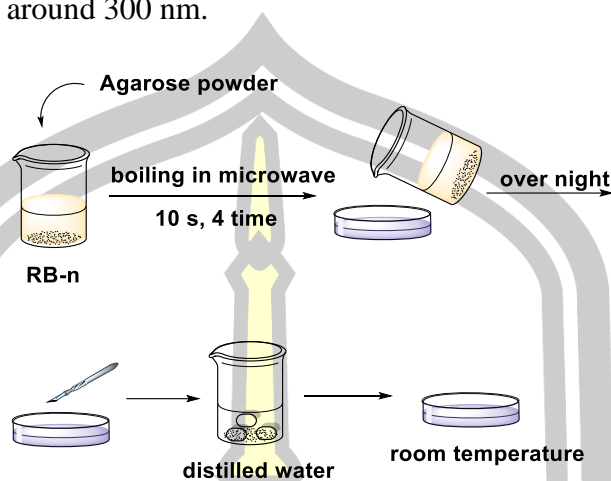


Figure 29 Preparation of **Agr-RhoL**.

3.2.3 Sensor response studies of Arg-RhoL

A 1 cm × 3 cm piece of the **Arg-RhoL** was immersed in 3 mL of 10^{-5} M each metal ion solution (Na^+ , K^+ , Ag^+ , Mg^{2+} , Ca^{2+} , Pb^{2+} , Co^{2+} , Ni^{2+} , Cu^{2+} , Zn^{2+} , Cd^{2+} , Hg^{2+} , Al^{3+} , Cr^{3+} , Fe^{3+} , Au^{3+} , Pt^{2+} and Ru^{3+}), then dried overnight at room temperature and **Arg-RhoL-M⁺** were investigated by many technique. UV-vis spectroscopy, Attenuated total reflectance Fourier transform infrared spectroscopy (ATR-FTIR), scanning electron microscope (SEM), Thermogravimetric analysis (TGA). And the composition of hybrid materials were investigated by X-Ray Diffraction Analysis (XRD).

3.3 Synthesize rhodamine derivative and dansyl chloride immobilized agarose hydrogel (**AAgr-RhoL+DNS**, **Agr-RhoL-DNS**)

3.3.1 Synthesize rhodamine ethylenediamine

Rhodamine B (0.20 g, 0.42 mmol) was dissolved in 30 mL of ethanol, and diethylenetriamine (0.22 mL, excess) were added dropwise to the solution and refluxed overnight (24 h) until the solution lost its red (figure 30). The solvent was removed by evaporation. Water (20 mL) was added to the residue and the solution was extracted with CH_2Cl_2 (20 mL × 2). The combined organic phase was washed twice with water and dried over anhydrous Na_2SO_4 . The solvent was removed by

evaporation. The crude product of rhodamine ethylenediamine was purified by column chromatography (dichloromethane/methanol/triethylamine 9:1:0.05) [45]. ^1H NMR (400 MHz, CDCl_3) δ 7.86–7.81 (m, 1H, ArH), 7.45–7.32 (m, 2H, ArH), 7.08–7.03 (m, 1H, ArH), 6.42 (s, 1H, ArH), 6.39 (s, 1H, ArH) 6.37 (s, 2H, ArH), 6.38–6.21 (m, 2H, ArH), 3.32 (q, $J = 6.8$ Hz, 8H, NCH_2CH_3), 3.12 (t, $J = 6.8$ Hz, 2H, NCH_2CH_2), 2.23 (t, $J = 6.8$ Hz, 2H, $\text{NCH}_2\text{CH}_2\text{NH}_2$), 2.05 (s, 2H, $\text{CH}_2\text{CH}_2\text{NH}_2$) and 1.16 (t, $J = 7.2$ Hz, 12H, NCH_2CH_3) and IR spectrum (ATR, ν , cm^{-1}): 628, 703, 763, 785, 813, 1018, 1077, 1117, 1150, 1219, 1287, 1300, 1330, 1352, 1378, 1427, 1466, 1513, 1545, 1614, 1683, 1879, 2015, 2047, 2164, 2872, 2893, 2928, 2968.

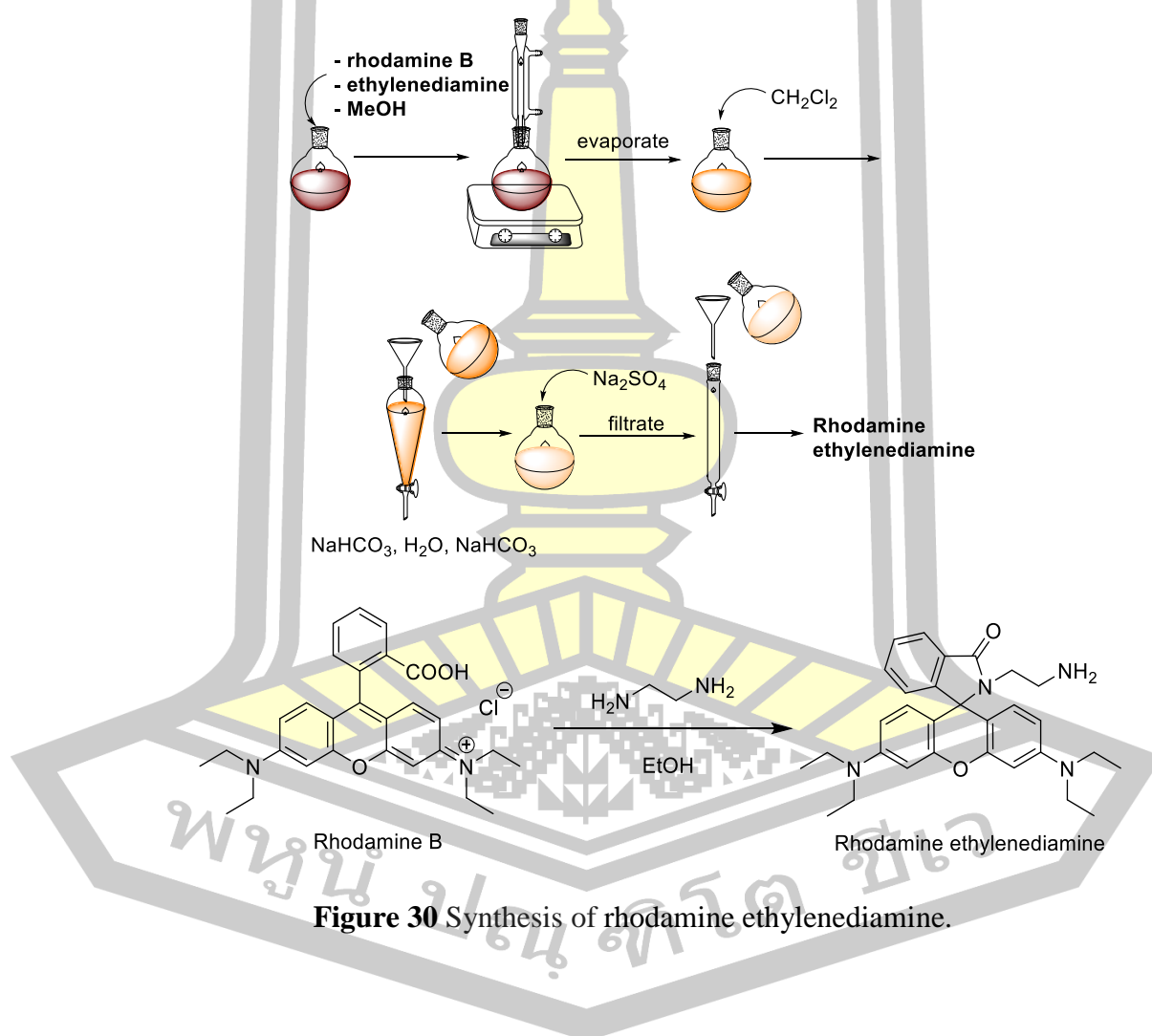
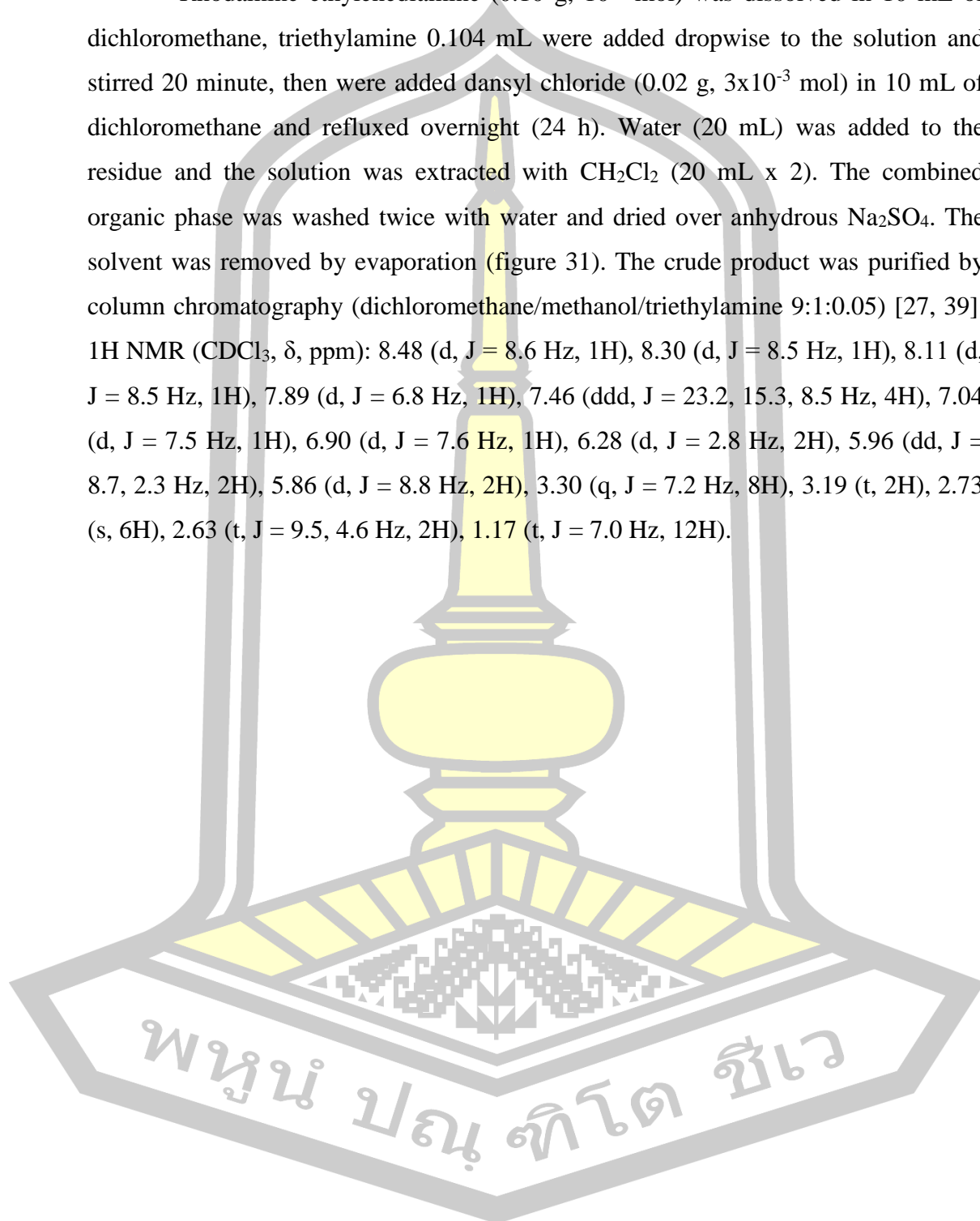


Figure 30 Synthesis of rhodamine ethylenediamine.

3.3.2 Synthesize rhodamine-dansyl

Rhodamine ethylenediamine (0.10 g, 10^{-3} mol) was dissolved in 10 mL of dichloromethane, triethylamine 0.104 mL were added dropwise to the solution and stirred 20 minute, then were added dansyl chloride (0.02 g, 3×10^{-3} mol) in 10 mL of dichloromethane and refluxed overnight (24 h). Water (20 mL) was added to the residue and the solution was extracted with CH_2Cl_2 (20 mL x 2). The combined organic phase was washed twice with water and dried over anhydrous Na_2SO_4 . The solvent was removed by evaporation (figure 31). The crude product was purified by column chromatography (dichloromethane/methanol/triethylamine 9:1:0.05) [27, 39]. ^1H NMR (CDCl_3 , δ , ppm): 8.48 (d, $J = 8.6$ Hz, 1H), 8.30 (d, $J = 8.5$ Hz, 1H), 8.11 (d, $J = 8.5$ Hz, 1H), 7.89 (d, $J = 6.8$ Hz, 1H), 7.46 (ddd, $J = 23.2, 15.3, 8.5$ Hz, 4H), 7.04 (d, $J = 7.5$ Hz, 1H), 6.90 (d, $J = 7.6$ Hz, 1H), 6.28 (d, $J = 2.8$ Hz, 2H), 5.96 (dd, $J = 8.7, 2.3$ Hz, 2H), 5.86 (d, $J = 8.8$ Hz, 2H), 3.30 (q, $J = 7.2$ Hz, 8H), 3.19 (t, 2H), 2.73 (s, 6H), 2.63 (t, $J = 9.5, 4.6$ Hz, 2H), 1.17 (t, $J = 7.0$ Hz, 12H).



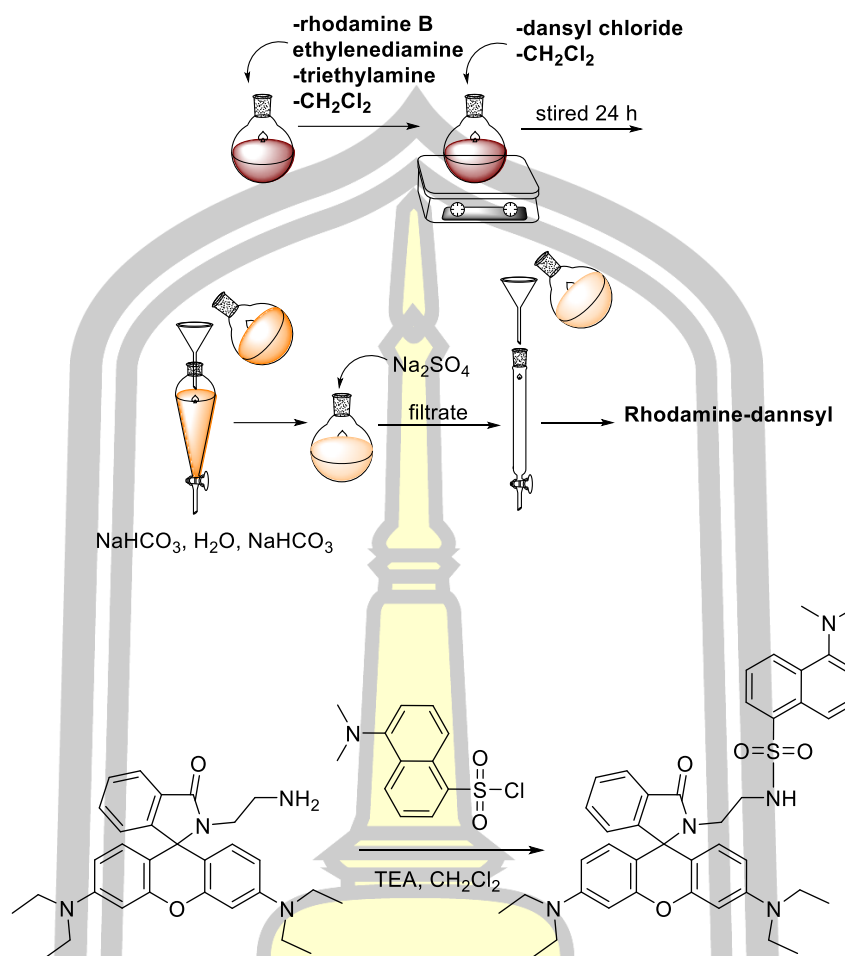


Figure 31 Synthesis of rhodamine-dansyl.

3.3.3 Immobilization of rhodamine and dansyl chloride to agarose hydrogel

3.3.3.1 Activation of agarose hydrogel

Dissolving 0.4 g of agarose powder in 10 mL of distilled water followed by boiling in microwave for 30 s, film casting was done by pouring the above solution into a petri dish and cooling to room temperature for about 1 h and stored in distilled water at overnight (1x1 cm) [1]. The agarose gel (1x1 cm) were added 25 mL of 2 mol L⁻¹ sodium hydroxide and 3.2 mL epichlorohydrine solution. The mixture was heated to 40°C in a incubator for 36 h. After cooling, the epoxy-activated membranes were thoroughly washed with distilled water and stored in water at 4°C (figure 32) [46].

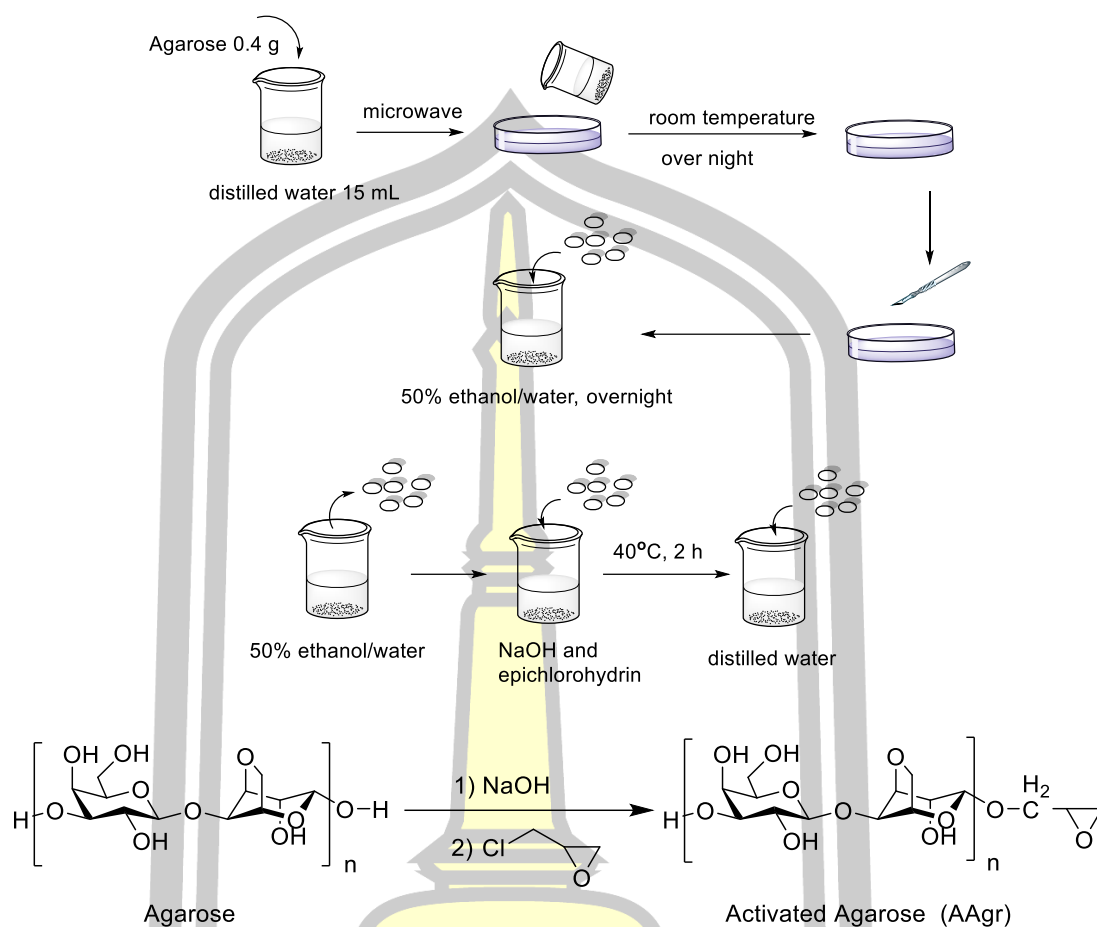


Figure 32 Activation of agarose gel membranes.

3.3.3.2 Immobilization of rhodamine and dansyl chloride

The activated gel were dried and transferred into a beaker containing an 25 mL solution of 10^{-3} mol L⁻¹ rhodamine ethylenediamine in ethanol. Then incubated 40°C and shook for 36 h the immobilization agarose gel and transferred into a beaker containing an 25 mL solution of 10^{-3} mol L⁻¹ dansyl chloride in 3 solvent, such as MeOH, DMF and DMSO. Then incubated at 40°C and shook for 36 h after that, it was washed with distilled water and stored in distilled water at 4°C [18]. UV-visible spectrum exhibited absorbance peak at around 400 nm, namely $\pi - \pi^*$, $n - \pi^*$ which was a characteristic of dansyl group (figure 33) [47].

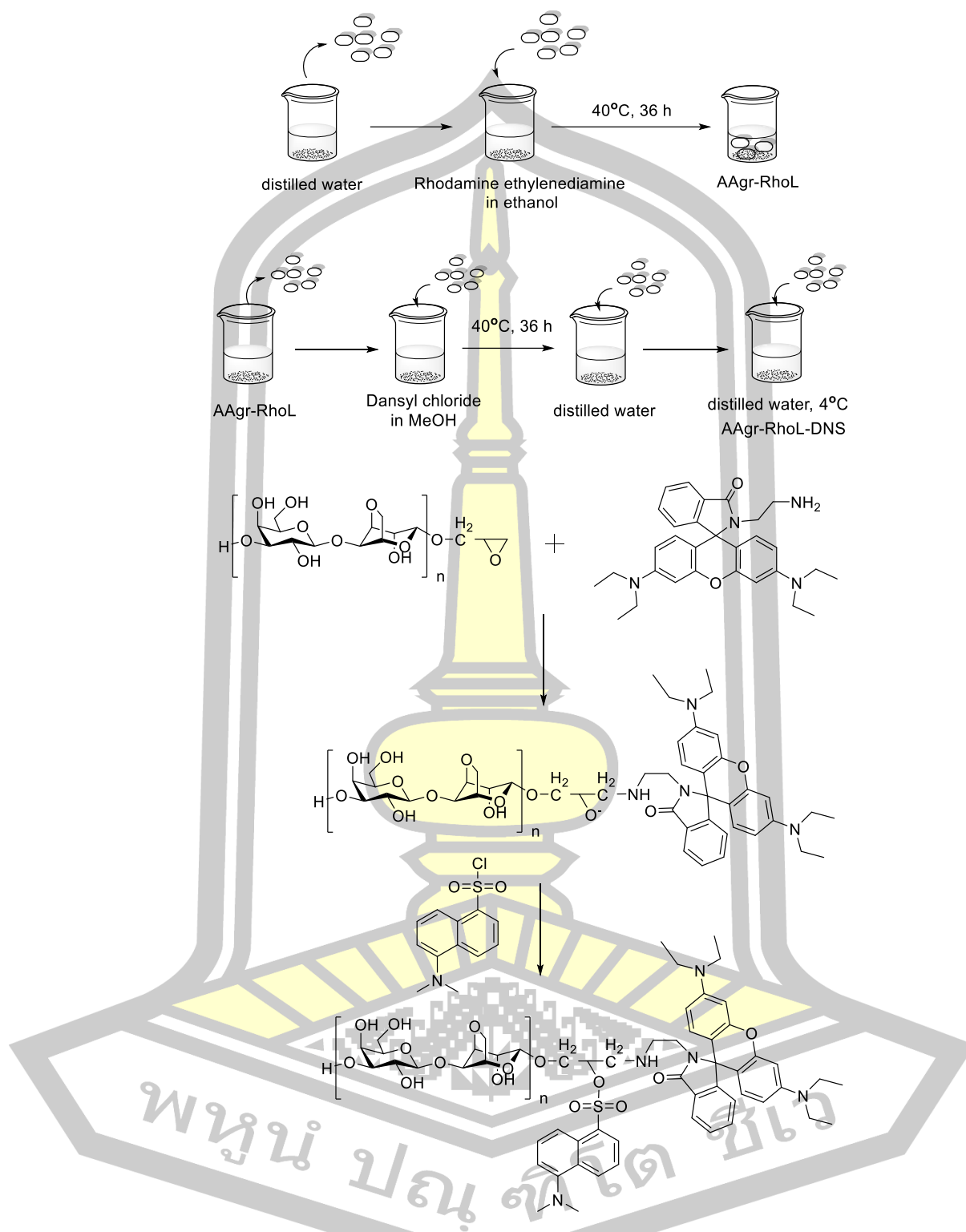


Figure 33 Immobilization of rhodamine derivative and dansyl chloride to agarose hydrogel.

3.3.4 Immobilization of rhodamine and dansyl chloride to agarose powder

3.3.4.1 Activation of agarose powder

Dissolving 0.4 g of suction dried agarose powder in 22 mL of distilled water and 1.6 mL of 2 mol L⁻¹ then added 1.2 mL of epichlorohydrin. The mixture was heated to 40°C in a incubator for 36 h. After cooling, the epoxy-activated membranes were thoroughly washed with distilled water and dried in room temperature (figure 34) [46].

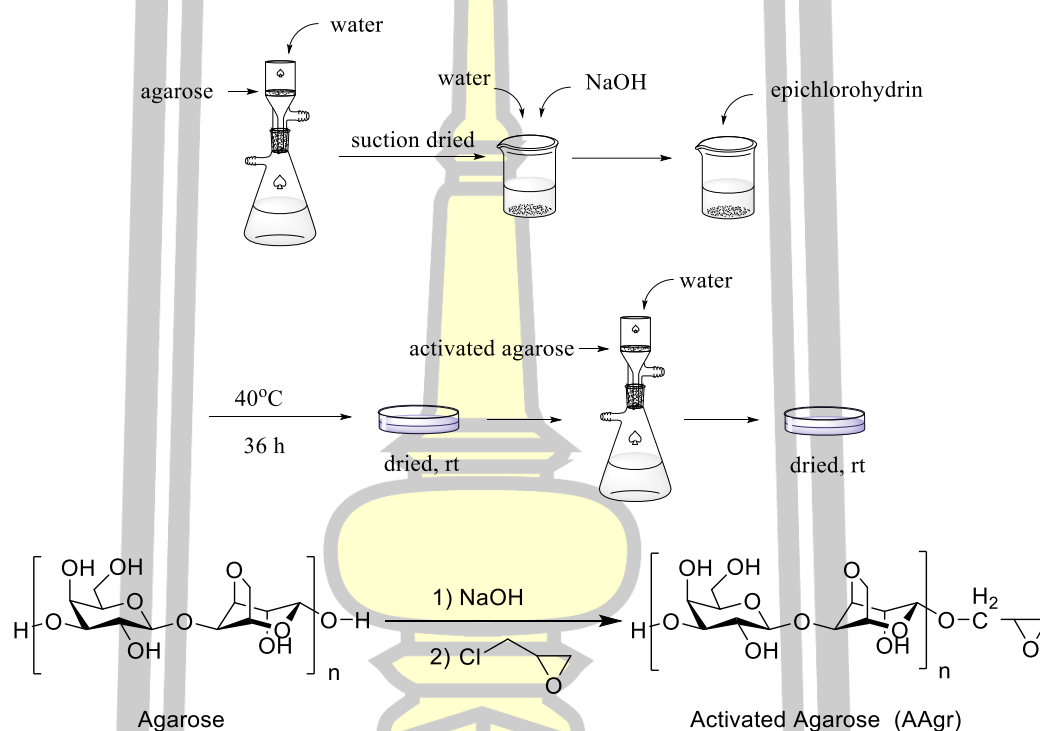
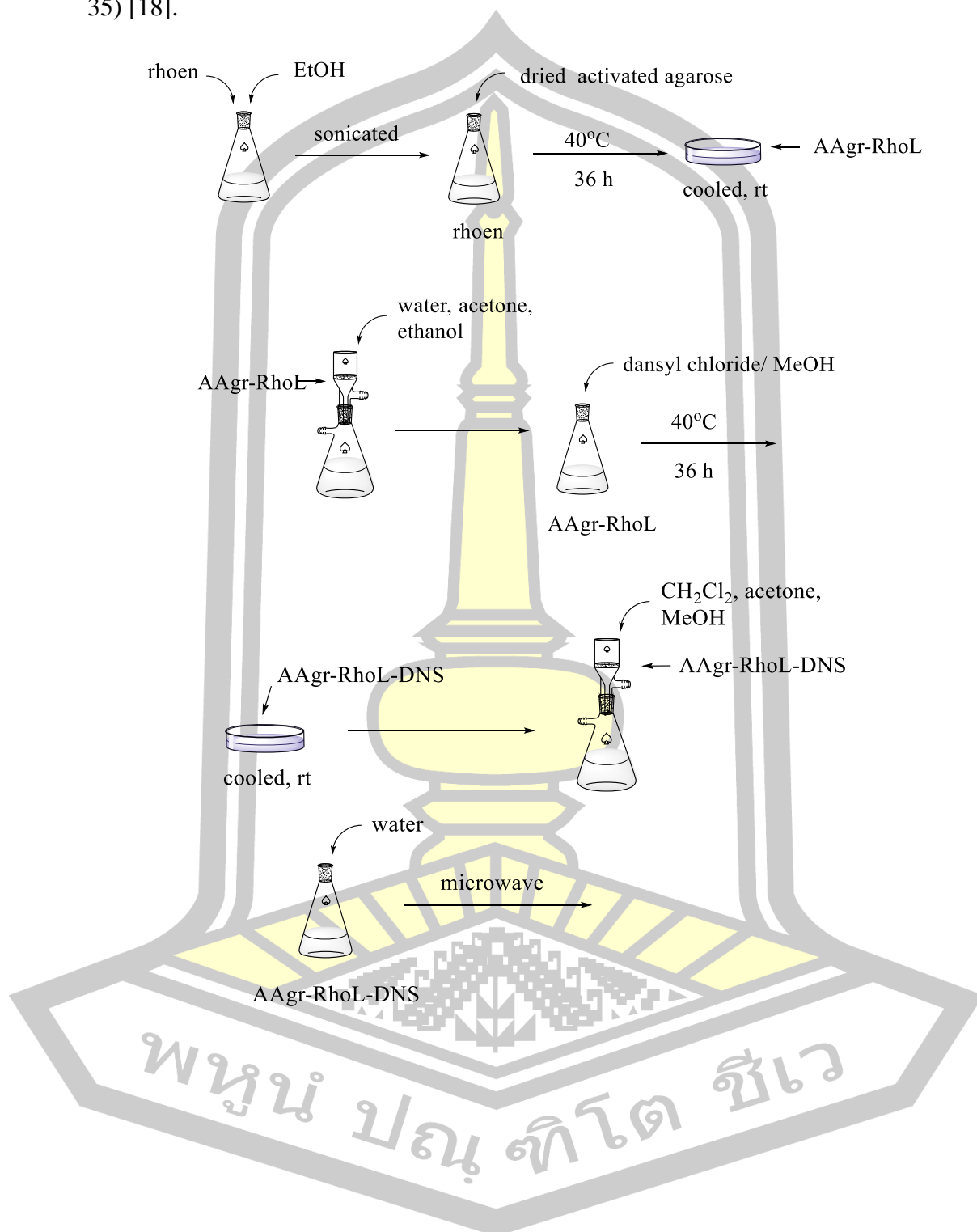


Figure 34 Activation of agarose powder.

3.3.4.2 Immobilization rhodamine and dansyl chloride

The activated powder was suction dried and transferred into a beaker containing an 20 mL solution of 10⁻² mol L⁻¹ rhodamine ethylenediamine in ethanol. Then incubated 40°C and shook for 36 h the immobilization agarose gel and transferred suction dried powder into a beaker containing an 20 mL solution of 4x10⁻³ mol L⁻¹ dansyl chloride in methanol. Then incubated 40°C and shook for 36 h after that, it was washed with methanol and dried in room temperature. The mixture was

dissolved in distilled water and then heated in microwave for hydrogel sensor (figure 35) [18].



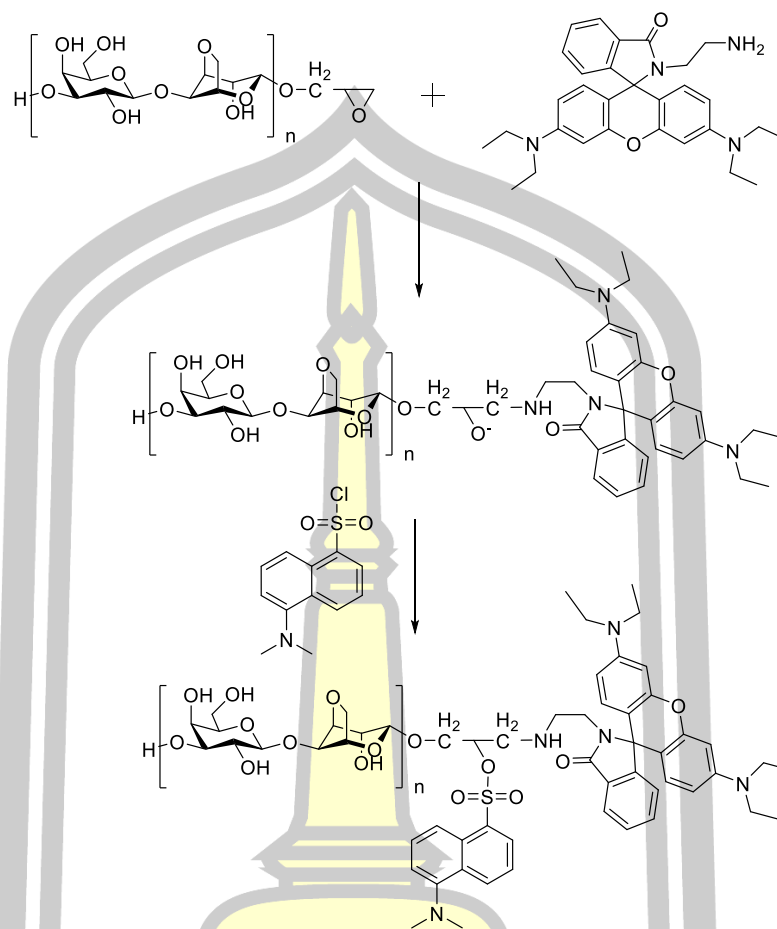


Figure 35 Immobilization of rhodamine derivative and dansyl chloride to agarose powder.

3.3.5 Immobilization of rhodamine-dansyl

The agarose hydrogels (figure 36) were dried and transferred into a beaker containing an 25 mL solution of 10^{-3} mol L⁻¹ rhodamine-dansyl in ethyl acetate. Then incubated 40°C and shook for 36 h after that, it was washed with distilled water and stored in distilled water at 4°C (figure 37) [18]. UV-visible spectrum exhibited absorbance peak at around 400 nm, namely $\pi - \pi^*$, $n - \pi^*$ which was a characteristic of dansyl group [47].

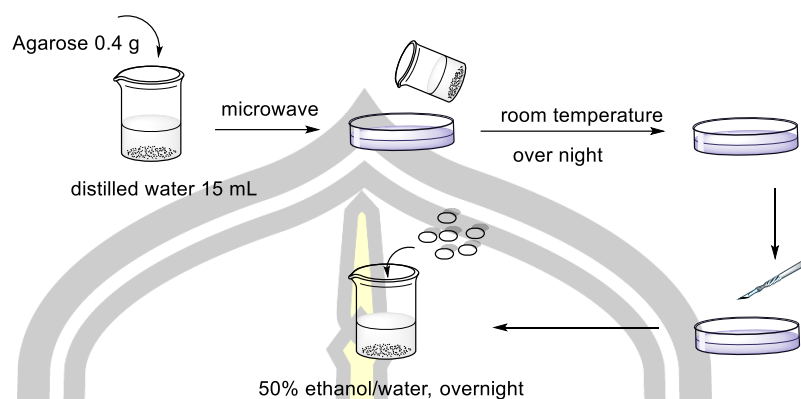


Figure 36 Preparation of agarose gel membranes.

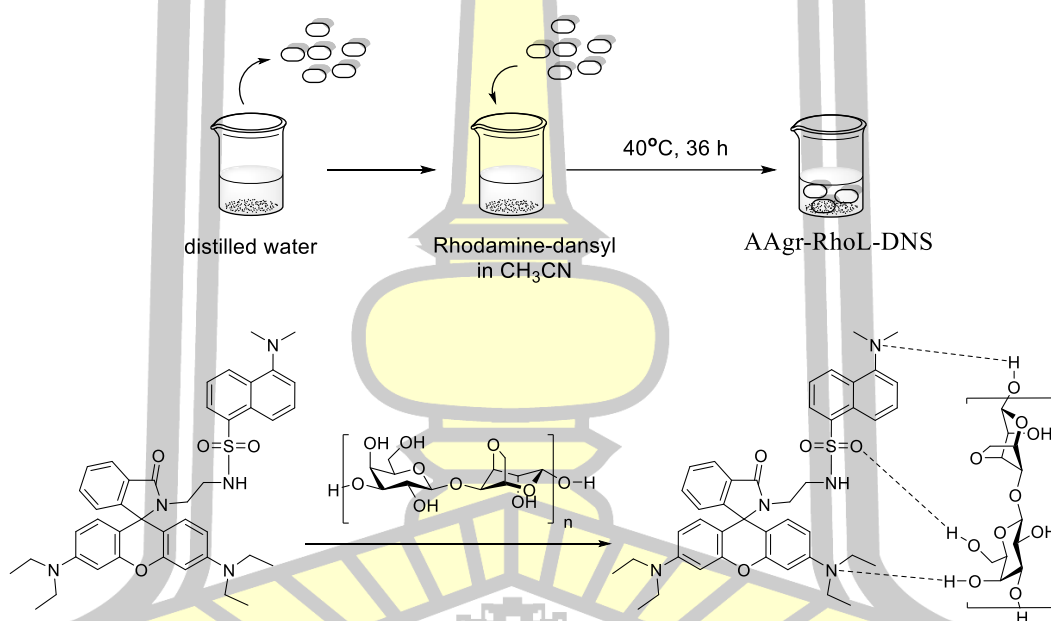


Figure 37 Immobilization of rhodamine-dansyl.

พหุ ประถมศึกษา

CHAPTER IV

RESULTS AND DISCUSSION

4.1 Synthesize agarose hydrogel (Agr-RhoL)

4.1.1 The formation of the rhodamine lactone colorless L-form

The rhodamine lactone (**RhoL**) was synthesized by slight modification to the methods described previously. In this work, we also added NaOH to help a transformation of the zwitterion into the lactone form in H₂O:THF (1:1.39) solution [26]. No emission and absorption spectra were demonstrated in this condition, which strongly indicated that the equilibrium was shifted toward the lactone form (figure 38).

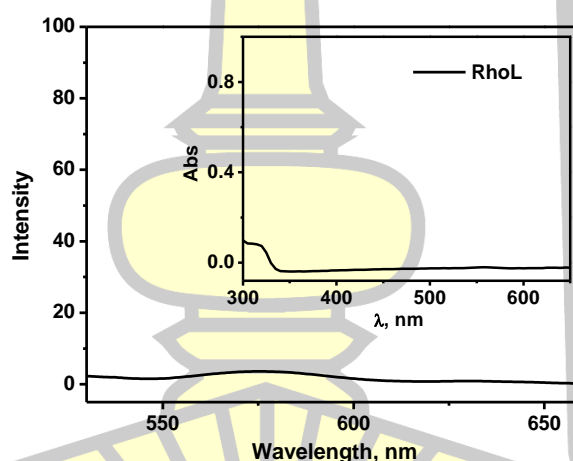


Figure 38 Visible absorption and emission spectra of rhodamine lactone in H₂O: THF solution.

4.1.2 Characterization of Arg-RhoL

After immobilization of **RhoL** on agarose membranes, to form **Arg-RhoL**, ATR-FTIR, SEM, TGA and UV-vis were employed to characterize the sensing material. First, ATR-FTIR is useful to investigate the functional groups present on the adsorbent and is also useful in checking on the loading of dye onto the hydrogel (figure 39). The FTIR spectra of **Arg-RhoL** showed a weak intensity band at 1150

cm^{-1} (plane bending), 888 cm^{-1} (out of plane bending) and at 690 cm^{-1} (wagging vibrations) attributed to aromatic C–H vibrations and the band at 1638 cm^{-1} is characteristic of the C=O stretching vibration of Rhodamine constituents [48], While the band at 3343 cm^{-1} is associated with O–H bond stretching of agarose constituent [49]. IR spectrum (FTIR, ν , cm^{-1}): 3343, 2932, 1638, 1371, 1150, 1039, 930, 888, 770, 690.

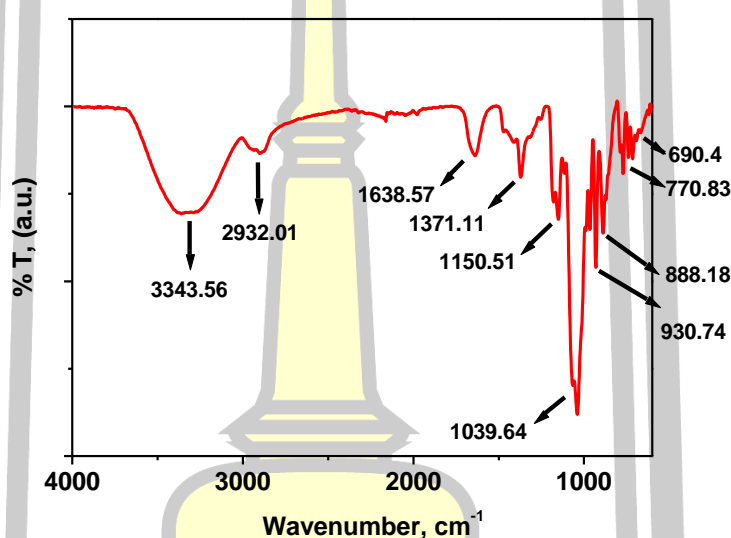


Figure 39 Attenuated total reflectance Fourier transform infrared spectroscopy (ATR-FTIR) spectrum of **Arg-RhoL**.

The loading of dye within agarose hydrogel was also monitored by SEM techniques. The distribution of **RhoL** on the agarose hydrogel film was revealed from the SEM images of **Arg-RhoL** (up) (figure 40), which demonstrated a significant increase in surface roughness. However, such distribution was absent in hydrogel film and in fact the film surface was found to be smooth in comparison to that of **Arg** (below) [50].

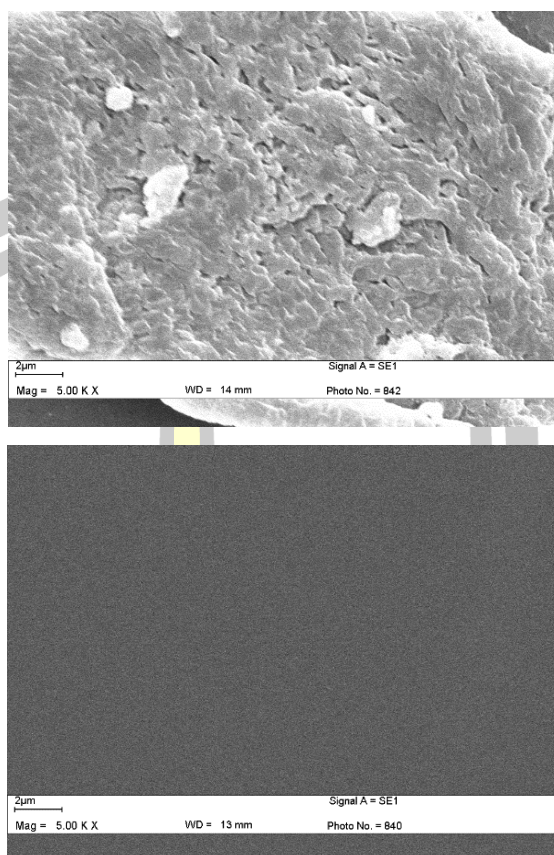


Figure 40 Scanning electron microscope (SEM) image of **Arg-RhoL** (up) and **Arg** (below).

The electrostatic interactions between the hydrogel and rhodamine B also effected the thermal behavior of hydrogel films investigated by thermogravimetric analysis (TGA) under nitrogen flow TGA profiles (figure 41). The decomposition of **Arg** and **Arg-RhoL** composite materials took place in two stages in which the first transition occurred below 100°C due to weight loss of samples by moisture vaporization; in the second stage degradation occurred from 180°C to 320°C, which was attributed to thermal degradation temperature of native and composite materials. In addition, **Arg-RhoL** was more stable than **Arg** at high temperature due to the interaction of hydrogel with Rhodamine B [51].

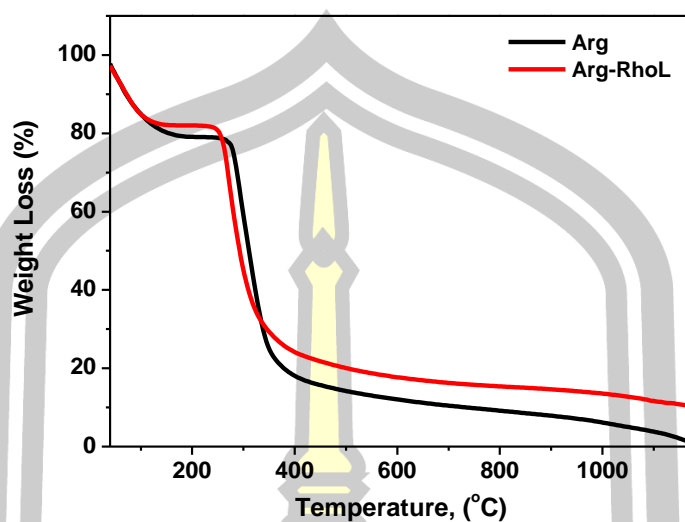


Figure 41 Thermogravimetric analysis of **Arg** and **Arg-RhoL**.

The UV-visible analysis was done in reflectance mode from 750 to 220 nm wavelength range to study the behavioral change in **Arg** and **Arg-RhoL** (figure 42). The **Arg-RhoL** UV-visible spectrum exhibited an absorbance peak at around 300 nm, namely $\pi - \pi^*$, $n - \pi^*$ which was a characteristic of rhodamine B. In the case of agarose hydrogel, no absorption peak was observed around 300 nm [31, 32].

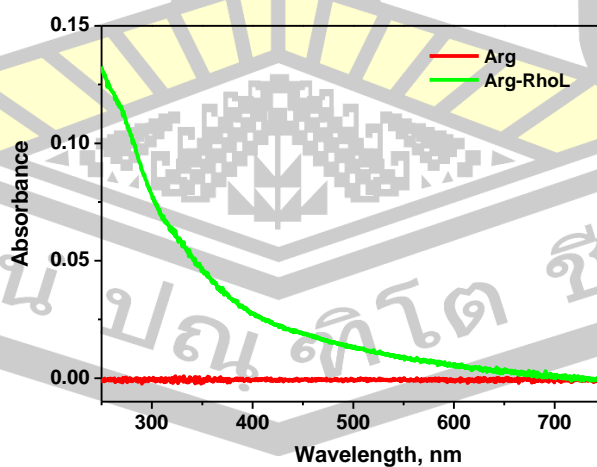


Figure 42 UV-visible spectra of **Arg** and **Arg-RhoL**.

All the techniques mentioned above (ATR-FTIR, SEM), TGA and UV-vis) showed evidences that RhoL can be immobilized into an agarose hydrogel.

4.1.3 Selectivity of Arg-RhoL

The UV-vis spectra changes of **Arg-RhoL** were investigated to determine its cation binding abilities in aqueous solution. The UV-vis spectra of **Arg-RhoL** in the presence and absence of 10 mM of various cations. Normally, the absorption spectra of **Arg-RhoL** exhibited absorbance peaks from 450 to 650 nm. Upon the addition of metal solutions, (such as transition metals (Ni^{2+} , Co^{2+} , Cd^{2+} , Hg^{2+} , Pb^{2+} , Zn^{2+} , Ag^+ , Cu^{2+} , Pt^{2+} , Fe^{3+} , Au^{3+} , Ru^{3+}), alkali metals (Li^+ , Na^+ , K^+) and alkaline earth metals (Ca^{2+} , Mg^{2+}) (figure 43), It can be observed that only Au^{3+} produced an obvious absorbance enhancement at about 540 nm as a result of Au^{3+} -induced ring opening of the spiro lactam form [52].

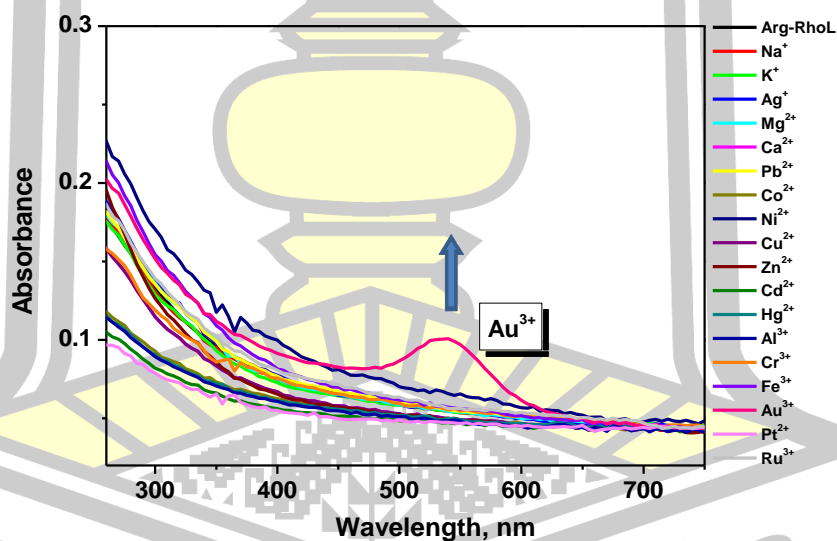


Figure 43 UV-vis spectra changes of **Arg-RhoL** after the addition of 10 μM of various cations.

This can be explained by the suitable distance and the soft properties of the receptor structure (**Arg-RhoL**) to form a complex with Au^{3+} ions (figure 44). In addition, no significant absorbance spectra changes of solution occurred in the presence of other metal ions under identical conditions and the color changes observable with the naked eye upon immersing **Arg-RhoL** into various cations. **Arg-RhoL** showed a distinct color change from colorless to pink only upon addition of Au^{3+} . These results suggested that the immobilization of rhodamine lactone to agarose hydrogel could be a good colorimetric chemosensor for Au^{3+} .

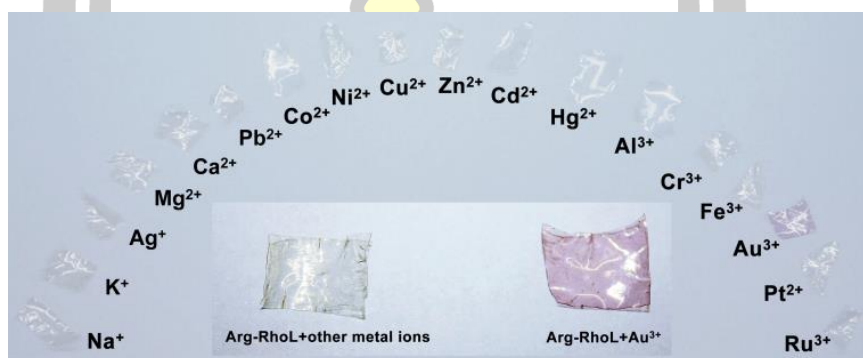


Figure 44 Color changes of the **Arg-RhoL** with various cations.

In order to further explore the formation of **Arg-RhoL**+ Au^{3+} complexes, **Arg-RhoL** in the presence and absence of Au^{3+} was investigated by X-Ray Diffraction Analysis (figure 45). The presence of **Arg-RhoL**+ Au^{3+} film produced distinct spectra showing the characteristic diffraction peaks of gold (III) ions which were lacking in **Arg-RhoL** without Au^{3+} . For **Arg-RhoL** treated with Au^{3+} , the gold experimental diffraction peak was found to be at 2θ values of 38.1° which was the Au (III) peak according to the JCPDS card (NO.1-1172) [53].

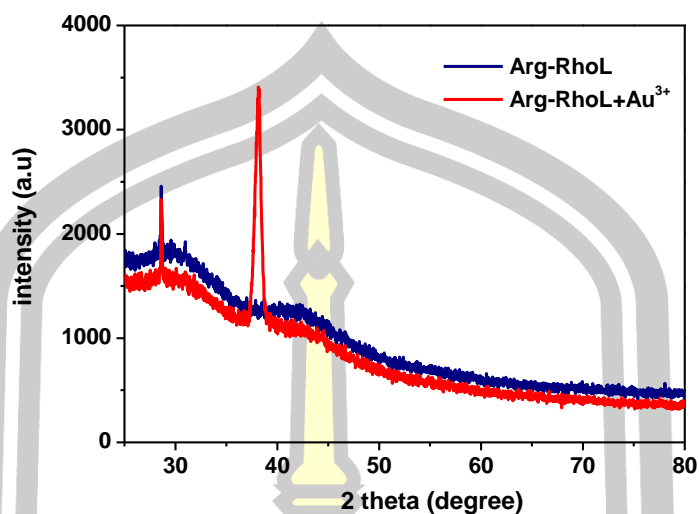


Figure 45 The XRD analysis of the **Arg-RhoL** and **Arg-RhoL+Au³⁺** films.

4.1.4 Computational methods

The structural and electronic properties of the **Arg-RhoL** and **Arg-RhoL+Au³⁺**, and the highest selectivity metal complexes were calculated using the density functional theory (DFT) method using the Gaussian 09 program [54].

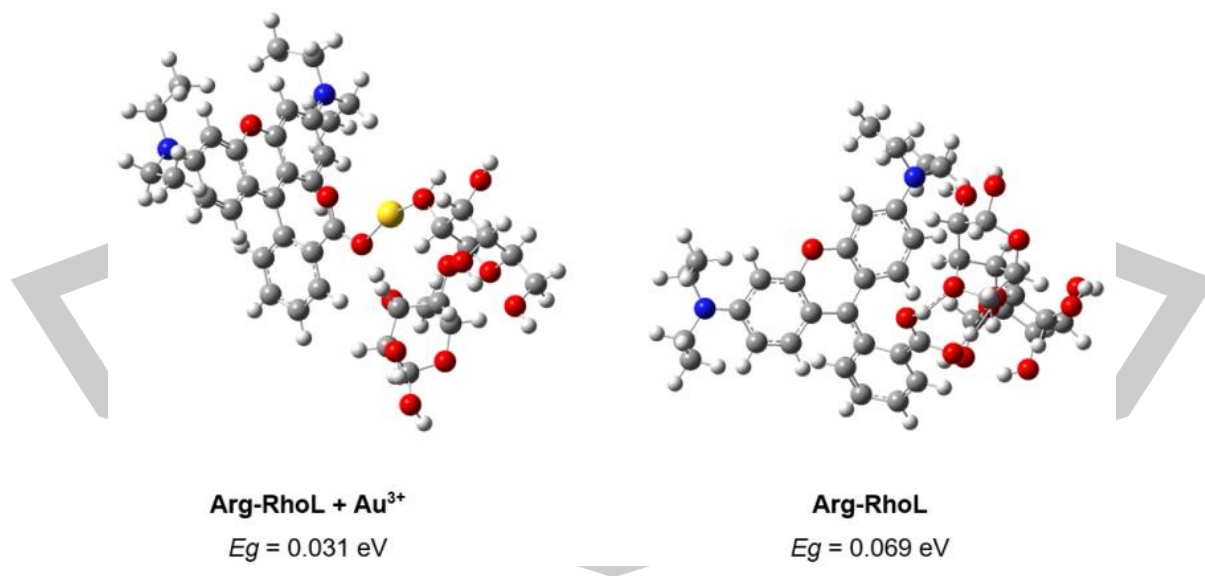
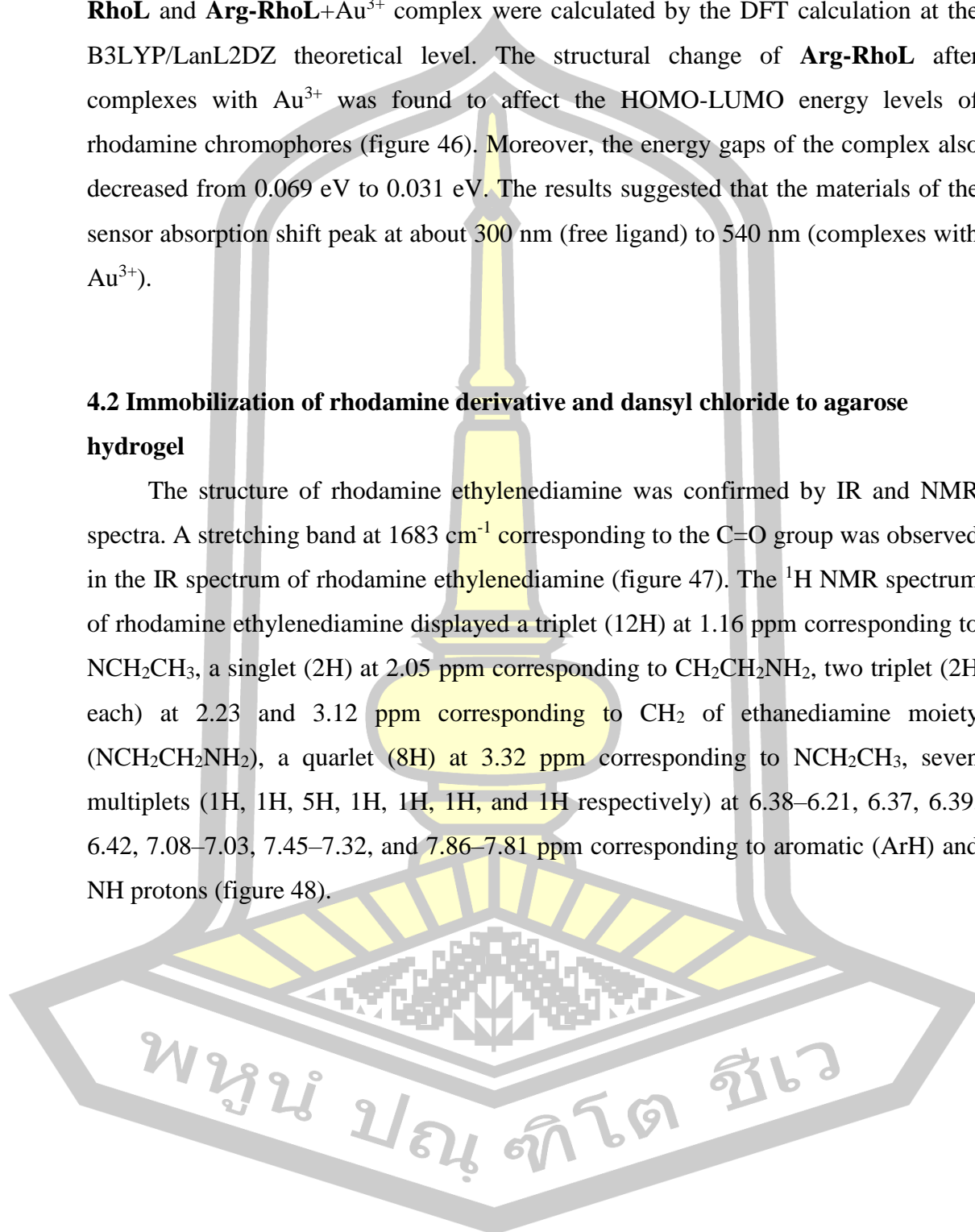


Figure 46 The optimized structures of **Arg-RhoL** and **Arg-RhoL+Au³⁺** complexes, the gap energies ($E_g = E_{LUMO} - E_{HOMO}$).

The optimized geometries and the HOMO and LUMO energies of the **Arg-RhoL** and **Arg-RhoL**+Au³⁺ complex were calculated by the DFT calculation at the B3LYP/LanL2DZ theoretical level. The structural change of **Arg-RhoL** after complexes with Au³⁺ was found to affect the HOMO-LUMO energy levels of rhodamine chromophores (figure 46). Moreover, the energy gaps of the complex also decreased from 0.069 eV to 0.031 eV. The results suggested that the materials of the sensor absorption shift peak at about 300 nm (free ligand) to 540 nm (complexes with Au³⁺).

4.2 Immobilization of rhodamine derivative and dansyl chloride to agarose hydrogel

The structure of rhodamine ethylenediamine was confirmed by IR and NMR spectra. A stretching band at 1683 cm⁻¹ corresponding to the C=O group was observed in the IR spectrum of rhodamine ethylenediamine (figure 47). The ¹H NMR spectrum of rhodamine ethylenediamine displayed a triplet (12H) at 1.16 ppm corresponding to NCH₂CH₃, a singlet (2H) at 2.05 ppm corresponding to CH₂CH₂NH₂, two triplet (2H each) at 2.23 and 3.12 ppm corresponding to CH₂ of ethanediamine moiety (NCH₂CH₂NH₂), a quartet (8H) at 3.32 ppm corresponding to NCH₂CH₃, seven multiplets (1H, 1H, 5H, 1H, 1H, 1H, and 1H respectively) at 6.38–6.21, 6.37, 6.39, 6.42, 7.08–7.03, 7.45–7.32, and 7.86–7.81 ppm corresponding to aromatic (ArH) and NH protons (figure 48).



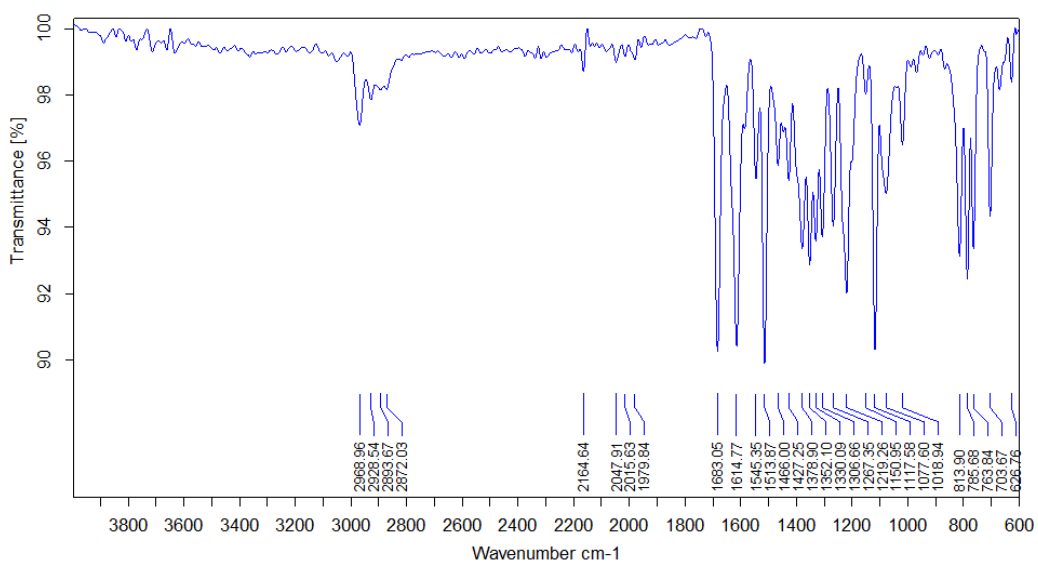


Figure 47 IR spectrum of rhodamine ethylenediamine.

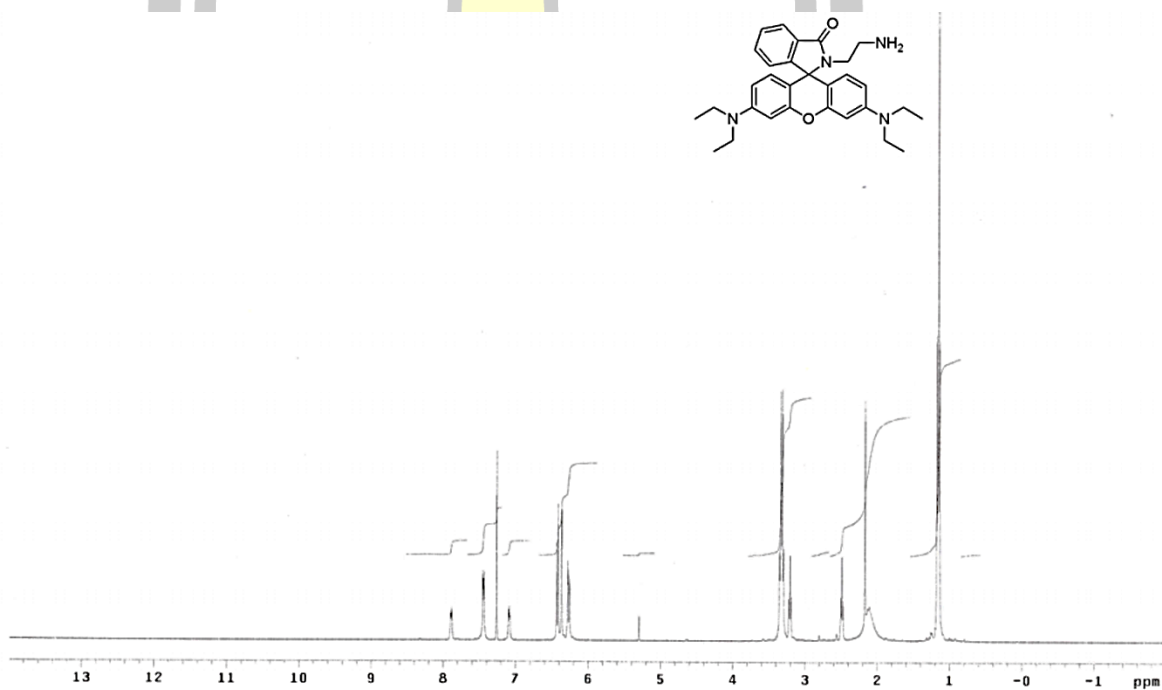


Figure 48 ¹H NMR spectrum of rhodamine ethylenediamine.

The activated gels were dried and transferred into a beaker containing an 25 mL solution of 10^{-3} mol L⁻¹ of rhodamine ethylenediamine and dansyl chloride respectively. This was become hydrogel sensor. The hydrogel sensors were showed selective with 10^{-3} mol L⁻¹ of Au³⁺ in water solution due to open spirolactam ring of rhodamine derivative. The open spirolactam ring of rhodamine was investigated by absorption peak of UV-Vis spectrometry at around 580 nm [53, 55]. Which is absorption of rhodamine (figure 49). But we had excited of dansyl at 380 nm resulted in the emission of rhodamine not showed peak around 580 nm (figure 50). Thus, we can confirm that the fluorescence of the hydrogel-Au³⁺ complex occurred due to **FRET** from the dansyl energy donor to the rhodamine energy acceptor but hydrogel sensor were not **FRET** due to the dansyl energy donor cannot transfer energy to rhodamine [56].

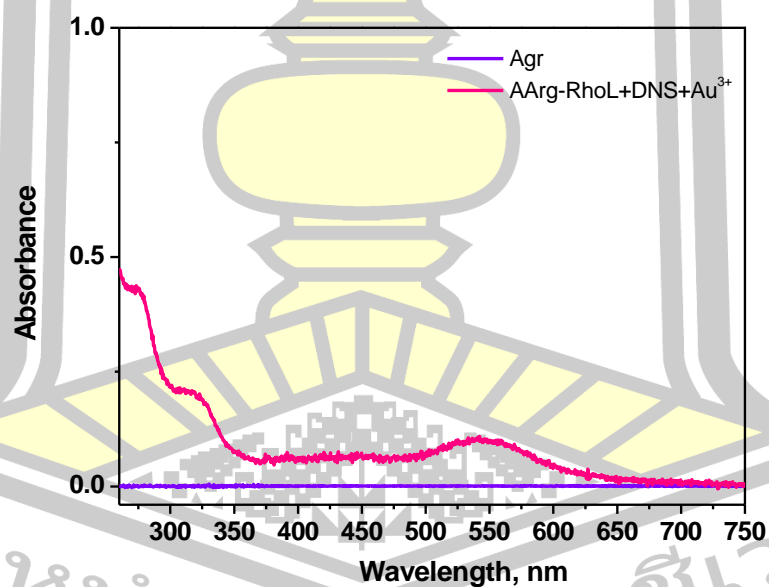


Figure 49 UV-Vis spectrum change of Arg and AArg-RhoL+DNS+Au³⁺.

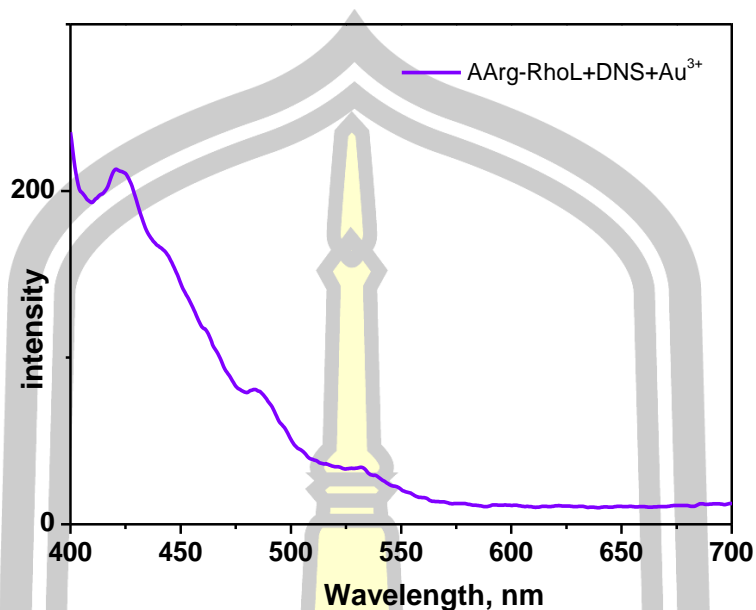


Figure 50 Fluorescent spectrum of AArg-RhoL+DNS+Au³⁺.

4.3 Immobilization of rhodamine derivative and dansyl chloride to agarose powder

The activated agarose powder was suction dried and transferred into a beaker containing an 20 mL solution of 10^{-2} mol L⁻¹ rhodamine ethylenediamine and 4×10^{-3} mol L⁻¹ dansyl chloride. Then incubated 40°C and shook for 36 h after that, it was washed with methanol and dried in room temperature. Then dissolving in distilled water and heated in microwave for hydrogel sensor. However, rhodamine-dansyl powder cannot form hydrogel due to insoluble of rhodamine-dansyl powder (figure 51).

พหุ ประถมศึกษา ชีวะ

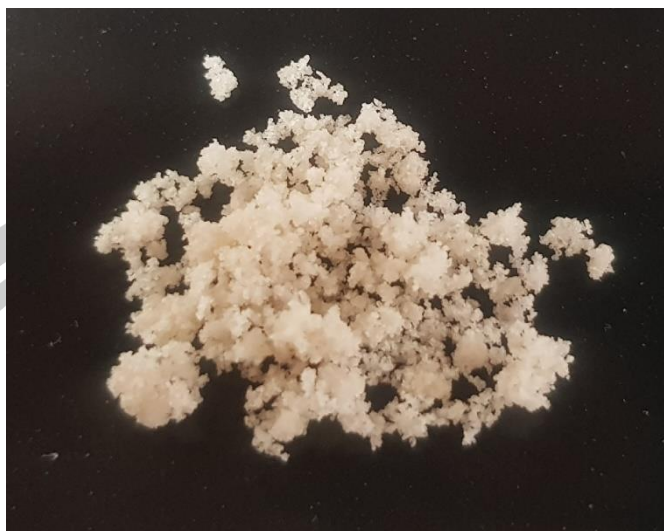
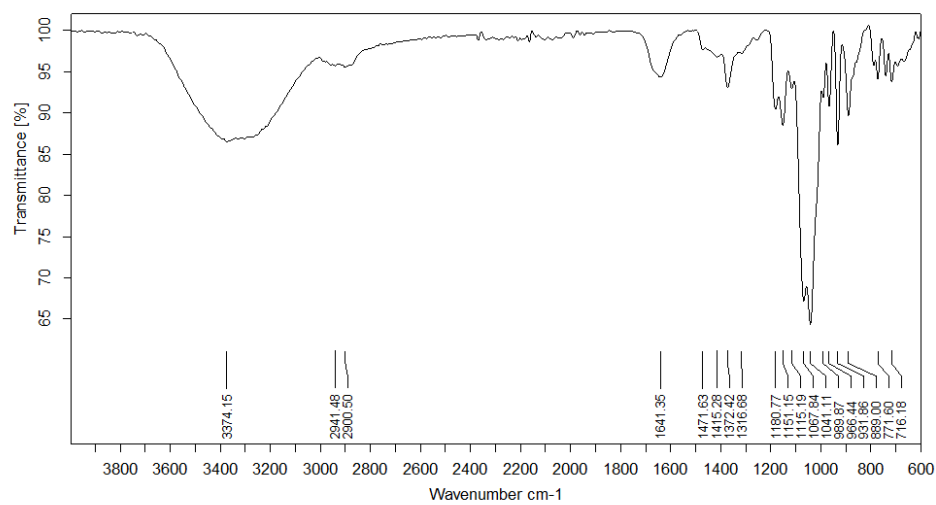


Figure 51 rhodamine-dansyl powder.

4.4 Immobilization of rhodamine-dansyl.

Rhodamine-dansyl was facilely prepared by a simple condensation reaction between rhodamine ethylenediamine and dansyl chloride at room temperature. A stretching band at 1678 cm^{-1} corresponding to the C=O group was observed in the IR spectrum of rhodamine-dansyl (figure 42). The structure of rhodamine-dansyl was confirmed by NMR spectra and IR spectra. The ^1H NMR spectrum of rhodamine-dansyl displayed a triplet (12H) at 1.14 ppm corresponding to the methyl protons, a singlet (6H) at 2.78 ppm corresponding to the methyl protons, two triplet (2H each) at 2.60–2.65 and 3.18–3.21 corresponding to CH_2 of ethanediamine moiety, a quarlet (8H) at 3.25–3.32 ppm corresponding to the methylene protons, three mutiplets (2H each) at 5.83–5.93, 5.94–5.97 and 6.27–6.28 ppm corresponding to aromatic protons, seven multiplets (1H, 1H, 5H, 1H, 1H, 1H and 1H respectively) at 6.90–6.92, 7.02–7.04, 7.38–7.51, 7.88–7.90, 8.09–8.12, 8.28–8.31 and 8.47–8.50 ppm corresponding to aromatic and NH protons (figure 53).



Date of Measurement : 3/7/2561	Sample Name : DNS-K
--------------------------------	---------------------

Figure 52 IR spectrum of rhodamine-dansyl.

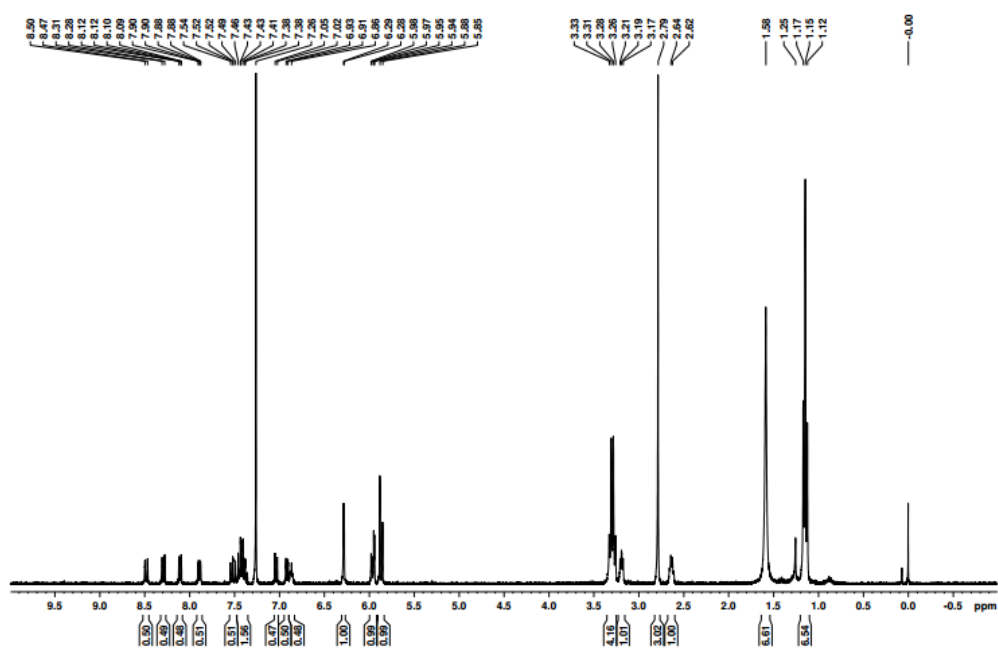


Figure 53 ¹H NMR spectrum of rhodamine-dansyl.

The activated gels were dried and transferred into a beaker containing an 25 mL solution of 10^{-3} mol L⁻¹ of rhodamine ethylenediamine and dansyl chloride respectively. This was become hydrogel sensor. The hydrogel sensors were showed selective with 10^{-3} mol L⁻¹ of Au³⁺ in water solution due to open spirolactam ring of rhodamine derivative. The open spirolactam ring of rhodamine was investigated by absorption peak of UV-Vis spectrometry at around 580 nm [53, 55]. Which is absorption of rhodamine (figure 49). But we had excited of dansyl at 380 nm resulted in the emission of rhodamine not showed peak around 580 nm (figure 50). Thus, we can confirm that the fluorescence of the hydrogel-Au³⁺ complex occurred due to **FRET** from the dansyl energy donor to the rhodamine energy acceptor but hydrogel sensor were not **FRET** due to the dansyl energy donor cannot transfer energy to rhodamine [56].

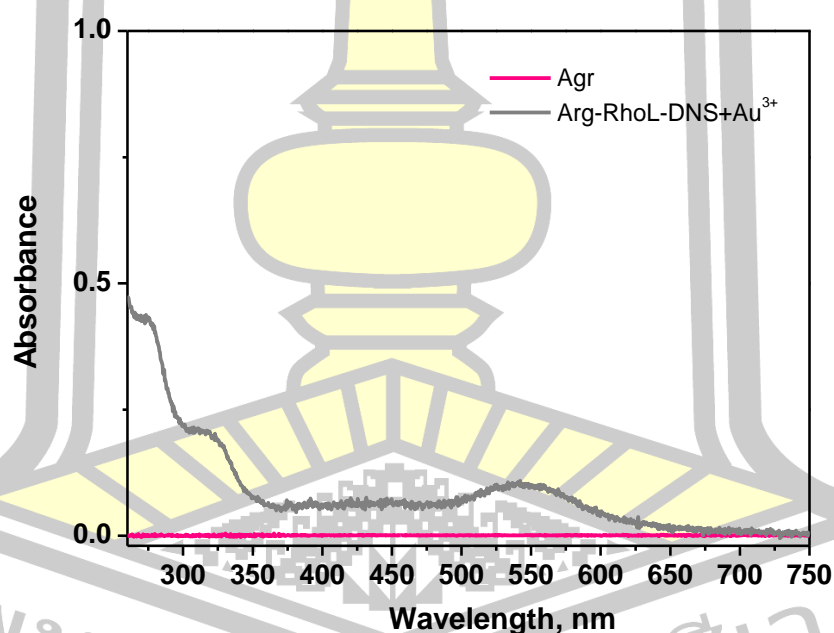


Figure 54 UV-vis spectra changes of Arg and Arg-RhoL-DNS+Au³⁺.

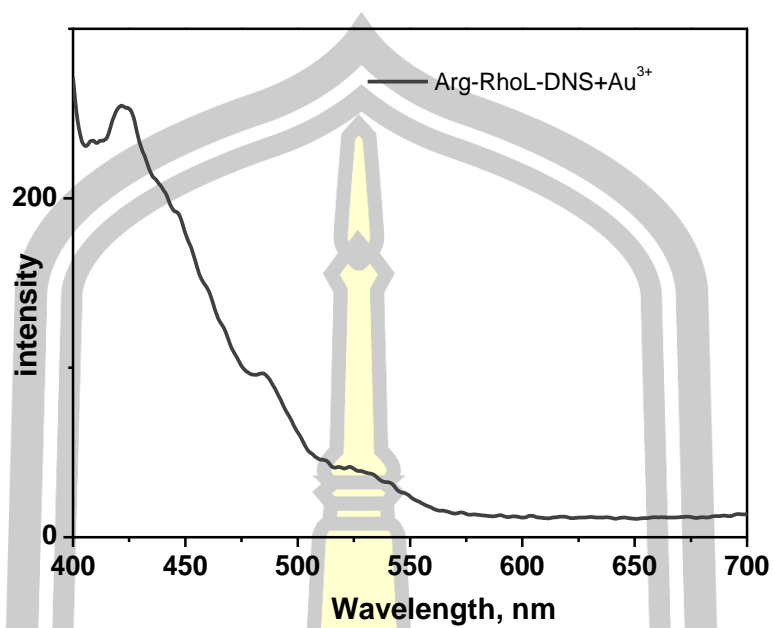
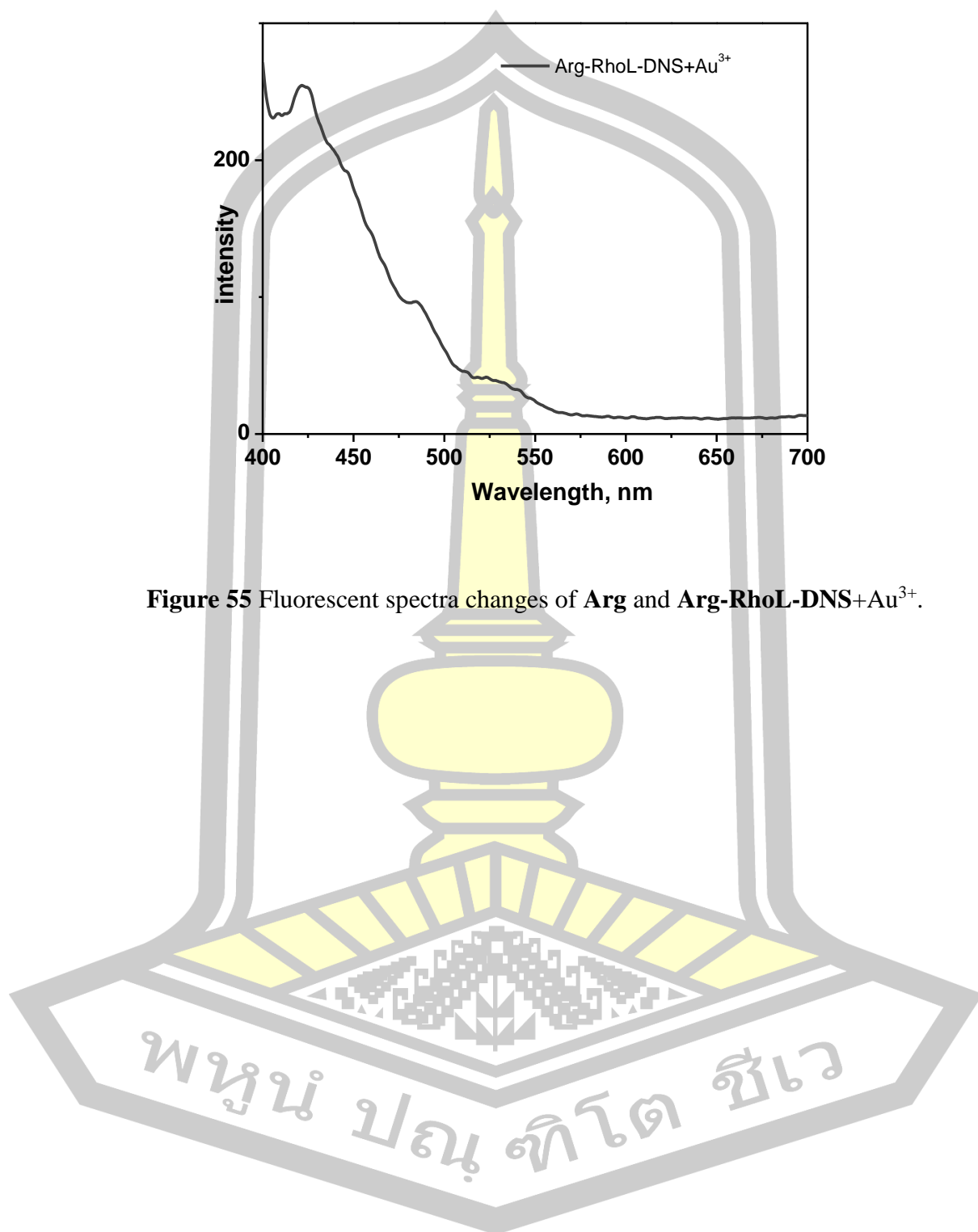


Figure 55 Fluorescent spectra changes of **Arg** and **Arg-RhoL-DNS+Au³⁺**.



CHAPTER V

CONCLUSIONS

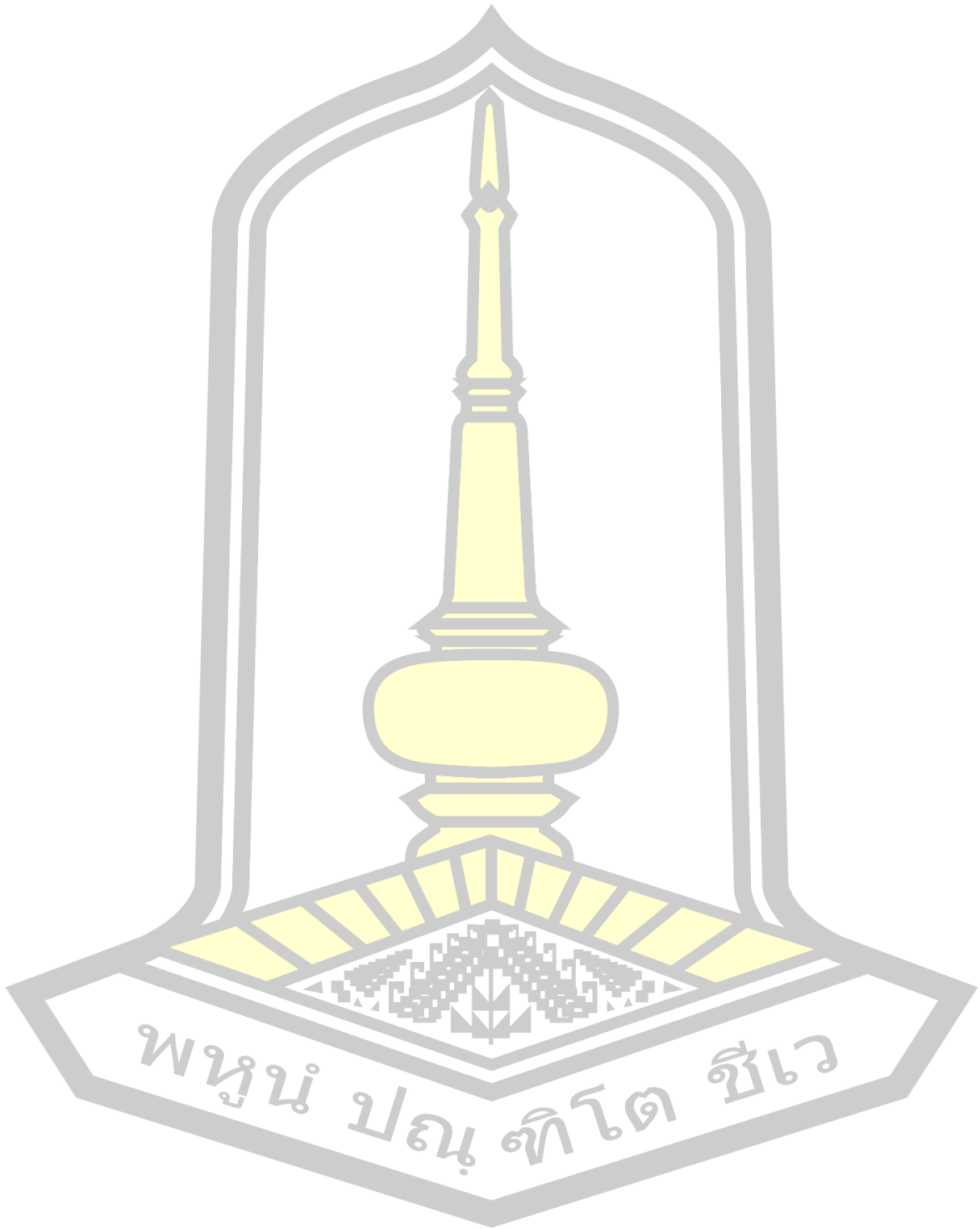
1. The immobilization of rhodamine lactone form into agarose hydrogel, immobilization of rhodamine+dansyl chloride, immobilization of rhodamine+dansyl chloride (powder) and immobilization of rhodamine-dansyl for use as in colorimetric-optical hydrogel film detection of Au^{3+} ions in real systems have been designed and synthesized by ours. The ATR-FTIR, SEM, TGA and UV-vis techniques provided evidence that **RhoL** can be immobilized into an agarose hydrogel.

2. The color change (colorless to pink) was observed in **Arg-RhoL** hydrogel film and was produced by the formation of **Arg-RhoL-Au³⁺** chelates leading to Au^{3+} -induced ring-opening of the rhodamine spiro-lactam. The results suggested that the materials of the sensor absorption shift peak at about 300 nm (free ligand) to 540 nm (complexes with Au^{3+}).

3. The immobilization of rhodamine+dansyl chloride onto agarose hydrogels formed complexes with Au^{3+} via a carboxylic group of rhodamine, sulfonyl group of dansyl and an alcohol group. However, rhodamine+dansyl chloride onto agarose hydrogels are not **FRET** due to the dansyl energy donor cannot transfer energy to rhodamine. Immobilization of rhodamine+dansyl chloride to agarose powder are not hydrogel formed because agarose+rhodamine+dansyl chloride are not soluble in water.

The immobilization of rhodamine-dansyl onto agarose hydrogel formed complexes with Au^{3+} via a carboxylic group of rhodamine, sulfonyl group of dansyl and an alcohol group. However, rhodamine-dansyl onto agarose hydrogels are not **FRET** due to the dansyl energy donor cannot transfer energy to rhodamine. We believe that, this approach may provide an easily measurable and inherently sensitive method for Au^{3+} detection in environmental and biological applications.

REFERENCES



Bibliography

- [1] N. Gogoi, M. Barooah, G. Majumdar, and D. Chowdhury, "Carbon dots rooted agarose hydrogel hybrid platform for optical detection and separation of heavy metal ions," *ACS Appl. Mater. Interfaces*, vol.7, pp. 3058–3067, 2015.
- [2] K. Zargoosh and F. F. Babadi, "Highly selective and sensitive optical sensor for determination of Pb^{2+} and Hg^{2+} ions based on the covalent immobilization of dithizone on agarose membrane," *Spectrochim. acta part a Mol. Biomol. Spectrosc*, vol. 137, pp. 105–110, 2015.
- [3] S. Yusuf and K. Shehu, "Heavy metals pollution on surface water sources in kaduna metropolis, Nigeria" *Sci World J.*, vol. 10, no. 2, pp. 1–5, 2015.
- [4] A. American, "Gold recovery from carbon-in-pulp eluates by precipitation with a mineral acid ii. gold bullion production from precipitate , treatment of barren solution , the settling rate of precipitate and assisting precipitation by addition of CuS ," vol. 21, pp. 243–248, 1988.
- [5] C. P. Gomes, M. F. Almeida, and M. Loureiro, "Gold recovery with ion exchange used resins," vol. 24, pp. 35–57, 2001.
- [6] F. J. Alguacil, P. Adeva, M. Alonso, A. Gregorio, and C. Universitaria, "Processing of residual Gold (III) solutions via ion exchange," pp. 9–13, 2005.
- [7] M. Navarro, "Gold complexes as potential anti-parasitic agents," vol. 253, pp. 1619–1626, 2009.
- [8] P. Claus, "Heterogeneously catalysed hydrogenation using gold catalysts," vol. 291, pp. 222–229, 2005.
- [9] P. Goodman, "Current and future uses of gold in electronics," no. 2, pp. 21–26, 2002.
- [10] N. T. Patil, V. S. Shinde, M. S. Thakare, and P. H. Kumar, "Chemcomm exploiting the higher alkynophilicity of Au-species : development of a highly selective fluorescent probe for gold ions," pp. 11229–11231, 2012.
- [11] A. Kundu, R. K. Layek, A. Kuila, and A. K. Nandi, "Highly fluorescent graphene oxide-poly (vinyl alcohol) hybrid: an effective material for specific Au^{3+} Ion Sensors," 2012.
- [12] J. Park, S. Choi, T. Kim, and Y. Kim, "Highly selective fluorescence turn-on sensing of gold ions by nanoparticle generation / C-I bond cleavage sequence," pp. 1–19, 2012.

- [13] W. D. Block and E. L. Knapp "Metabolism, toxicity, and manner of action of gold compounds in the treatment of arthritis." *J Pharmacol Exp Ther.*, vol. 83, no. 4, pp. 275-278, 1945
- [14] E. G. Shcherbakova *et al.*, "Supramolecular sensors for opiates and their metabolites," *J. Am. Chem. Soc.*, vol. 139, no. 42, pp. 14954–14960, 2017.
- [15] C. G. Claessens and J. F. Stoddart, " π - π Interactions in self-assembly," vol. 10, pp. 254–272, 1997.
- [16] N. Kannan and S. Vishveshwara, "Aromatic clusters : a determinant of thermal stability of thermophilic proteins," vol. 13, no. 11, pp. 753–761, 2000.
- [17] J. F. Stoddart, "Synthetic supramolecular chemistry," vol. 30, 1997.
- [18] P. Hashemi and M. M. Abolghasemi, "Preparation of a novel optical sensor for low pH values using agarose membranes as support," vol. 115, pp. 49–53, 2006.
- [19] M. Beija and C. A. M. Afonso, "Synthesis and applications of rhodamine derivatives as fluorescent probes," 2009.
- [20] H. Zheng, Z. Qian, L. Xu, F. Yuan, and L. Lan, "Switching the recognition preference of rhodamine b spirolactam by replacing one atom : design of rhodamine B thiohydrazide for recognition of Hg (II) in aqueous solution," no. 4, pp. 7386–7387, 2006.
- [21] A. K. Pikaev, L. I. Kartasheva, and V. N. Chulkov, "A new highly-sensitive dosimetric composition based on a solution of rhodamine B lactone in chloroform," vol. 7, no. 5, pp. 178–179, 1997.
- [22] K. Li *et al.*, "Reversible photochromic system based on rhodamine B salicylaldehyde hydrazone metal complex," 2014.
- [23] T. Tokimoto, S. Tsukahara, and H. Watarai, "Lactone cleavage reaction kinetics of rhodamine dye at liquid / liquid interfaces studied by micro-two-phase sheath flow / two-photon excitation fluorescence microscopy," no. 8, pp. 1299–1304, 2005.
- [24] Y. Zhou, F. Wang, Y. Kim, S. Kim, and J. Yoon, " Cu^{2+} -Selective ratiometric and ' off-on ' sensor based on the rhodamine derivative bearing pyrene group," vol. 11, no. 19, pp. 2–5, 2009.
- [25] Q. A. Best, R. Xu, M. E. Mccarroll, L. Wang, and D. J. Dyer, "Design and investigation of a series of rhodamine-based fluorescent probes for optical measurements of pH," vol. 12, no. 14, pp. 2007–2009, 2010.

- [26] C. Kaewtong, "A solvatochromic-based sensor for chromium (iii) in real systems," *New J. Chem.*, 2018.
- [27] P. Xie, F. Guo, R. Xia, Y. Wang, D. Yao, and G. Yang, "A rhodamine – dansyl conjugate as a FRET based sensor for Fe³⁺ in the red spectral region," vol. 145, pp. 849–854, 2014.
- [28] J. Piao, J. Lv, X. Zhou, T. Zhao, and X. Wu, "A dansyl – rhodamine chemosensor for Fe (III) based on off – on FRET," *Spectrochim Acta A.*, vol. 128, pp. 475–480, 2014.
- [29] X. Wang, M. Song, and Y. Long, "Synthesis, characterization, and crystal structure of the lactone form of rhodamine B," *J. Solid State Chem.*, vol. 156, no. 2, pp. 325–330, 2001.
- [30] D. A. Hinckley and P. G. Seybold, "A spectroscopic/thermodynamic study of the rhodamine B lactone \rightleftharpoons zwitterion equilibrium," *Spectrochim. Acta Part A Mol. Spectrosc.*, vol. 44, no. 10, pp. 1053–1059, 1988.
- [31] A. Abdalfahdaw *et al.*, "Effect of solvents on the dipole moments and fluorescence quantum yield of rhodamine dyes. vol. 9, no. 16, pp. 34–42, 2016.
- [32] N. Mergu, A. K. Singh, and V. K. Gupta, "Highly sensitive and selective colorimetric and off-on fluorescent reversible chemosensors for Al³⁺ based on the rhodamine fluorophore," pp. 9097–9111, 2015.
- [33] F. H. Wang, C. W. Cheng, L. C. Duan, W. Lei, M. Z. Xia, and F. Y. Wang, "Highly selective fluorescent sensor for Hg²⁺ ion based on a novel rhodamine B derivative," *Sensors Actuators, B Chem.*, vol. 206, pp. 679–683, 2015.
- [34] D. Shi *et al.*, "Rhodamine derivative functionalized chitosan as efficient sensor and adsorbent for mercury (II) detection and removal," *Mater. Res. Bull.*, vol. 70, pp. 958–964, 2015.
- [35] Y. Jiao, L. Zhang, and P. Zhou, "A rhodamine B-based fluorescent sensor toward highly selective mercury (II) ions detection," *Talanta*, vol. 150, pp. 14–19, 2016.
- [36] P. Venkatesan, N. Thirumalivasan, and S. P. Wu, "A rhodamine-based chemosensor with diphenylselenium for highly selective fluorescence turn-on detection of Hg²⁺: In vitro and in vivo," *RSC Adv.*, vol. 7, no. 35, pp. 21733–21739, 2017.
- [37] M. H. Lee, H. J. Kim, S. Yoon, N. Park, and J. S. Kim, "Metal ion induced FRET OFF – ON in tren / dansyl-appended rhodamine," pp. 1–4, 2008.

- [38] P. Xie, F. Guo, L. Wang, and S. Yang, "A dansyl-rhodamine ratiometric fluorescent probe for Hg^{2+} based on FRET mechanism," 2015.
- [39] S. Yuan, W. Su, and E. Wang, "A dansyl-rhodamine based fluorescent probe for detection of Hg^{2+} and Cu^{2+} ," pp. 638–643, 2017.
- [40] P. Hashemi, R. A. Zarjani, and M. M. Abolghasemi, "Agarose film coated glass slides for preparation of pH optical sensors," vol. 121, pp. 396–400, 2007.
- [41] P. Hashemi, M. M. Abolghasemi, K. Alizadeh, and R. A. Zarjani, "A calmagite immobilized agarose membrane optical sensor for selective monitoring of Cu^{2+} ," *Sensors Actuators, B Chem.*, vol. 129, no. 1, pp. 332–338, 2008.
- [42] K. Alizadeh, R. Parooi, P. Hashemi, B. Rezaei, and M. R. Ganjali, "A new Schiff's base ligand immobilized agarose membrane optical sensor for selective monitoring of mercury ion," *J. Hazard. Mater.*, vol. 186, no. 2–3, pp. 1794–1800, 2011.
- [43] F. N. Serenjah, P. Hashemi, A. R. Ghiasvand, and F. Rasolzadeh, "A new optical sensor for selective quantitation of uranium by the immobilization of arsenazo III on an agarose membrane," *Anal. Methods*, vol. 8, no. 21, pp. 4181–4187, 2016.
- [44] R. Heydari, M. Hosseini, A. Amraei, and A. Mohammadzadeh, "Preparation of a novel pH optical sensor using orange (II) based on agarose membrane as support," *Mater. Sci. Eng. C*, vol. 61, pp. 333–337, 2016.
- [45] C. Kaewtong, B. Wannoo, Y. Uppa, N. Morakot, B. Pulpoka, and T. Tuntulani, "Facile synthesis of rhodamine-based highly sensitive and fast responsive colorimetric and off-on fluorescent reversible chemosensors for Hg^{2+} : Preparation of a fluorescent thin film sensor," *Dalt. Trans.*, vol. 40, no. 46, pp. 12578–12583, 2011.
- [46] I. Matsumoto, Y. Mizuno, and N. Seno, "Activation of sepharose with epichlorohydrin and subsequent immobilization of ligand for affinity adsorbent," *J. Biochem.*, vol. 85, no. 4, pp. 1091–1098, 1979.
- [47] T. Ft-ir, "The spectroscopic (FT-IR, FT-Raman, UV and NMR) first order hyperpolarizability and HOMO-LUMO analysis of Dansyl chloride," *Spectrochim. Acta part A Mol. Biomol. Spectrosc.*, 2013.
- [48] R. M. Dukali, "Electrospinning of the laser dye rhodamine B-doped poly (methyl methacrylate) nanofibers," vol. 79, no. 7, pp. 867–880, 2014.
- [49] B. Samiey and F. Ashoori, "Adsorptive removal of methylene blue by agar : effects of NaCl and ethanol," vol. 1, no. c, pp. 1–13, 2012.

BIOGRAPHY

NAME	Mr. Sastiya Kampaengsri
DATE OF BIRTH	August 20, 1993
PLACE OF BIRTH	Nongbualamphu, Thailand
ADDRESS	7/1 Moo 7, Tumbol Nonmeang, Aumphur Nonsang, Nongbua amphu 39140, Thailan
EDUCATION	2009 Junior High School, Sriboonruang Witthayakarn School 2012 Senior High School, Udonpattanakarn Witthayakarn School 2016 Bachelor of Science degree in Chemistry (B.Sc.), Mahasarakham University 2018 Master of Science degree in Chemistry (M.Sc.), Mahasarakham University
Research grants & awards	Center of Excellence for Innovation in Chemistry (PERCH-CIC)
Research output	Sastiya Kampaengsri, Banchob Wannoo, Thawatchai Tuntulani, Buncha Pulpoka, Chatthai Kaewtong. Immobilization of rhodamine derivative on agarose hydrogel as gold probe.

